NTNU
Norwegian University of
Science and Technology

Wet-chemical deposition of silicon quantum dots for enhanced solar cell efficiency

Åsne Århus

Chemical Engineering and Biotechnology
Submission date: June 2011
Supervisor: Mari-Ann Einarsrud, IMTE
Co-supervisor: Malin Sletnes, IMT
Mustafa Balci, IMT
Jerome Maria, IFY

Norwegian University of Science and Technology
Department of Materials Science and Engineering

Erklæring (Declaration)

Jeg erklærer at arbeidet med denne diplomoppgaven er utført sjølstendig og i samsvar med reglement for sivilarkitekt- og sivilingeniøreksamen ved NTNU.

(I herby declare that the work on this master thesis has been done independently, and in accordance with the examination regulations for the technology studies at The Norwegian University of Science and Technology.)

Trondheim, 17. juni 2011

Åsne Århus

Acknowledgements

This master thesis has been carried out at The Department of Materials Science and Engineering, in the spring of 2011. A project work was performed in the autumn of 2010, which is linked to the work of this master thesis. No parts of the report are directly copied from the project work, but some sections may be similar.

I want to thank all the people who have helped me with this project, for all their guidance, support and inspiration during the semester. Both helping me with experimental work, and also supporting me theoretically by giving advices and answering my questions. This work could not have been done without them.

First of all I would like to thank my supervisor, Prof. Mari-Ann Einarsrud for being very helpful and positive, and for organising meetings for discussion of the results. The help I have got from Mustafa Balci and Malin Sletnes is invaluable; they have been outstanding helping me with experimental details and were kind and patient when answering my questions. Mustafa and Malin synthesised the octoxy capped silicon quantum dots, by the potassium naphthalide and the alkalide synthesis, respectively.

I want to thank chief engineer Yingda Yu for doing TEM characterisation of the quantum dots and Jerome Maria at The Department of Physics for being available for discussions and performing material investigations by diffuse reflectance spectroscopy. Thanks to Pål Ulseth for help with the grinding of the Al substrates, and to Prof. Ursula Gibson, Department of Physics, for lending us the Langmuir trough and help with the set-up. All the experimental work except characterisation was done in the NTNU Nanolab and I would like to thank the engineers working there for providing excellent working conditions.

Abstract

Silicon quantum dots were synthesised wet-chemically by three different methods based on reduction of silicon tetrachloride with the reduction agents potassium naphthalide, sodium cyclopentadiene and the alkalide of potassium. The purpose of these quantum dots was to deposit them on a substrate in order to use them as down converters on top of photovoltaic solar cells for enhanced solar cell efficiency. One possible method for the formation of down converting layers is to incorporate quantum dots into silica thin films by deposition of quantum dots in an ethanol based silica sol, followed by spin coating. It is believed that when the quantum dots are water dispersible, this will make it easier to bind them to the silica network, and a good dispersion in the film is facilitated. The different hydrophilic functionalisations investigated were pentenoxy capping, oxidised pentenoxy capping, oxidised acrylic acid capping and ethanolamine capping. Challenges were encountered during the synthesis of water dispersible quantum dots, the most important were related to agglomeration and purification of the quantum dots. This was believed to be due to the tendency of hydrophilic surface groups to attract each other, interaction with the polar solvent and similar solubility characteristics of the quantum dots and the byproduct salts.

Si quantum dots with hydrophobic octoxy capping were also synthesised. Dispersions of these quantum dots were deposited onto solid substrates followed by solvent evaporation. This was done to see whether it was possible to deposit the synthesised quantum dots by this simple approach, to investigate the fundamentals upon evaporation, the degree of agglomeration and the byproducts present in the quantum dot dispersions. It was found that agglomeration was very pronounced after the solvent had evaporated and that quite large amounts of byproducts were present in the final quantum dot dispersions. The most important reasons to this were believed to be too weak steric repulsive forces between the particles, too fast evaporation of the solvent and an insufficient purification procedure. For the use of Si quantum dots synthesised wet-chemically as down converters in solar cells, improvements of the particles are needed.

Contents

List of abbreviations

Abbreviation	Term
e^-	Electron
EDS	Energy Dispersive X-ray Spectroscopy
FTIR	Fourier Transform Infrared Spectroscopy
IPS	Isopropanol
LB	Langmuir Blodgett
L	Ligand
M	Alkali metal
M^+	Alkali metal cation
M^-	Alkali metal anion
NMR	Nuclear Magnetic Resonance
QD	Quantum Dots
SAED	Selected Area Electron Diffraction
SEM	Scanning Electron Microscopy
STEM	Scanning Transmission Electron Microscopy
TEM	Transmission Electron Microscopy
THF	Tetrahydrofuran
TMCS	Trimethylchlorosilane
XRD	X-Ray Diffraction
2D	Two Dimensional

1. Introduction

1.1. Motivation and background

The sun has an unlimited potential as power source and is therefore a very valuable resource of energy. In less than one hour, enough energy is supplied to the earth from the sun to satisfy the energy demand for a whole year. Due to this large potential and the climate changes, solar cells have been subject to massive research during the last decades. The development of efficient photovoltaic solar cells is considered very important for sustainable and environmentally friendly generation of electricity in the future. The major drawback is a high capital cost; at present the installation of photovoltaic devices is subsidised or dependent on financing mechanisms to spread the payments over the system lifetime. The use of solar power is steadily increasing, doubling every two, or fewer, years. If it continues with the same rate as up to now, solar power would become the dominant energy source within a few decades.

Currently, single-junction crystalline silicon solar cells dominate the market, although the potential of them certainly is not fully utilised yet. Silicon is the second most abundant material on the earth, is non-toxic and inexpensive, has good mechanical and electronic properties and is for that reason the principal material for semiconductor devices. In Si solar cells, the sunlight is converted directly into electricity using photovoltaics. The two most important power loss mechanisms in single band gap photovoltaic cells are the inability to absorb photons with energy less than the band gap and the thermalisation of photon energy exceeding the band gap [1].

The aim for researchers on the field is to enhance the effect of the solar cells and to reduce the production costs, since the solar modules up to date are too expensive and have a too low efficiency to compete with energy produced from e.g. fossil fuels. So-called third generation solar cells are now emerging. The aim for third generation solar cells is to provide higher efficiency and lower costs per watt of electricity generated. The red area in Figure 1.1 represents third generation solar cells. They should also be made of abundant materials that do not cause toxicity and should be easily produced, in practice this generally means by thin film deposition techniques.

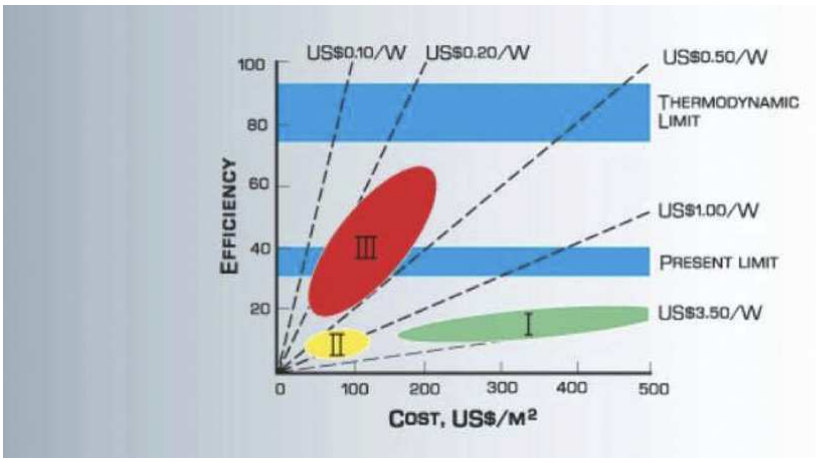

Figure 1.1: Solar cell efficiency as a function of cost per unit area showing the present status in the solar cell market. Generation I cells (green area) are based on bulk single and polycrystalline Si. Generation II cells (yellow area) are based on thin films of various compositions. Generation III solar cells (red area) utilise various proposed energy conversion concepts [2].

The primary aim, at least initially, is to enhance the conversion efficiency of existing Si solar cells. Quantum dots (QD) have remarkable characteristics that differ from their bulk material, such as optical and electronic properties. Down-conversion of the solar spectrum is the most realistic application of quantum dot structures in solar cells. In these cells, the incoming radiation is converted to energies that better fit the absorption properties of the solar cells by a layer of semiconductor quantum dots in a dielectric matrix. Using a silicon solar cell with an ideal down converter, a conversion efficiency of 38.6 % could be achieved under unconcentrated sunlight [3]. This is in comparison to the limiting efficiency of 30.9 % for the same solar cell without a down converting layer present.

Considerable efforts have been invested in the research of silicon nanostructures, because they are advantageous in respect of their chemical simplicity, technical maturity, feasible surface functionalisation and biocompatibility compared to that of most other quantum dots [4]. The biocompatibility of Si makes luminescent silicon particles dispersed in liquid phase an ideal candidate for bio-applications such as drug delivery, bio imaging and fluorescent tags [5]. This will eliminate toxicology problems of inorganic nanocrystals in living systems that might arise from the otherwise well-established and deeply investigated cadmium-based semiconductors. There are many possible routes to the synthesis of quantum dots, among them are solution-based chemical methods as well as chemical and physical vapour deposition methods. Synthesis of Si quantum dots is challenging since they are very air- and water sensitive, and it is also demanding to produce monodisperse and crystalline quantum dots with a simultaneous control of surface chemistry and optical properties.

1.2. Previous work

Silicon quantum dots have for some time been synthesised and investigated here at the Department of Materials Science and Technology. These Si nanoparticles have previously been dispersed in silica thin films by spin coating in a project work carried out in the autumn of 2010 [6]. Ethanol based silica sol used for the spin coating was produced by the sol-gel method. Quantum dots were incorporated into the thin films by dispersion in silica sol prior to spin coating. This is a very simple means to produce such thin films. Different hydrophobic functionalisations of the quantum dots were investigated. However, it turned out that quantum dots with hydrophobic cappings do not mix readily with the silica sol. The work in this master thesis is based on the assumption that water dispersible quantum dots would be easier to disperse in ethanol based silica sols, since the nanoparticles possibly could form bondings to non-condensated OH-groups in the silica sol. When the quantum dots are well dispersed in the dispersions, the homogeneous distribution in the resulting spin coated silica films is also more probable.

1.3. Aim of the work

The first aim of this work is to produce silicon quantum dots by wet chemical synthesis, in order to make them water dispersible. This should be achieved by functionalisation of the quantum dots with different water soluble cappings. These are oxidised pentenol, oxidised acrylic acid and ethanolamine. Capping of the quantum dots is also desirable because it prevents the quantum dots from agglomeration and oxidation when exposed to air, and thereby makes the nanoparticles more stable. The quantum dots are supposed to act as down converters when dispersed in a layer on top of a Si solar cell. These films with quantum dots should be thin to reduce losses due to absorption and

scattering in the film, and the quantum dots should be homogeneously distributed and have a high packing density to achieve an efficient down conversion layer.

It is very challenging to synthesise water dispersible silicon quantum dots and they tend to have a low stability due to agglomeration and efficient oxidation. It is also demanding to characterise Si quantum dots in silica films because of the low contrast between silica and Si during TEM investigation. Because of these challenges, other techniques for the deposition on substrates should be investigated. The deposition of quantum dots on Si and Al substrates should be done simply by solvent evaporation of the quantum dot dispersions. Deposition should also be done for hydrophobic quantum dots in order to see if it is possible to deposit quantum dots onto solid substrates by this simple approach, to investigate the fundamentals upon evaporation, to characterise the degree of agglomeration and the byproducts present in the final quantum dot dispersions.

Dispersions of the differently functionalised quantum dots should be investigated by Fourier Transform Infrared (FTIR) spectroscopy to confirm the surface modification is successful, by Scanning Transmission Electron Microscopy (STEM) and Transmission Electron Microscopy (TEM) to see if the quantum dots are well dispersed, to investigate their size distribution, and to confirm eventual crystallinity. For the deposition of the quantum dots onto substrates, the most important characterisation tool will be Scanning Electron Microscopy (SEM). This thesis is organised as a two-step process. In the first part, silicon quantum dots are synthesised and characterised. Next, the quantum dots are deposited on substrates by solvent dispersion, followed by characterisation.

2. Theory

2.1. Power losses in solar cells

According to the quantum nature of light, it consists of photons carrying an energy corresponding to their wavelength [7]. Only those photons having energy in excess of the band gap can be converted into electricity by the solar cell, the photons with a lower energy will not be absorbed at all. This mismatch represents one of the fundamental losses in a solar cell. For a silicon solar cell with a band gap of 1.1 eV, the photon flux which can be converted is about two thirds of the total flux, shown as the shaded area in Figure 2.1a. This means that practically all the generated electron-hole pairs have energy in excess of the band gap. The extra energy is given off by decay of the charge carriers to states near the edges of their respective bands, as illustrated in Figure 2.1b. The excess energy is lost as heat and can not be converted into useful power. A very small energy gap is useful for absorbing most of the solar photons but deleterious because of the resulting unwanted small open-circuit voltage. A rather high value of the energy gap, on the other hand, is harmful because most of the solar radiation can then not be absorbed by the semiconductor. The band gap of silicon lies in the range of the optimal band gap for a one-junction semiconducting solar cell [3].

a) **b)**

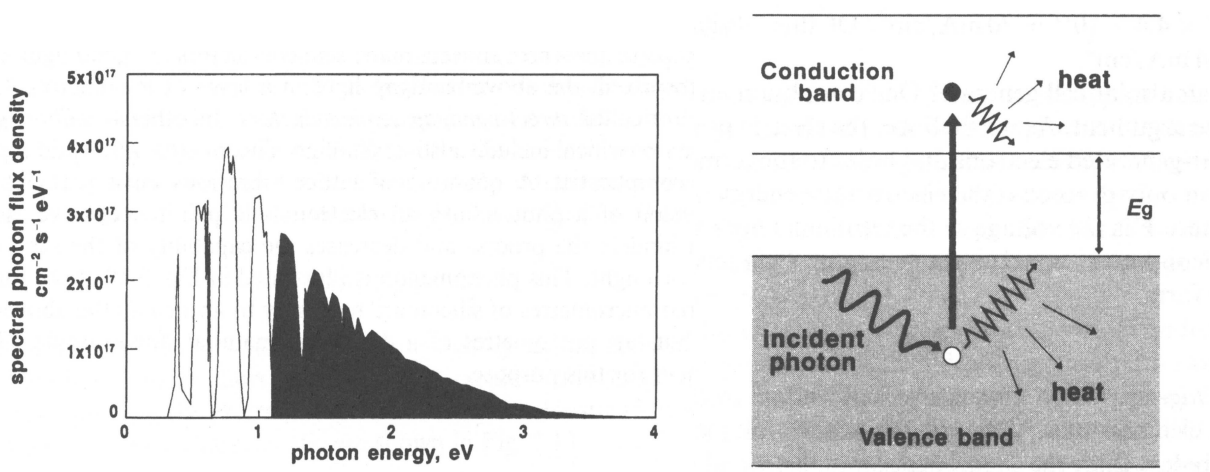

Figure 2.1: a) The shaded area represents the photon flux which can be utilised by a silicon solar cell, i.e. these photons have an energy larger than the band gap of 1.1 eV. **b)** Photons with energy in excess of the band gap loose the extra energy as heat during generation of an electron-hole pair [7].

Another important loss mechanism is recombination. This is the process when a generated electron-hole pair recombines before migrating over the p-n-junction. Recombination is most common at impurities or defects in the crystal structure, or at the surface of the semiconductor where there are many unsatisfied bonds. In these recombination processes, energy levels may be introduced inside the energy gap which act as stepping stones for the electrons to fall back into the valence band and recombine with holes. This is called indirect recombination. Other losses generally associated with solar cells are shading contacts on the top, light reflection from the top surface, ohmic losses and voltage losses at high temperatures [7].

2.2. Quantum dots

Quantum dots are zero-dimensional nanocrystals, their sizes are in the range 2-20 nm in diameter [8]. Due to their small size and emerging quantisation effects, quantum dots have different optical and electronic properties than their bulk material. A great advantage over their bulk material is that their optical and electronic properties are easy to control, since the absorption edge of quantum dots can be easily changed by adjusting the size. The absorption edge in nanostructures corresponds to the energy gap in bulk material, but the term band gap is often used for nanostructures too, even though continuous energy bands are not formed. The unusual properties of quantum dots can be attributed to two main factors: the large surface to volume ratio and the confinement of charge carriers in a quantum mechanical box. The difference in electronic structure between an atom, the bulk and a quantum dot of the same material is illustrated in Figure 2.2.

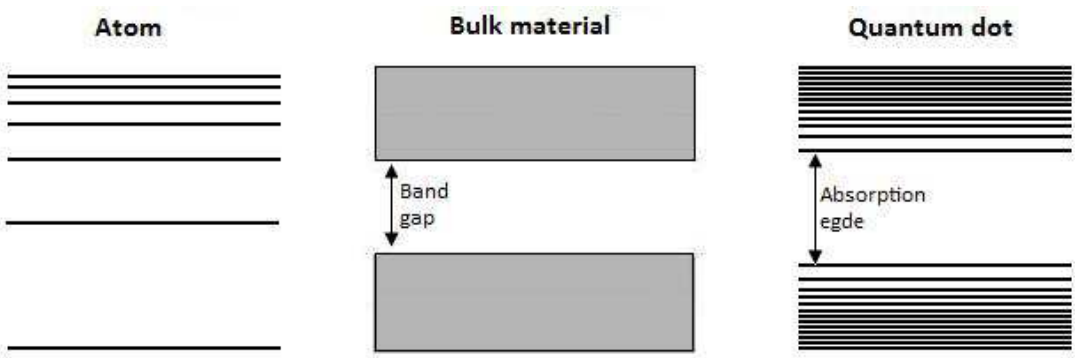

Figure 2.2: Difference in electronic structure between a single atom, the bulk and a quantum dot of the same material. The energy levels in bulk material form continuous bands, whereas in single atoms and in quantum dots, the energy levels remain discrete [9].

Due to an increasing surface-to-volume ratio, surface properties become more important with decreasing particle sizes. It is theoretically predicted that the surface morphology drastically affects the electronic charge distribution, and thus, the optical properties can be modified by surface-capping agents [10]. This is particularly true for silicon, which is known to be a material that is very sensitive to surface termination and usually requires a special treatment for passivation.

The quantum dot properties can be explained by the theory of quantum confinement which is related to the exciton Bohr radius, the natural separation distance between a hole and an electron in a given semiconductor. This effect can be observed when the diameter of a particle is of the same magnitude as the wavelength of the electron wave function. When the size of a nanoparticle reaches this limit, the energy spectrum turns to discrete, meaning that there is a small and finite separation between the energy levels, opposed to the continuous energy bands in the bulk material [8]. Particles with a size smaller than this limit are called quantum dots. As a result, the band gap becomes size dependent and there is a blue shift in optical illumination as the size of the particles decreases, i.e. the value for the band gap increases.

The difference in electronic structure for bulk material and quantum dots can also be explained with the theory about how energy bands form. When atoms of the same material come into close proximity, their orbitals overlap [11]. For every atom in the material, one molecular orbital is formed.

For bulk materials, which contain an infinite number of atoms, the distance between the single orbitals becomes infinitely small, and thus a continuous energy band is formed. In contrast, quantum dots contain so few atoms that the atomic energy levels remain discrete. The distance between the lowest and highest energy level increases as the number of atoms increases, leading to a wider energy band as shown in Figure 2.3. Since this is true for both the valence and the conduction band, it follows that the value of the band gap decreases as more atoms are introduced. This is illustrated in Figure 2.4.

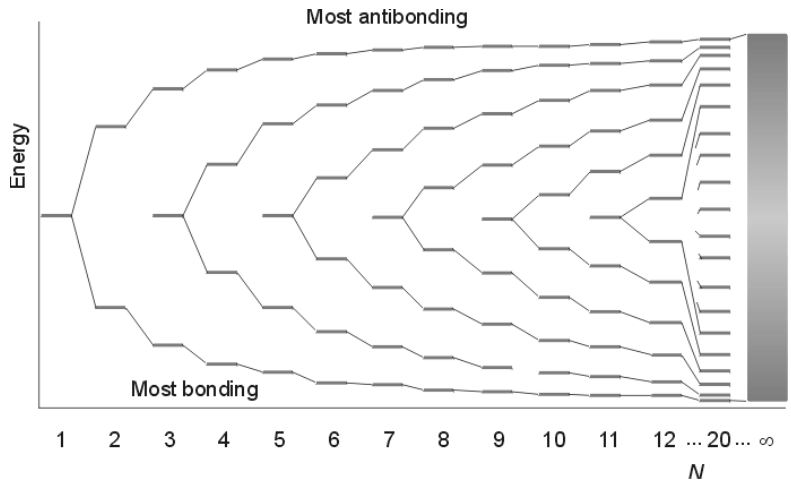

Figure 2.3: The orbitals belonging to the atoms in a solid material overlap and form energy bands. The width of the energy bands increases with increasing number of atoms [11].

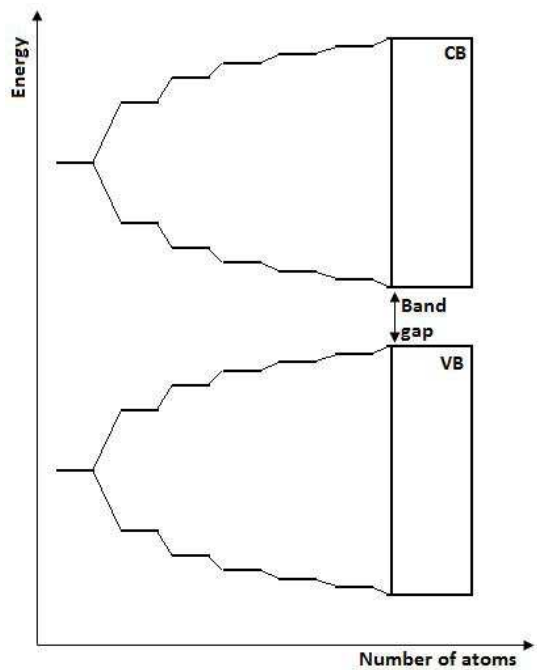

Figure 2.4: An illustration of how the band gap increases with decreasing number of atoms, i.e. with decreasing quantum dot size [9].

2.2.1. Quantum dots for solar cell applications

One of the major efficiency loss mechanisms leading to low energy conversion efficiencies of solar cells is the thermalisation of charge carriers by the absorption of high-energy photons. These losses can be reduced significantly if the incoming radiation is converted to wavelengths that can be better utilised by the solar cell. Quantum dot structures can be used to generate two lower energy photons from an incident photon with energy larger than twice the band gap of the solar cell. This principle is called down conversion and is the most realistic application of quantum dots to solar cells. The opposite can also be done for photons with a lower energy than the band gap by up conversion, which is the creation of one photon with higher energy than the band gap from two low-energy photons. Research of efficient down-conversion mechanisms is less advanced to date, however it is conceptually easy to imagine the inclusion of a down-converting luminescent species within the solar cell antireflection coating [12].

Quantum dots are characterised by very wide absorption spectra and narrow emission peaks, giving the possibility to transform a large part of the solar spectrum into nearly monochromatic light, suitable to the band gap of the solar cell. Combined with a high rate of impact ionisation because of the many discrete electronic states in quantum dots, this makes them efficient for down conversion layers. The principle of impact ionisation is illustrated in Figure 2.5.

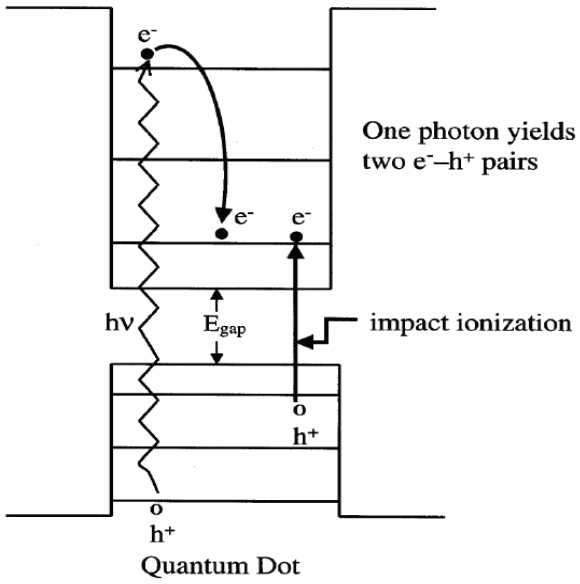

Figure 2.5: Illustration of impact ionisation. A high energy photon decays to a lower energy state upon creation of a second electron–hole pair [9].

Indirect band gap materials, such as silicon, show remarkable changes in their optical properties when the size of a crystallite is reduced to the nanoscale, since crystal momentum need not be conserved in a zero dimensional structure [10]. With decreasing dot size, there is spatial localisation of the electron and hole wavefunctions, and hence the indirect band gap of silicon becomes more direct. As the maximum of the valence band and the minimum of the conduction band approach each other with respect to momentum, the radiative lifetime decreases to nanosecond range since no longer a phonon is involved in the transition process. This enhances the rate for radiative

recombination, i.e. the recombination of an electron with a hole to produce a photon, and causes luminescence. Bulk silicon is basically an inefficient light emitter, whereas silicon nanostructures below the exciton Bohr radius emit light efficiently at room temperature [5]. However, it is complicated to interpret the photoluminescence spectrum of Si quantum dots because of the presence of both indirect and direct band gap transitions [13]. In silicon, this requires the physical dimensions of the quantum dots to be on the order of or less than the bulk exciton Bohr radius of 4 nm.

Some other properties that make Si very interesting for use in solar cells, are that silicon is the second most abundant material on the earth, is non-toxic and inexpensive, has good electronic properties and is the principal material for semiconductor devices [14]. The well-understood silicon chemistry makes it possible to update existing silicon-based devices to their corresponding nanostructured versions. Other advantages for Si are that the electrical conductivity can be controlled over a wide range, its oxidised state is a very good insulator and it also has superior chemical and mechanical properties.

2.2.2. Synthesis of Si quantum dots

Synthesis of silicon quantum dots is demanding and has been an object of thorough research during the recent years. There are many challenges related to the synthesis of Si quantum dots, among them control of particle size, size distribution, surface chemistry, crystallinity and optical properties. Control of the size is especially crucial since the properties of the material vary considerably with only small variations in particle size. Additionally, Si quantum dots are very air- and water sensitive, which is an additional challenge and requires that the syntheses take place under inert conditions. There are two main approaches to synthesise silicon quantum dots: "top-down" based on high-energy dispersing of bulk material, and "bottom-up" based on formation of nanoparticles from precursor molecules [15]. Several different routes are available, including both solid-state, gas-phase and solution phase methods. Each method has its own advantages and disadvantages with respect to the wanted properties. Wet chemical synthesis is the method utilised in this master thesis and will have the main focus in the following presentation. Electrochemically etching and some gasphase syntheses are other widely used synthesis methods and will be shortly presented to explain why wet chemical methods are chosen for the synthesis of quantum dots which are going to be used as down converters in solar cells. Other available synthesis methods of silicon quantum dots which will not be further presented here, are heterogeneous solution based reduction of silicon halides via Zintl salts, reduction through sodium by sonification, preparation under high pressure and temperature with hydrothermal synthesis and rapid methathesis reaction of sodium silicofluoride (Na_2SiF_6) with sodium azide (NaN_3) at 950−1000 °C [15-17].

Electrochemically etching

One possibility is to produce silicon nanoparticles by electrochemically etching. This can be done by ultrasonic dispersion of thin sections of porous silicon in a variety of organic solvents. The method has attracted much interest due to the simplicity of the preparation procedure. Another advantage with this synthesis is that water dispersible quantum dots capped with carboxylic acid and OH groups have been synthesised by this method [18],[19]. An illustration of the synthesis of Si quantum dots from porous silicon followed by the functionalisation with carboxylic acid is provided in Figure 2.6. The largest disadvantage by this synthesis method is that it is very difficult to achieve a narrow

size distribution. Thus, the optical properties of the quantum dots synthesised by this procedure are impossible to control, and they can not be utilised as effective down converters in solar cells.

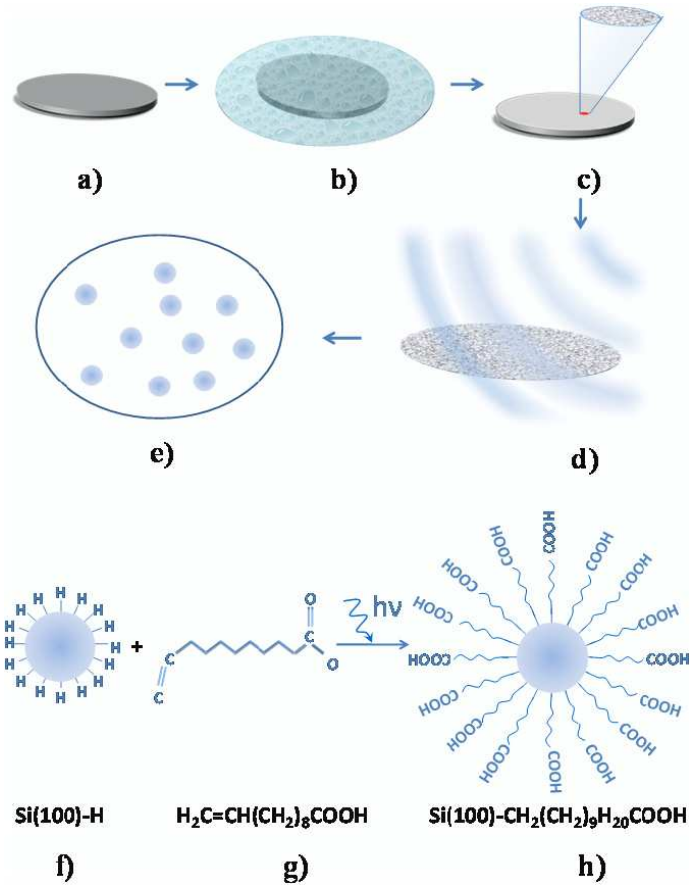

Figure 2.6: A silicon wafer **(a)** being electrochemically etched in HF/ethanol solution **(b)** to produce porous silicon **(c)**. Porous silicon is then sonicated **(d)** in toluene/ethanol solution to obtain Si nanocrystals **(e)**. The carboxyl-acid terminated monolayer on the surface of the nanoparticles **(h)** can be achieved through the photochemical hydrosilylation of undecylenic acid **(g)** with a hydrogen-terminated Si (100) surface **(f)** of the Si quantum dots [18].

Gasphase synthesis

Different gasphase methods are also possible for the preparation of nanoparticles. One of them is high energy decomposition of silane in a gas flow reactor, followed by etching with HF/HNO_3 in water to reduce the nanoparticle size. By controlling the flow rates and the laser power, the nanoparticle sizes can be controlled to a certain extent. Another gasphase synthesis is the co-sputtering technique, where two targets (usually pure silicon and quartz) are simultaneously exposed to ions, producing a mixed layer of silicon and oxide. Excess silicon is then used to create Si nanocrystals after high temperature annealing. The size distribution can be controlled by adjusting the excess silicon volume content. These gasphase techniques produce Si nanoparticles with a narrow size distribution, but it is impossible to produce nanoparticles on a large scale, to manipulate the surface of the particles and hence, to obtain water dispersible quantum dots which can be incorporated into silica thin films for solar cell applications. Another consequence of the lack of ability to modify the nanoparticle's surfaces, is that it will be difficult to avoid agglomeration since

the formed particles are not charged and are not protected against agglomeration by proper capping agents.

Wet chemical synthesis

Methods based on wet chemistry have the potential of high yield, size control, manipulation of the surface and crystallinity. Quantum dots synthesised via solution-phase reduction of silicon salts also show strong quantum confinement [13]. Wet chemical techniques are, because of the simple apparatus required, well suited for upscaling to industrial processes. The solution phase processes allow capping of quantum dots at early stages of their formation, thus preventing agglomeration that results in rather narrow particle size distributions.

Control of the size and the ability to manipulate the surface were the limiting factors for the synthesis of quantum dots via electrochemically etching and from the gasphase, respectively. These are both overcome in most wet chemical methods. In general, the sizes of Si quantum dots prepared by wet chemical reduction methods can be controlled by adjusting the concentration of reduction agent, by changing the balance between growth and nucleation speeds through the reaction temperature, by the choice of surface ligands or by adjusting the reaction time. Most of the wet chemical methods presented here use silicon tetrachloride as the precursor, and the resulting quantum dots are initially terminated with chlorine atoms that allow a lot of possible options for further functionalisation or stabilisation.

One possible wet chemical method is the use of inverse micelles (water droplets in oil, stabilised by a surfactant). Inverse micelles form when surfactants with hydrophilic headgroups and hydrophobic tails are in hydrophobic organic solvents with a low water content at concentrations exceeding the critical micelle concentration. Various chemical methods can be carried out inside the micelle to synthesise nanoparticles, like reduction of silicon halides with lithium or sodium naphthalide and $LiAlH_4$ [17]. The growth above nanometer scale is hindered by the surfactant molecules and thus, the size can be easily controlled. Very small particles with narrow size distributions have been obtained by the utilisation of inverse micelles. Tilley and co-workers prepared monodisperse silicon nanoparticles in size of 1.8 ± 0.2 nm via reduction of $SiCl_4$ with $LiAlH_4$ in inverse micelles using tetraoctyl ammonium bromide as a surfactant [5]. The same system without inverse micelles present led to a large size distribution of the nanoparticles [20]. However, the shape of the quantum dots is difficult to control with this method, and the synthesised particles are typically only partly functionalised [20].

Alkaline metals have been widely used as reduction agents. One of the first procedures investigated was the reduction with sodium metal in a nonpolar organic solvent at high temperature (385 °C) and high pressure (> 100 atm) [5]. Most of the later syntheses are performed at room temperature and ambient pressure, but use some kind of complexant to make the alkaline metal soluble in an organic solvent. For instance, Kauzlarich et al. used sodium naphthalide in aprotic polar organic solvents such as glyme to reduce silicon tetrachloride [21]. Sodium naphthalide is a soluble one-electron reductant, consisting of sodium ions coordinated with ether molecules and paired with naphthalene radicals. They demonstrated size and surface chemistry control, but the size distribution was found to be broad. A broad size distribution is not wanted for quantum dots which are going to be used as down converters in solar cells because this makes it impossible to characterise the optical properties. To change the size distribution, one has to take nucleation theory into consideration.

The formation of crystals is generally considered to follow a process consisting of three stages: pre-nucleation stage (I), nucleation stage (II), and the growth stage (III) [17]. The nucleation stage is very important to increase the yield during nanocrystal production. Together with the growth stage, the nucleation stage is also critical to obtain a narrow size distribution [22]. A fast nucleation process would be accomplished with higher reactivity, and growth control would be achievable with less electronegative reduction agent. Since the dissociation constant of potassium naphthalide in tetrahydrofuran is higher than of sodium naphthalide [17], it can be deduced that potassium naphthalide will be more soluble in glyme than sodium naphthalide and thus providing faster homogeneous nucleation. On the basis of this, Balci et al. explored the sodium naphthalide route further, using potassium naphthalide instead of sodium naphthalide as the reduction agent. Crystalline Si quantum dots with a higher yield and a with narrower size distribution (3.1 nm ± 0.6 nm) [17] were obtained. A tunable size for the quantum dots prepared by this synthesis was observed as a function of reaction time and concentration; as the concentration of the reduction agent decreases, the particle size increases [17].

Other very powerful reducing agents possible for the wet chemical reduction of silicon halides are alkalides and electrides. In solution, they are able to reduce nearly all metallic cations to form nanoscale metal particles [23]. The unique feature of alkalides and electrides is the ability to produce stoichiometric crystalline salts in which trapped electrons (e^-) or alkali-metal anions (M^-) serve as the anions [24]. This is achieved by using powerful cation complexants such as crown ethers, to protect the alkali-metal cation from reduction by M^- or e^-. Crown ethers are organic ring compounds, typically larger than 12 atoms in the cycle, that contain oxygen, nitrogen, sulphur, or other heteroatoms [25]. Crown ethers are named by first giving the total number of atoms in the ring, followed by the word crown and at last the number of oxygen atoms. The ability for crown ethers to complex cations is explained by their electronic distribution. The electrostatic potential surface consists of two regions: an electron-rich interior associated with the oxygens and a hydrocarbon-like exterior associated with the CH_2 groups, an illustration of this is provided in Figure 2.7. Ions of a particular size can find their place within the internal cavity of a specific crown ether. This results in strongly complexed cations, masked by nonpolar CH_2 groups which permit the complex to dissolve in nonpolar solvents.

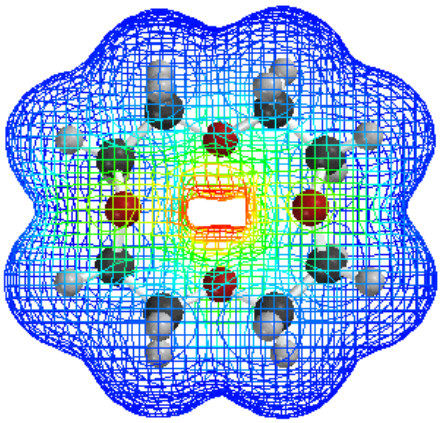

Figure 2.7: An electrostatic potential map of 12−crown−4. The region of highest electron density (red) is associated with the negatively polarised oxygens and their lone pairs. The outer periphery of

the crown ether (blue) is relatively nonpolar (hydrocarbon-like) and causes the molecule to be soluble in nonpolar solvents [26].

The preparation of concentrated alkali metal solutions can be accomplished by addition of a crown ether or a cryptand to an aprotic solvent. There is direct contact of the metal surface with the crown ether, the crown ether is adsorbed on the metal surface and the process of metal dissolution can be roughly described by the following equations [27], where M is the alkali metal, e.g. potassium or sodium, and L is the complexant, e.g. 15-crown-5:

$$L + M(s) \leftrightarrow M^{+}(L) + e^{-}\ (solv) \quad \textbf{(2.1)}$$

$$e^{-} + M(s) \leftrightarrow M^{-} \quad \textbf{(2.2)}$$

As shown in these equations, alkalides and electrides form M^{-} and solvated e^{-} when dissolved in a nonreducible solvent. The removal of M^{+} from the metal lattice is normally a relatively slow process involving a potential energy barrier which is reduced by the adsorption of a ligand and formation of a soluble $M^{+}(L)$ complex. Thus, the resulting solution contains mainly crowned metal cations and metal anions, since most of the solvated electrons are used for the formation of metal anions. The process is strongly dependent on temperature, contact time of a ligand with metal surface, nature of ligand, etc. Playing with these factors one can control the process of metal dissolution and eventually the composition of the final solution. The stability of the solution is strongly affected by temperature. Alkalides and electrides are air sensitive and thermally unstable; at higher temperatures (above 10−15 °C) the concentration of M^{-} tends to decrease and the decomposition of the ligand occurs [27]. Hence, the synthesis must be done at low temperatures in the absence of air and moisture. The type of ligand and solvent used also affect the stability of the solution. It has been shown that tetrahydrofuran (THF) produces the most stable system when crown ethers are used as the ligand [27].

The major challenges for the method based on reduction of silicon halides by use of alkalides are related to the solubility and solution stability of the precursor compounds, the stability of the alkalide solution, and the removal of byproducts of the reduction reaction. Silicon quantum dots have not yet been synthesised in large amounts by alkalide syntheses, but research is currently going on. The particle sizes become smaller when more dilute solutions are used [24]. A major advantage of this method for producing nanoscale metal particles in nonaqueous solvents is that the reactions occur rapidly with homogeneous solutions. This has permitted formation of intermetallic compounds or alloys when two metal salts are reduced simultaneously [28]. The less reactive noble metals Au, Pt etc. are easiest to isolate and characterise.

2.2.3. Surface functionalisation of Si quantum dots

Lack of sufficient stability and difficulty in surface manipulation for functionality are barriers that to a large extent hinder the practical application of silicon quantum dots. Because of their air-sensitivity, the surface of the nanoparticles has to be passivated by some kind of capping ligands to enhance their stability, otherwise they will experience a rapid and efficient surface oxidation. Besides chemical stability towards oxidation and Ostwald ripening, passivation of the silicon quantum dots surfaces reduces defect states at surfaces caused by dangling bonds. A non-dense capping can also lead to agglomeration of quantum dots because of non-optimal surface chemistry. Basically, just by slightly changing the polarity of the terminal group, it is possible to tune and adjust the solubility of quantum

dots in a wide variety of solvents for specific applications. A suitable capping ligand should also have a negligible effect on the optical properties of the silicon core, i.e. the effective band gap should be relatively unperturbed by the surface capping.

The functionalisation process is often multistepped, since it is then easier to control the target functionality [29]. When attaching functional molecules to the surface of silicon quantum dots, some of the moleceules tend to have more than one reactive moiety. For example, molecules with an oxygen containing functional group such as carboxylic group or hydroxyl group and a double bond may preferentially react with the oxygen functionality, not the carbon double bond. This can be overcome by more than one step in the functionalisation process.

Silanisation

Silanisation has been widely used to alter the surface characteristics of various nanoparticles, such as CdSe and Au nanoparticles but has also been used for Si [30]. An illustration of the structure on the surface of a silanised quantum dot is given in Figure 2.8. Different terminating groups are illustrated as Y's.

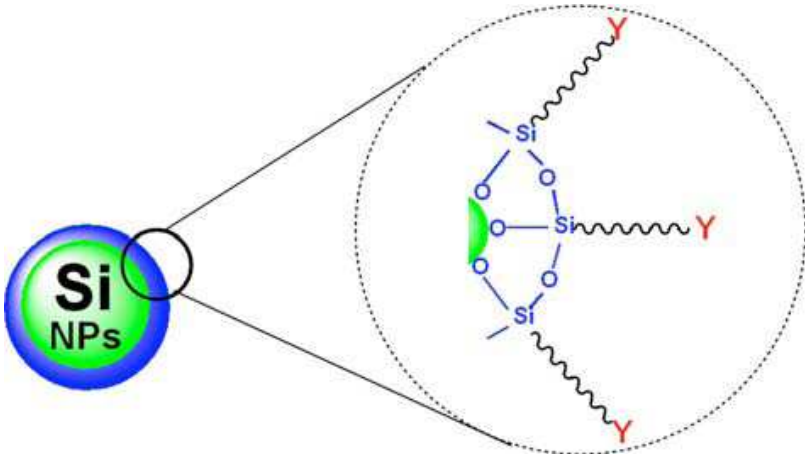

Figure 2.8: Illustration of the silicon core-silane shell structure of a silanised Si nanoparticle [30].

Silanised silicon quantum dots are often made from alkoxy-coated quantum dots, and various kinds of chlorosilanes can be used as the capping agent to obtain different terminating groups. In Figure 2.9 is shown a flow sheet of three different silanisation routes for the silanisation of silicon quantum dots resulting in different functionalisations. Silanisation-terminated silicon quantum dots afford the potential of easy manipulation for more complex functionalisations as the functionality can be tailored by choosing appropriate chlorosilanes.

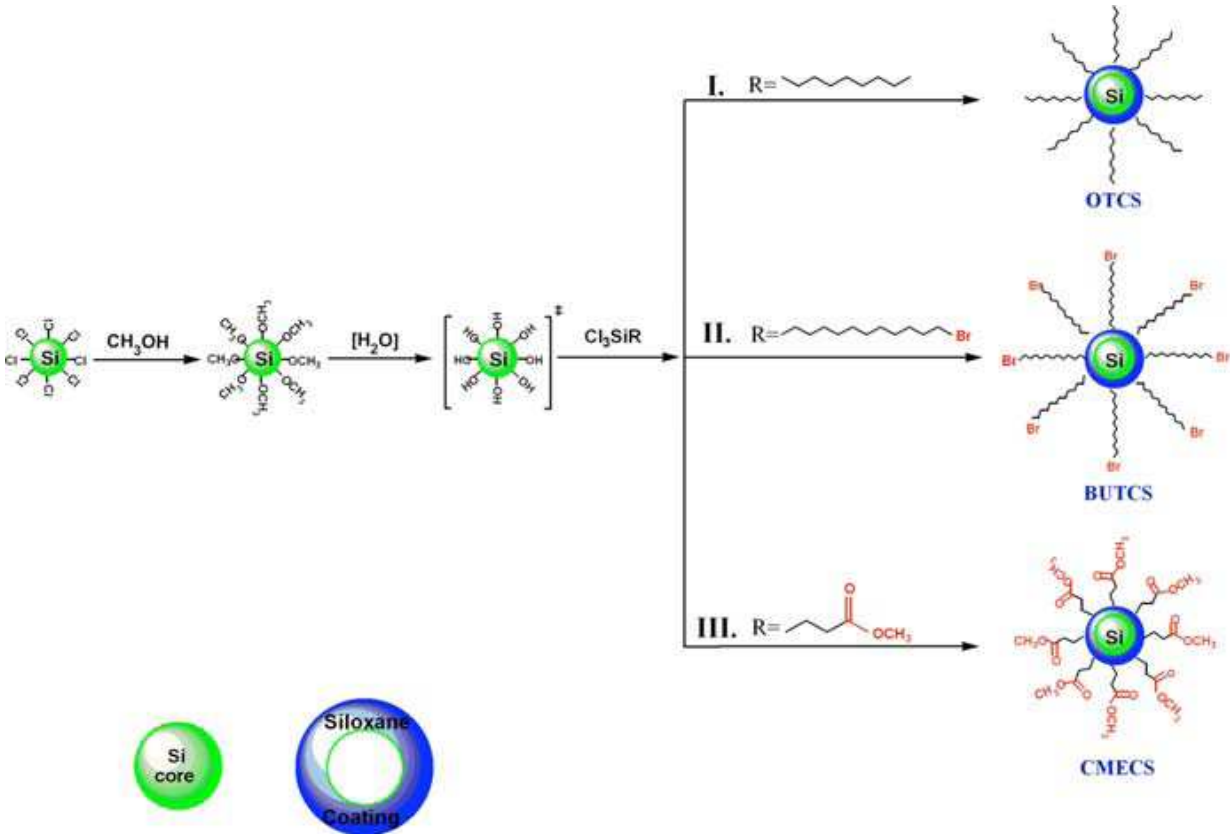

Figure 2.9: Three different silanisation routes for different termination of silicon quantum dots, via methoxy and hydroxyl coated quantum dots. The final quantum dots shown here are (from top to bottom) alkyl-terminated, bromo-terminated and ester-terminated [30].

A siloxane coat on the silicon quantum dot enhances the particle stability significantly and maintains the crystallinity of the quantum dot [30]. The photoluminescent properties of silanised Si nanoparticles remain approximately constant for two months, which is a very long time compared to silicon quantum dots capped with other ligands [31]. In addition to type of capping agent, the stability also depends on the level of surface coverage. Insufficient coverage on the particle surface provides sites for moisture or air to attack and replace either residual Si-Cl bonds or Si-OR bonds. With a dense layer, the stability of silanised silicon nanoparticles can be remarkably improved, by up to years.

Water dispersible quantum dots

Water dispersible quantum dots are very interesting for the application of quantum dots in solar cells because the quantum dots can then be incorporated in films made for instance by sol-gel method. Water dispersible quantum dots are also useful for other applications, the most important is probably the use in biomedical applications. In particular, silicon is a common trace element in biological systems and is naturally absorbed and extracted by a number of different tissues. Thus, silicon quantum dots have a high biocompatibility and low toxicity and are preferable over quantum dots containing for instance CdSe for use in biomedical applications ranging from contrast agents to biological labelling.

There have been many challenges in creating stable, water-dispersible quantum dots, including instability of photoluminescence due to oxidation in an aqueous environment and difficulty in attaching hydrophilic molecules to silicon surfaces without inducing oxidation. Quantum dots could be made directly in water but often have narrow available size ranges and wide size distribution [32]. Hence a challenge is how to make the high-quality hydrophobic quantum dots soluble in water and also retain their expedient optical properties.

For the wet-chemical synthesis of silicon quantum dots, the most important technique is to reduce silicon tetrachloride with some reduction agent. Silicon tetrachloride is a classic electrophile in its reactivity and reacts violently with water because of silicon's relatively large size and empty 3d orbitals that allows water molecules to attack. Equation 2.3 shows the reaction of silicon tetrachloride with water, giving white solid silicon dioxide and steamy fumes of HCl. Liquid $SiCl_4$ fumes in moist air for this reason - it is reacting with water vapour in the air.

$$SiCl_4 + H_2O \rightarrow SiO_2 + 4HCl \qquad \textbf{(2.3)}$$

Because of this, silicon quantum dots prepared from $SiCl_4$ have to be prepared in organic solutions. However, quantum dots synthesised in organic solvents are normally insoluble in water. Water dispersibility of quantum dots can be tuned via substituents on the surface, as long as the optical properties and other relevant features are not affected by the substitution. The dispersibility of quantum dots is controlled by the chemical nature of the surface coating. Terminating groups like for instance $-COOH$ or $-NH_2$ will make quantum dots water soluble.

Different approaches have been made to solubilise hydrophobic quantum dots in aqueous solvents. One approach is to replace the hydrophobic ligands of quantum dots synthesised in organic solutions by some water-soluble bifunctional molecules in which one end connects to quantum dot surface atoms and the other end is hydrophilic. However, ligand exchange inevitably alters the chemical and physical states of the quantum dot surface atoms and in most cases dramatically decreases the quantum efficiency of the quantum dots. Another possibility is to use molecules which have both hydrophilic and hydrophobic ends. They could encapsulate quantum dots by forming oil-in-water micelles through hydrophobic interaction between their hydrophobic ends and the surface ligands of the quantum dots and provide water-solubility via hydrophilic exterior ends [32]. This strategy of using amphiphilic polymers is generally superior to the ligand exchange, because (a) there is no direct interaction with the quantum dot surface atoms and therefore can preserve the original quantum efficiency, (b) the polymer's large number of hydrophobic side chains strengthens the hydrophobic interaction to form more stable water-soluble quantum dots, and (c) these polymers are generally commercially available with low prices.

An alternative route embeds the nanoparticles in a polymerised silica shell in a procedure similar to the one illustrated in Figure 2.9, but with a thicker silica layer and water soluble terminating groups [33]. Such silica-coated nanocrystals have a large stability in aqueous solutions and are easy to handle. The procedures to make a controllable silica layer around hydrophobic quantum dots are relatively complicated involving more steps and work comparing to the other strategies. Another limit is that silica coating needs to be carried out under dilute conditions, which is not suitable for large quantity production. However, silica encapsulation produces stable particles.

2.3. Deposition of quantum dots on solid substrates

Thin organic films one molecule in thickness (a monolayer) are the source of high expectations as being useful components in many practical and commercial applications such as sensors, detectors, displays and electronic circuit components. Amphiphiles or surfactants are the most common monolayer-forming materials and the simplest molecules to deposit into complex yet often predictable structures. The molecules will orient themselves at the interface between a solid and a liquid phase as they are deposited to minimise their free energy. This is illustrated in Figure 2.10. Molecules like amphiphiles or surfactants will all be aligned the same way on for instance a hydrophilic substrate. An organic thin film can be deposited on a solid substrate by various techniques such as thermal evaporation, sputtering, electrodeposition, molecular beam epitaxy, adsorption from solution, Langmuir-Blodgett (LB) technique, self assembly etc.

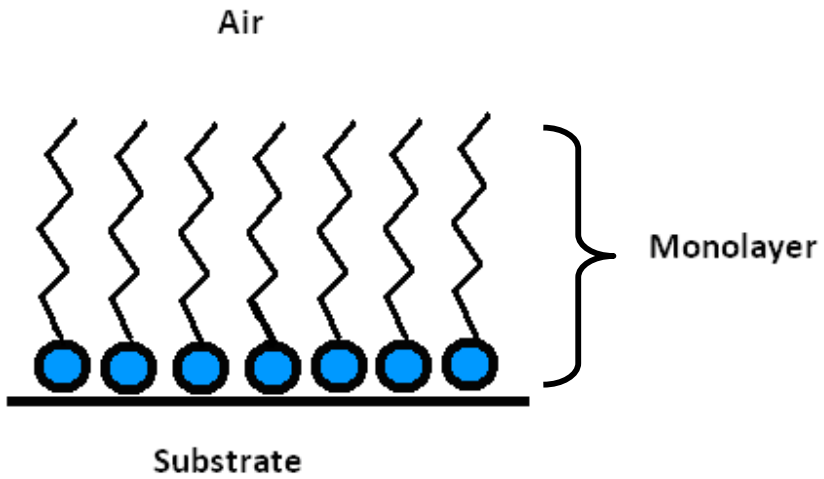

Figure 2.10: Illustration of a monolayer of amphiphilic molecules on a solid substrate. All molecules are oriented the same way because of the affinity towards the substrate of one of their ends.

A similar fabrication of nanoparticles into ordered morphologies is also possible when the nanoparticles are functionalised for instance with hydrophobic groups and deposited on a hydrophobic substrate. If quantum dots can be deposited into an ordered structure on a solid substrate, it would be very good for the application as down converting layers for solar cells. If nanoparticles are deposited and a well ordered structure is obtained, novel physical properties have been observed. This is a result of the interactions between particles [34]. Such collective properties are neither the properties of the individual particles, nor those of the bulk material, and they are favoured by the good organisation of the nanomaterial. It is important that these highly ordered structures are reproducible to make use of them. In spite of considerable efforts, it is still a great challenge for many research groups to develop a simple and reliable process to fabricate well-organised two dimensional (2D) nanoparticle structures which offer control over coverage and the spatial distribution of the particles on the surface. Whether an ordered structure will form or not is determined by the interactions between the particles, and will be described in the next section. In most cases, ordered monolayers will not form without any form of pre-treatment, like for instance charging up the nanoparticle surface or modifying the substrate with a monolayer [35].

2.3.1. Particle interactions

The assembly of nanoscale building blocks into macroscopic structures is driven by the interactions of particles with other particles, substrate, solvent, etc. Entropy can actually be the driving force for the ordering of particles because of the increased local free space available for each sphere in the ordered lattice compared to the disordered state [36]. In an ensemble of non-interacting particles entropy can be a sole driving force for the transition from disordered into long-range ordered state. However, semiconductor nanoparticles usually exhibit strong interparticle electrostatic interactions which should also be taken into consideration when predicting the ordering of particles into structures. When the dispersed particles are on the nanoscale, the surface forces dominate over other forces [37]. There are always attractive van der Waals forces acting between identical particles suspended in a medium. Origin of the van der Waals interactions lies in the mutual electro-magnetic influence of electric dipoles, both permanent and temporarily induced, present in atoms and molecules.

Repulsive forces act against the attracting forces, and the sum of the forces determine whether the particles will agglomerate or remain dispersed in the liquid. The main contributions to repulsive forces between nanoparticles will come from steric and electrostatic effects. The sign and the magnitude of these forces depend on the material and the solvent properties. The stability of quantum dots dispersed in a liquid depends on the force balance in the dispersion and the interactions can be modulated by changing the solvent properties and strength of the individual surface force component. Quantum dots without any repulsive barrier will stick together, but a sufficient stabilisation can often be obtained by ligands that can stabilise the surface of the nanoparticles. Stabilisation by control of the repulsive forces between particles is well known from ceramic engineering [38], and the same techniques apply to nanoparticles dispersed in a liquid. Steric stabilisation involves addition of chainlike organic molecules that are adsorbed onto the particles to provide a buffer zone around each particle. This is illustrated in Figure 2.11. The other most important approach for holding particles apart in a dispersion is to utilise electrostatic repulsion, which involves buildup of charges of the same polarity on all the particles so that they repel each other. Agglomerates with only weak interactions between them can be separated simply by ultrasonication.

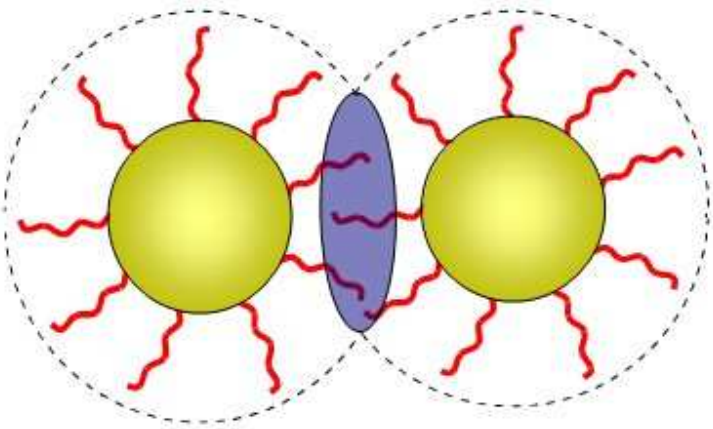

Figure 2.11: Adsorption of chain polymers onto the surface of nanoparticles to provide dispersion by steric hindrance.

2.3.2. Deposition by solvent evaporation

In the case of nanoparticles, the most popular and easiest approach to form ordered superstructures is to deposit a solution of nanomaterials on a flat solid substrate followed by gradual increase of particle concentration by solvent evaporation. Solvent evaporation is an extremely simple route to intriguing structures. However, the resulting structures are often randomly organised without controlled regularity. The process is strongly affected by the nature of the nanoparticles, solvent, substrate, wetting properties, nanoparticle concentration, temperature etc. If solvent and substrate show good wetting properties, dilute solutions of monodisperse nanoparticles can produce long-range ordered 2D superlattices as shown in Figure 2.12 [36]. Such arrays typically show hexagonal packing corresponding to maximal packing density of nanoparticles in 2D and the strongest van der Waals interactions. The spacing between crystallites in the monolayer is determined by the length of the surfactant molecules and can be adjusted by tailoring the capping ligands.

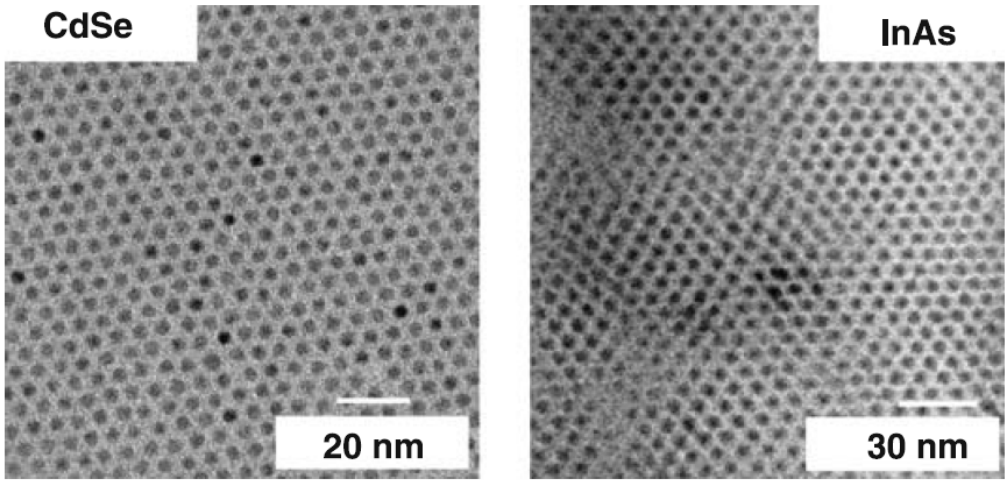

Figure 2.12: Examples of two-dimensional ordered arrays of semiconductor nanocrystals viewed in TEM [36].

The relatively weak attractions between nanocrystals become more important as the solvent evaporates and the nanoparticles become less mobile [39]. Dynamics of the solvent evaporation is very important and can be varied by changing the temperature and/or solvent. Generally, slow growth (i.e. slow evaporation) is important to obtain highly ordered structures. The arriving particles must have enough energy and time to find equilibrium sites in the growing structure. If new nanoparticles are arriving too fast or stick together irreversibly, they will land on top of each other and block the diffusion pathways for other particles. This will lead to the formation of an amorphous solid. If nanoparticles are poorly soluble in a given solvent due to insufficient sterical repulsion or lack capping ligands on the nanocrystal surface, no long-range ordered arrays are expected. Also, if repulsive forces dominate particle-particle interactions and these interactions are weak, there is no sufficient energy driving the formation of an ordered lattice.

3. Experimental

The first goal of this work was to produce water soluble silicon quantum dots wet chemically. The next part involved deposition of quantum dots onto silicon substrates, directly from the quantum dot dispersion. The synthesis of the quantum dots, the deposition of the silicon quantum dots by solvent evaporation and by spin coating, as well as the STEM and SEM characterisation was performed in NTNU Nanolab (clean room class 7) at room temperature.

3.1. Synthesis of Si quantum dots

Three different methods were utilised for the synthesis of the silicon quantum dots. These are described below and were based on reduction of silicon tetrachloride with different reduction agents, i.e. potassium naphthalide, sodium cyclopentadiene and the alkalide of potassium. A Schlenk line with argon gas was used in the syntheses to assure complete inert conditions, which were necessary because silicon quantum dots are very air- and water-sensitive. An image of the Schlenk line in NTNU Nanolab is provided in Figure 3.1.

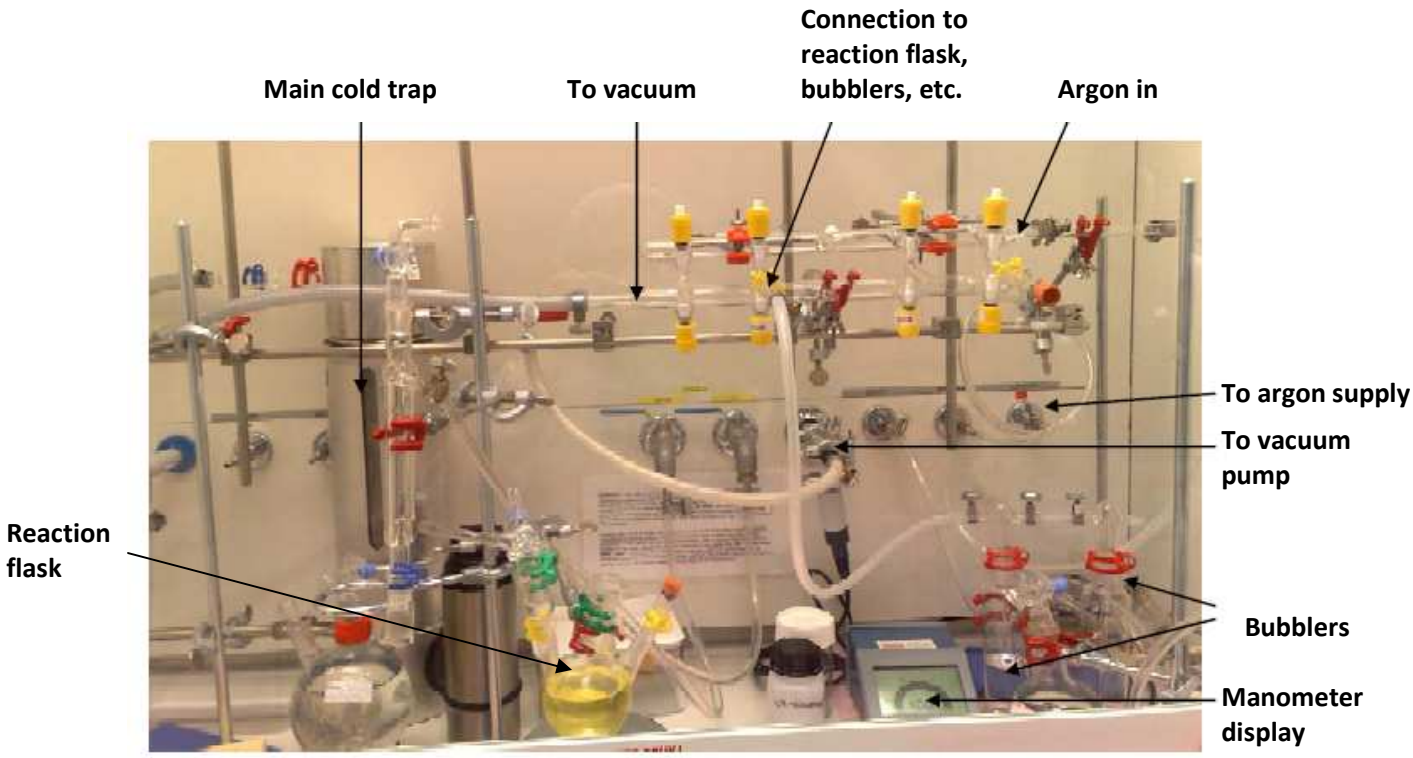

Figure 3.1: Schlenk line with argon gas in NTNU nanolab.

The Schlenk system consisted of a dual manifold with several ports. One manifold was connected to a source of purified argon gas. The gas was further purified by a triple trap gas purifier (Sigma Aldrich Supelco, SU 861026) containing different oxides, primarily aluminium oxide (80−90 %) and copper oxide (10−14 %) for the removal of hydrocarbons, moisture and oxygen below the ppm level. The other manifold was connected to a vacuum pump with an obtainable pressure of 10^{-3} mbar.

Special stopcocks allowed for vacuum or inert gas to be selected without the need for placing the sample on a separate line. The inert gas line was vented through an oil bubbler, while solvent vapours and gaseous reaction products were prevented from contaminating the vacuum pump through a liquid nitrogen cold trap. The high vacuum was used to remove the solvent from the reaction flasks by evacuation. For the removal of solvents, an extra cold trap with nitrogen was mounted between the line and the reaction flask and the reaction flask was evacuated. All chemicals were added to the Schlenk system using the counter flow technique, in which a flow of inert gas out of one of the reaction flask openings made it possible to carefully insert a syringe with a chemical into the opening and inject the chemical without introducing outside air into the reaction flask. All liquids were transferred via gas-tight syringes (not lubricated with silicon grease) which were first filled and emptied with argon gas at least three times.

When attaching empty equipment containing air to the line, the equipment was evacuated until a stable low pressure (at least < 10^{-2} mbar) was obtained, before filling it with inert gas. This procedure was repeated twice. Carbon grease was used instead of ordinary silicon grease to avoid contamination and the syringe tips were cleaned with ethanol before use to remove any lubrication. The solvents were dried with molecular sieves (3 Å, Sigma Aldrich) and degassed before use to remove the dissolved gases. The degassing was done by immersing the round bottom flask in liquid nitrogen until the solvent was completely frozen. The flask was evacuated for three minutes, and then remelted in a water bath at 30 °C. This procedure was repeated until no more gas bubbles escaped from the solvent during the heating. The other chemicals were used as supplied, without further purification.

3.1.1. A – Potassium naphthalide synthesis

One of the procedures to make silicon quantum dots was a synthesis route developed by Balci et al., based on reduction of silicon tetrachloride with potassium naphthalide [17]. Potassium naphthalide is prepared by stirring potassium metal with naphthalene in a polar solvent, e.g. dimethoxyethane, hereafter called glyme. The reaction between silicon tetrachloride and potassium naphthalide resulting in chloride capped silicon quantum dots is given in Equation 3.1. The amount of the chemicals used in the synthesis, as well as the purity and the supplier of each chemical are listed in Table 3.1.

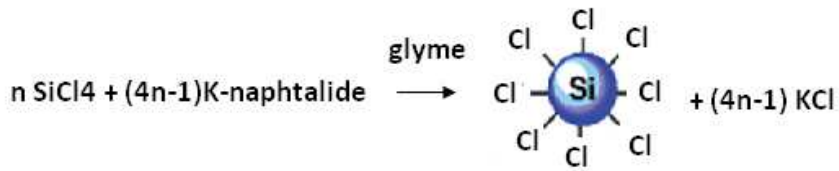

(3.1)

Table 3.1: Amount, supplier and purity of the reactants which were used in the potassium naphthalide synthesis of the silicon quantum dots.

Chemical	Amount	Supplier	Purity [%]
Potassium	0.182 g	Sigma Aldrich	98
Naphthalene	0.605 g	Sigma Aldrich	> 99
1,2-dimethoxyethane	10 ml (1st) + 30 ml (2nd)	Sigma Aldrich	99.5
Silicon tetrachloride	0.12 ml	Sigma Aldrich	99.998

First, potassium was weighed out in an argon glove box. The potassium was put into a two-neck round bottom flask (25 ml) together with naphthalene and glyme (1st portion). This solution was stirred with a magnetic stirrer overnight. The next day, a solution of $SiCl_4$ in glyme (2nd portion) was made in a new reaction flask (100 ml), and the potassium naphthalide solution was rapidly added. A dark brown suspension which turned to yellow after about 5 seconds was observed, and this solution was stirred for another 1.5 hour. Any capping agent could subsequently be added to the quantum dot dispersion.

3.1.2. B − Sodium Cyclopentadiene synthesis

A similar synthesis method was based on using sodium cyclopentadiene as the reduction agent. Commercially available sodium cyclopentadiene from Sigma Aldrich was used. The reaction between sodium cyclopentadiene and silicon tetrachloride yielding chloride capped Si quantum dots is given in Equation 3.2. The amount, supplier and the purity of each chemical used in the synthesis are given in Table 3.2. First, glyme was transferred to a two-necked round bottom flask together with a magnetic stirrer. Silicon tetrachloride and sodium cycolopentadiene were after the outgassing added to the reaction flask and stirred, and the transparent solution immediately turned to brown. After two hours of stirring, the chemical for functionalisation was added and the dispersion was stirred overnight.

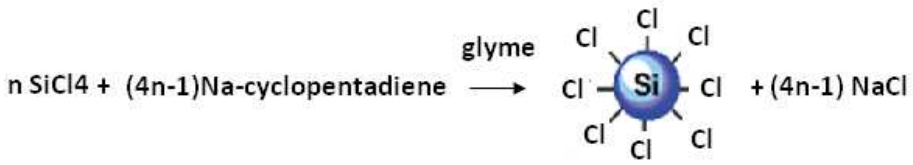

(3.2)

Table 3.2: Amount, supplier and purity of the reactants used in the silicon quantum dot synthesis, when using sodium cyclopentadiene to reduce silicon tetrachloride.

Chemical	Amount [ml]	Supplier	Purity/ concentration
1,2-dimethoxyethane	40	Sigma Aldrich	99.5 %
Silicon tetrachloride	0.15	Sigma Aldrich	99.998 %
Sodium cyclopentadiene	2.4	Sigma Aldrich	2.0 M

3.1.3. C − Alkalide synthesis

The last synthesis route utilised for producing Si quantum dots was a synthesis based on dissolving potassium with the help of crown ethers to form potasside, to reduce silicon tetrachloride. Potasside is the alkalide of potassium. The reaction which yields chloride capped Si quantum dots is shown in Equation 3.3. The amount, manufacturer and purity of the chemicals used in this synthesis are listed in Table 3.3.

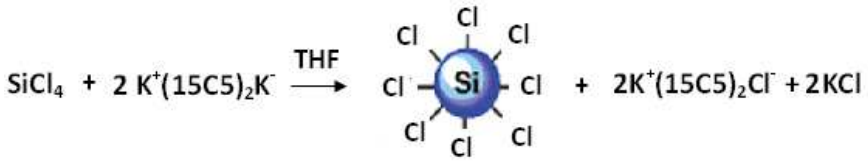

(3.3)

Table 3.3: Amount, supplier and purity of the reactants used in the silicon quantum dot synthesis, using the alkalide of potassium to reduce silicon tetrachloride.

Chemical	Amount	Supplier	Purity [%]
Potassium	0.195 g	Sigma Aldrich	98
15-Crown-5	1 ml	Sigma Aldrich	98
Tetrahydrofuran	20 ml + 20 ml	Sigma Aldrich	> 99.9
Silicon tetrachloride	0.143 ml	Sigma Aldrich	99.998

The three reaction flasks used in the synthesis were cleaned and heated at 150 °C overnight, followed by cooling in an argon glove box. Potassium was weighed out in an argon glove box and put into a round bottom flask (25 ml). To another round bottom flask was 15-crown-5 transferred. A magnetic stirrer was introduced to all the three round bottom flasks before they were closed with septa and taken out of the glove box again. Equal amounts of tetrahydrofuran (THF) were added to the flask with the crown ether and to the empty round bottom flask. Then, the solution of THF and 15-Crown-5 ether was transferred to the flask with the potassium and stirred for one hour. The colour of the solution first turned to light yellow and changed to dark blue as the potassium dissolved. Silicon tetrachloride was added to the round bottom flask with only THF. Both flasks were cooled in an ice bath until the temperature had equalised (after about twenty minutes), and the solution with silicon tetrachloride was transferred to the other reaction flask. The dark blue colour immediately turned to orange. This solution was then stirred for 45 minutes, before the capping agent could be added.

3.2. Functionalisation of Si quantum dots

Octoxy capped silicon quantum dots were previously investigated quite extensively by Balci et al. [17], synthesised via reduction of silicon tetrachloride with potassium naphthalide. Silicon quantum dots with methoxy capping and quantum dots silanised with octyltrichlorosilane have previously been synthesised here at the Department of Materials Science and Engineering, synthesised via the potassium naphthalide route [6]. However, water soluble silicon quantum dots have not yet been synthesised by this method.

New capping agents were investigated in this work in order to achieve water solubility of the quantum dots. Different chemicals were added for functionalisation, according to the procedures described below. An overview of the syntheses performed and the cappings investigated is given in Table 3.4. The syntheses are named according to synthesis route and functionalisation, where A is the K-naphthalide synthesis, B is the Na-cyclopentadiene synthesis and C the alkalide synthesis. Numbers represent the functionalisation, 1 is octoxy capping, 2 is pentenoxy capping, 3 is capping with acrylic acid and 4 is ethanolamine capping. When the terminating double bond was oxidised with water, this is marked with (ox) following the name of the product. When more parallels were done, this is marked with (a) and (b). These codes will be used for further reference.

Table 3.4: Overview over the different syntheses performed and the corresponding functionalisations. Each product is given a code for further reference.

Product	Synthesis route	Functionalisation
A−1	K-naphthalide	Octanol
A−2	K-naphthalide	4-penten-1-ol
A−2 (ox)	K-naphthalide	Ox 4-penten-1-ol
B−2 (ox)	Na-cyclopentadiene	Ox 4-penten-1-ol
C−1	Alkalide	Octanol
C−3	Alkalide	Acrylic acid
C−3 (ox)	Alkalide	Ox acrylic acid
C−4 (a)	Alkalide	Ethanolamine
C−4 (b)	Alkalide	Ethanolamine

An excess of all the capping ligands was added, corresponding to approximately five times the stoichiometric amount that should react with silicon tetrachloride. The amounts, the supplier and the purity are listed in Table 3.5. For each capping ligand, the respective amount was added and the solution was stirred for 12 hours for complete surface functionalisation. The capping agents investigated were 1-octanol, 4-penten-1-ol, acrylic acid and ethanolamine.

Table 3.5: Amount, supplier and purity of the chemicals used for the different functionalisations of the Si quantum dots.

Chemical	Amount [ml]	Supplier	Purity [%]
1-octanol	0.6 (A) and 1 (C)	Sigma Aldrich	> 99
4-penten-1-ol	1	Fluka	> 99
Acrylic acid	1	Sigma Aldrich	99
Ethanolamine	0.5	Sigma Aldrich	> 99.5

3.2.1. Functionalisation with octanol

Functionalisation with octanol was done for the quantum dots synthesised via synthesis route A and C. This resulted in products A−1 and C−1 in Table 3.4, to which 0.6 ml and 1 ml octanol was added for functionalisation, respectively. After the addition of the capping agent and stirring for 12 hours, a bright yellow solution with a white precipitate was obtained. The reaction between the quantum dots and the octanol is shown in Figure 3.2.

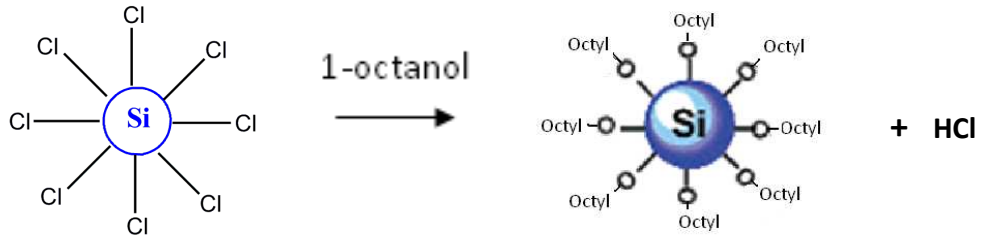

Figure 3.2: Illustration of the functionalisation process when capping the Si quantum dots with octanol.

The stirring was turned off, allowing the two phases to separate. After the separation, the yellow solution was taken out carefully and filtered (0.2 µm pore size) before the solvents were evaporated under reduced pressure. A yellow gel-like product was obtained and extracted with hexane. For purification of the quantum dots, the hexane phase was washed with deionised water in a separation funnel, followed by centrifugation (3500 rpm, 10 minutes) and filtration (0.2 µm pore size). This washing procedure is based on the immiscibility of water and hexane, and that the main byproduct KCl is soluble in water and will dissolve in the water phase, which can easily be separated from the hexane phase by extraction. Another salt, $K^+(15C5)_2Cl^-$, was an additional byproduct from synthesis C, and could also be removed by the same washing procedure. Finally the product was re-dispersed in a hexane and chloroform (3:1 volume ratio) mixture, giving a bright yellow colour.

3.2.2. Functionalisation with 4-penten-1-ol

In the case of pentenoxy capping, it was expected that the alcohol group as the most reactive functional group would bind to the surface of the silicon quantum dots, so that the double bond would stick out as the terminating end. The functionalisation process is illustrated in Figure 3.3, and was investigated for quantum dots synthesised via synthesis A and B, resulting in the products A−2 and B−2. The respective amount of 4-penten-1-ol was added to the solution, the amount is given in Table 3.5. This solution was stirred for 12 hours and a bright yellow solution with a white precipitate was obtained. The precipitate was allowed to settle, and the yellow solution was taken out carefully and filtered (0.2 µm pore size). The same procedure for evaporation, purification and re-dispersion as used for the octoxy capped quantum dots was followed for this functionalisation. At last, the quantum dots were redispersed in pure hexane (10 ml).

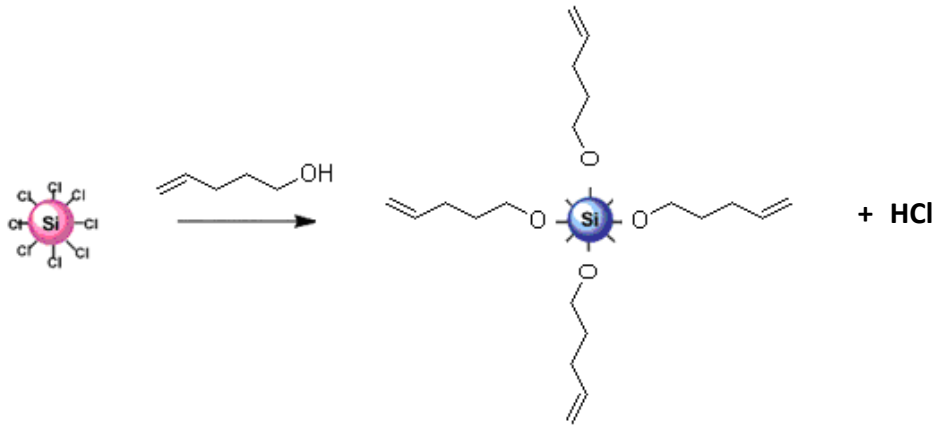

Figure 3.3: Illustration of the functionalisation process of the silicon quantum dots, resulting in product A−2 and B−2. The alcohol 4-penten-1-ol was added and expected to cap the quantum dots by reaction with the OH group to form a Si−O−C bond.

3.2.3. Functionalisation with acrylic acid

Acrylic acid was investigated as a capping agent for synthesis C, resulting in product C−3 in Table 3.4. After addition of the chemical, a bright yellow dispersion with a white precipitate was obtained. This dispersion was stirred for 12 hours, followed by settling of the precipitate and separation of the phases. The same procedure as for the octoxy capped quantum dots with extraction, filtration, evaporation, purification and re-dispersion in hexane (10 ml) was followed. The functionalisation

procedure is illustrated in Figure 3.4. As for the capping with 4-penten-1-ol, it was assumed that the hydroxyl group as the most reactive functional group would bind to the surface of the silicon quantum dots, resulting in quantum dots with double bonds as the terminating ends of their functionalisation.

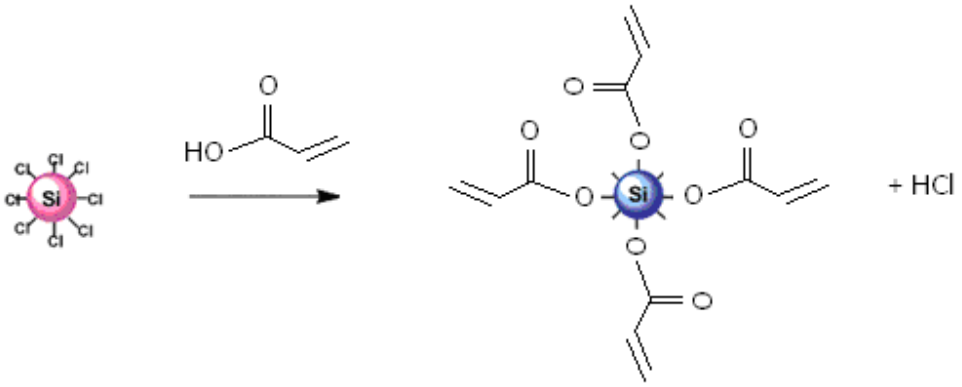

Figure 3.4: Illustration of the functionalisation process with acrylic acid. Acrylic acid was added and expected to cap the quantum dots by reaction with the OH group to form a Si−O−C bond, yielding product C−3.

3.2.4. Functionalisation with ethanolamine

Another capping agent investigated in this study was ethanolamine. The ethanolamine capping was only tried for the quantum dots synthesised via the alkalide synthesis. The reason for this was that ethanolamine mixes with THF which is the solvent used in synthesis C, but not with glyme, which was the solvent used in the two other syntheses. This functionalisation was repeated once, resulting in the products C−4 (a) and C−4 (b). An illustration of the functionalisation procedure is provided in Figure 3.5. It was assumed that the hydroxyl group would bind to the surface of the silicon quantum dots, rather than the amine group on the opposite end because of the higher reactivity of the OH-group towards the silicon quantum dot surface. According to these assumptions, the resulting quantum dots should be functionalised with amine groups and hence, be water dispersible.

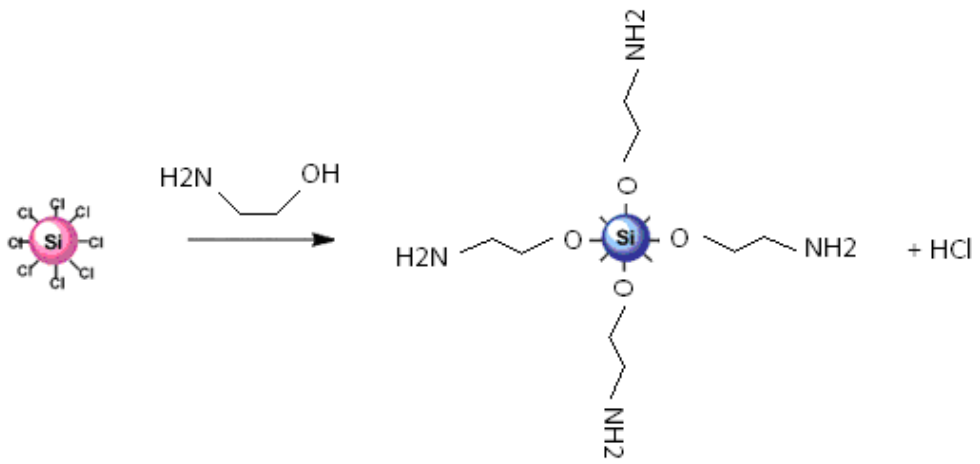

Figure 3.5: Illustration of the functionalisation procedure of the quantum dots for the capping with ethanolamine. It was assumed that the OH group, which is more reactive than the amine group, would bind to the surface of the silicon quantum dots to give Si−O−C bonds. Two syntheses with this functionalisation were performed, resulting in product C−4 (a) and C−4 (b).

After addition of ethanolamine to the quantum dots dispersed in THF, the colour of the dispersion turned from yellow to an orange solution with a white precipitate. The solution was stirred for 12 hours for complete surface functionalisation. The stirring was turned off, and the precipitate was allowed to settle. The solution was taken out with a pipette, centrifuged and filtered (0.2 µm pore size) before the solvents were evaporated under reduced pressure. The remaining yellow gel-like product was redispersed in ethanol (10 ml).

3.2.5. Oxidation of terminating double bonds

When pentenol and acrylic acid were added as capping agents, it was expected that the terminating end of the functionalisation would be a double bond. Since the aim for the synthesised quantum dots was to achieve water solubility of them, it was tried to oxidise the terminating double bonds by addition of deionised water under acidic conditions to obtain OH groups as part of the surface capping. The amount, the supplier and the purity of the acid and the water are given in Table 3.6. In this work, the oxidation was done in a second step after the addition of capping agent and 12 hours of stirring. The oxidised products are marked as B−2 (ox), A−2 (ox) and C−3 (ox) in Table 3.4. The amount of water added corresponded to the stoichiometric amount of capping agent.

Table 3.6: The amount, supplier and purity of the chemicals used for the oxidation of the quantum dot's terminating double bond.

Chemical	Amount	Supplier	Purity/ resistivity
Hydrochloric acid	3 µl	Sigma Aldrich	37 %
Deionised water	0.40 ml	NTNU Nanolab	18 MΩ/cm

For the oxidation, hydrochloric acid was first added to the quantum dot dispersion which had been stirred for 12 hours, followed by the addition of deionised water and stirring for two hours. Markovnikov's rule was assumed to be valid for the oxidation reaction, i.e. the hydrogen adds to the carbon that has the greater number of hydrogens, and the water adds to the carbon having fewer

hydrogens [26], leading to an OH-group on the fourth carbon atom of the pentenoxy capping. The oxidation process is illustrated in Figure 3.6 for the pentenoxy capped Si quantum dots. The same oxidation of the terminating double bond was assumed to take place for the quantum dots capped with acrylic acid, yielding an OH-group on the second carbon atom.

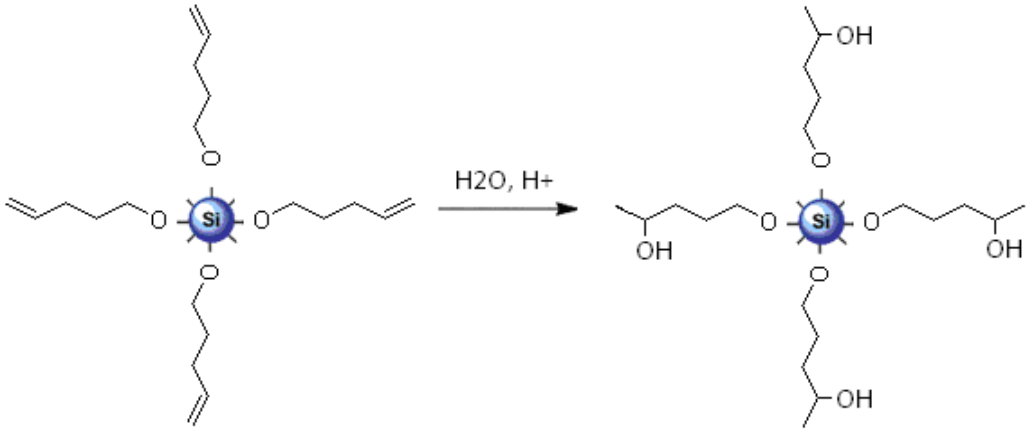

Figure 3.6: The oxidation of the pentenoxy capped silicon quantum dots via the addition of water, resulting in the products A−2 (ox) and B−2 (ox). The same procedure was followed in the case of quantum dots capped with acrylic acid, giving product C−3 (ox) (not shown here).

A yellow solution with a white precipitate was obtained and the liquid phase was extracted after two hours. This phase was centrifiuged, and the yellow solution was taken out carefully and filtered (0.2 µm pore size) before the solvents were evaporated under reduced pressure. The products were re-dispersed in ethanol (10 ml). Finally, the quantum dot dispersions were filtered again (0.2 µm pore size). The normal purification procedure involving washing the quantum dots with water could not be performed for any of the quantum dots with a water dispersible functionalisation, because the products were not dispersible in any chemical which did not mix with water. It was not found any alternative way to remove the byproducts from the final quantum dot dispersions in this work and hence, none of the water dispersible quantum dots were washed.

3.2.6. Functionalisation with other chemicals

The possibility to use solid chemicals as cappings was also investigated. Examples of these are L-arginine, β-alanine, L-glutamic acid and L-glutamine. The structural formulas of these chemicals are given in Figure 3.7. However, it was difficult to find a suitable solvent for them, since many requirements should be fulfilled simultaneously for this solvent: It should dissolve the polar solid easily, it should mix well with the organic quantum dot dispersion and also make it possible to remove the byproducts afterwards. Solvents like alcohols could not be used, since the alcohol molecules would have acted like a capping agent and substituted the chlorine atoms on the surface of the quantum dots. Aprotic solvents, which tend to have large dipole moments would probably be the best alternative to fulfil all these requirements at once. Different aprotic solvents were tried, such as acetone, dimethylformamide (DMF) and acetonitrile, but unfortunately, none of these dissolved the solids shown in Figure 3.7.

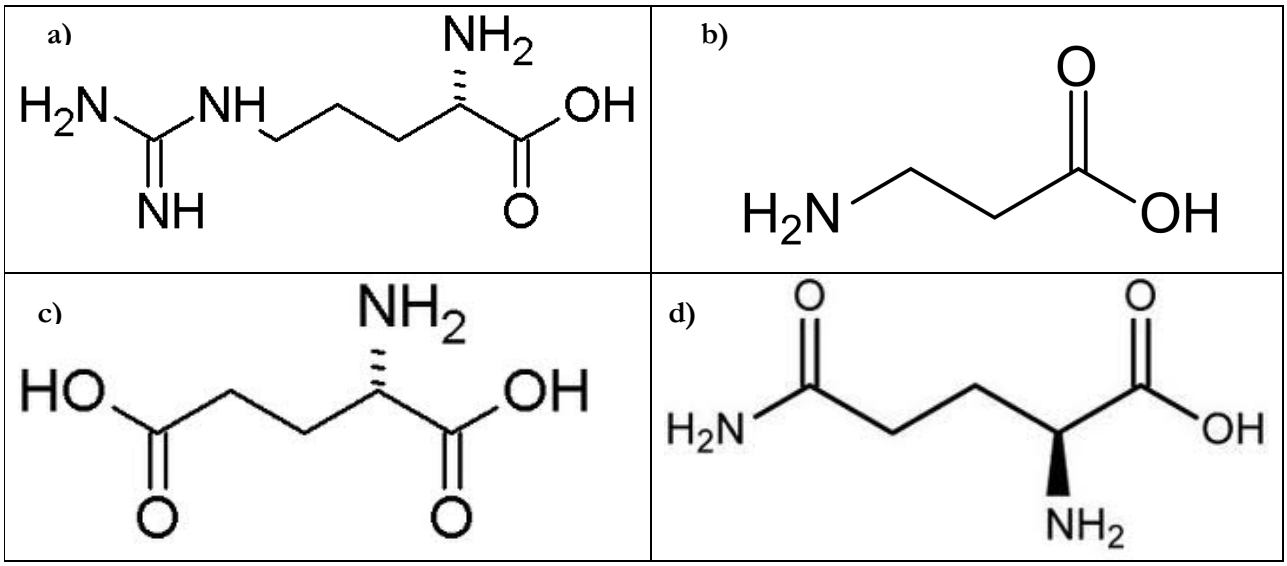

Figure 3.7: Overview over solids which could possibly be used as capping agents for the silicon quantum dots. **a)** L-arginine, **b)** β -alanine, **c)** L-glutamic acid and **d)** L-glutamine.

3.3. Deposition of quantum dots on solid substrates

Dispersions with hydrophobic quantum dots were deposited onto solid substrates in order to see if it was possible to disperse quantum dots on a solid substrate by simple techniques like solvent evaporation and spin coating. In the case of a successful deposition, it would be interesting to investigate how the quantum dots dispersed on a substrate, the degree of agglomeration and the byproducts present in the final quantum dot dispersions. Before deposition, the quantum dots were dispersed by using an ultrasonic bath for ten minutes. The most frequently used substrates used for the deposition were monocrystalline silicon wafers. Details about the wafers are given in Table 3.7.

Table 3.7: Characteristics of the monocrystalline Si wafers used for the spin coating.

Diameter	2”
Thickness	256-306 µm
Orientation	<100>
Polish	Single side
Doping	Phosphorous
Resistivity	5-10 Ohm cm
Supplier	Si-Mat

Other substrates used for the deposition of the Si QD were Al sample holders designed for a Hitachi S-5500 S(T)EM. Al substrates were used, because then EDS spectra could be recorded and used to confirm the presence of Si. This technique was not possible when Si was used as the substrate. Before use, the Al substrates were grinded with a P4000 SiC grinding paper because of the rough surface structure of the sample holders. The surface of the substrate can influence the ability of the quantum dots to disperse on the substrate significantly. After the deposition onto the Al sample holders, the solvent was evaporated at 120 °C in a vacuum furnace overnight.

The first Si substrates were plasma cleaned for five minutes prior to the deposition to remove eventual organic contamination from the wafer surface. A Plasma cleaner Femto was used for cleaning of the Si wafers. The generator had a frequency of 40 kHz and the power used was 100 W. Plasma cleaning is a dry wafer cleaning method and is advantageous when compared to wet chemical cleaning techniques, which have been widely used to remove contaminants from wafer surfaces. The plasma cleaning is very easy, safe, does not produce any waste and is of low cost when compared to wet chemical methods like RCA cleaning. In the plasma enhanced cleaning, glow discharge generates reactive species which react with contaminated molecules on wafer surfaces and produce CO_2 and H_2O which are desorbed from the surfaces, by exciting a gas in a low pressure chamber by a supply of energy. UV radiation helps breaking down long-chain complex carbon compounds, and the surface is also physically cleaned by the ion bombardment during the procedure. Oxygen plasma was used, which creates radical sites on the surface, leaving it hydrophilic. After the deposition and the solvent had evaporated, some of the samples were plasma cleaned again for ten minutes, before characterising them in an SEM.

An overview over the different attempts for depositing quantum dots on solid substrates is given in Table 3.8. Two different approaches were utilised when depositing the quantum dots; solvent evaporation and spin coating. The two techniques will be described in Section 3.3.2 and Section 3.3.3, respectively. Different amounts of the quantum dot dispersions were deposited (5 µl and 100 µl), and different concentrations of the quantum dots in their respective dispersions were investigated, as listed in Table 3.8.

Table 3.8: Overview over the investigations performed for deposition of quantum dots onto solid substrates.

Quantum dots/ synthesis	Substrate	Deposition technique	Amount (µl)	Concentration (x times diluted)	Plasma cleaning after deposition
CdSe QD	Si	Solvent evaporation	5, 100	Original dispersion, (10, 20, 100, 200, 500)	Yes
CdSe QD	Si	Spin coating	100	Original dispersion, (10, 20, 100, 200, 500)	No
A−1	Si	Solvent evaporation	100	Original dispersion	Yes
A−1	Hydrophobic Si	Solvent evaporation	100	Original dispersion	No
C−1	Si	Solvent evaporation/ Spin coating	100	Original dispersion	No
C−1	Hydrophobic Si	Solventevaporation/ Spin coating	5, 100	Original dispersion, (100)	No
C−1	Al	Solvent evaporation	100	Original dispersion	No
A−2 (ox)	Si	Solvent evaporation	100	Original dispersion	Yes

3.3.1. Deposition of CdSe quantum dots

Commercially available CdSe/ZnS core/shell quantum dots were dispersed on a silicon susbtrate in an attempt to investigate quantum dots of a heavier element compared to the substrate and to see whether it was possible to deposit quantum dots on substrates and characterise them by SEM investigation. The CdSe quantum dots were supplied as a 49.9 nmol/ml dispersion in toluene from Evident Technologies, with a diameter of 4 nm and an amine capping agent used as a stabiliser. The exact chemistry of the capping was unknown. Different concentrations of the quantum dots and different amounts of the quantum dot dispersions were investigated, as given in Table 3.8. The quantum dots were diluted with toluene and ethanol, dilution between 10 and 500 times was used. Combining wetting of the substrate with no agglomeration of the quantum dots was a difficult task. Ethanol was used because it wets the Si substrate much better than toluene does. To prevent agglomeration upon dilution with ethanol, it was tried to add microlitre amounts of hydrochloric acid to the ethanol before it was mixed with the quantum dot dispersion.

3.3.2. Deposition by solvent evaporation

Quantum dots were simply deposited, by means of a microdispenser, microlitre amounts of the quantum dot dispersion on a silicon substrate, permitting the solution to spread spontaneously and the solvent to evaporate. This is a very simple route for the deposition of nanoparticles onto a solid substrate. Small rectangular pieces of the silicon substrate were cut to pieces with a diamond scriber to a size of about 10 * 5 mm to fit in the S(T)EM sample chamber. Silicon quantum dots with octoxy capping, i.e. the product of synthesis A−1 and C−1, as well as quantum dots with oxidised pentenoxy capping, i.e. product A−2 (ox) in Table 3.4 were deposited on substrates, heat treated in a vacuum furnace at 120 °C overnight and characterised in an SEM.

3.3.3. Quantum dot deposition by spin coating

The quantum dot dispersions were also spin coated onto silicon substrates. The spin coating was conducted using a Laurell Spin Processor WS-400B-6NPP-Lite, an image of the spin coater is shown in Figure 3.8. A blow gun with nitrogen gas was used to remove any dust particles present on the Si wafer before it was plasma cleaned and placed in the spin coater. For the spin coating, the circular silicon wafers were cut into four equal pieces. The silicon wafers were placed carefully in the middle of the spin chuck and held in place by vacuum suction. A purge flow of nitrogen gas through the spin coater was turned on. The dispersion was deposited onto the middle of the Si wafer using a glass pipette. For complete covering of the substrate, one drop was found to be the ideal amount. The spin program was started immediately and run for 2 minutes with a speed of 2000 rpm and an acceleration of 540 rpm/s. The quantum dot dispersions which were deposited on substrates by spin coating are given in Table 3.8. Only some of the quantum dot dispersions were deposited on substrates by spin coating, these are listed in Table 3.8.

Figure 3.8: Spin coating equipment available in NTNU NanoLab.

3.3.4. Treatment of the Si substrate by silylation

For the deposition of octoxy capped silicon quantum dots (product A−1 and C−1) on Si substrates, it was tried to make the wafers hydrophobic by silylation in order to improve the wetting and thereby make it easier to disperse the quantum dots on the wafer surface. The silylation was performed following a modified recipe suggested by Lee, Kim and Hyun for waterglass silica [40]. The wetting properties of the surface can be controlled by choosing a silane with a specific ligand; a terminating alkane group results in a hydrophobic surface while a primary amine renders it hydrophilic. The method involved mixing hexane-solved trimethylchlorosilane (TMCS) with isopropanol (IPA), forming isopropoxytrimethylsilane and a gaseous HCl product. The isopropoxytrimethylsilane reacts further with a surface hydroxyl group, forming a trimethylsilicon group bonded to the surface:

$$\text{TMCS} + \text{IPA} \leftrightarrow (CH_3)_3 - Si - O - CH(CH_3)_2 + HCl \qquad \textbf{(3.3)}$$

$$(CH_3)_3 - Si - O - CH(CH_3)_2 + \equiv Si - OH \rightarrow \equiv Si - O - Si(CH_3)_3 + \text{IPA} \qquad \textbf{(3.4)}$$

where ≡Si represents a silicon atom on the surface of a silicon lattice. The recipe used had a molar ratio of IPA : TMCS of 1:1 and the volumetric ratio n-Hexane : TMCS was 10 : 1. The wafers were cut in wanted sizes for deposition and spin coating, before they were put in a water bath of deionised water to obtain −OH groups on the surface and dried with a blow gun with nitrogen gas. Then the wafer pieces were submerged in the silylation solution for 24 hours in a closed container, whereupon they were extracted and dried at ambient conditions.

3.4. Characterisation

Holey carbon grids were used for STEM characterisation with a Hitachi S−5500 ultra high resolution In-lens microscope and also for TEM characterisation with a JEOL JEM−2010 instrument, operated at 300 kV. For the investigation of merely the quantum dots, the quantum dot dispersion was dripped onto holey carbon grids (3 µl) and dried in a vacuum furnace at 120 °C overnight. The S(T)EM microscope was used in SEM mode for investigation of quantum dot dispersions on silicon wafers. The S(T)EM was equipped with a Quantax EDS system from Bruker. An acceleration voltage of 10 kV was used when recording the EDS spectra.

Two different approaches were utilised when the FTIR spectra were recorded (Bruker, IFS−66V). The first approach was to use KBr pellets, a few drops of the quantum dot dispersion was dropped onto the discs and thereafter heated in a vacuum furnace at 120 °C overnight before the IR spectra were recorded. The other approach was to measure FTIR spectra from liquid samples contained between KBr windows. When measuring FTIR spectra for liquid samples, one had to be very careful which solvent was used, as the bands of the solvent should not interfere with the interesting bands for the sample.

The solid film left on the silicon substrate after deposition of quantum dots from synthesis A and heat treatment at 200 °C was investigated by diffuse reflectance UV-visible spectroscopy. The set-up consisted of a fiber optic reflectance accessory from Labsphere (RSA-FO-150), connected to a fiber-based spectrometer operating in the UV-visible region from Hamamatsu (C10082CA). This film was also investigated by FTIR spectroscopy, by scraping twenty mg of the film off as a powder and mixing 20 mg of it with the KBr powder for the subsequent pressing of a pellet. An overview over the characterisation methods and the corresponding specific instruments used is given in Table 3.9.

Table 3.9: Overview over the characterisation methods used and the corresponding instruments.

Characterisation method	Instrument
S(T)EM	Hitachi S−5500
EDS	Bruker Quantax EDS
TEM	JEOL JEM−2010
FTIR	Bruker IFS−66V
Diffuse reflectance	Fiber optics: Labsphere (RSA−FO−150)
	Spectrometer: Hamamatsu (C10082CA)

4. Results

4.1. A−Potassium naphthalide synthesis

4.1.1. Octoxy capping (A−1)

Size distribution, degree of agglomeration and crystallinity

Octoxy capped silicon quantum dots synthesised via the potassium naphthalide synthesis were characterised in previous work [6]. STEM images of these quantum dots are included here, shown in Figure 4.1. The dark spots are assumed to be the quantum dots, and it seems as if they are quite well dispersed on the grid. The average diameter of the quantum dots is from these images determined to be about 4 nm, and their size distribution is quite narrow.

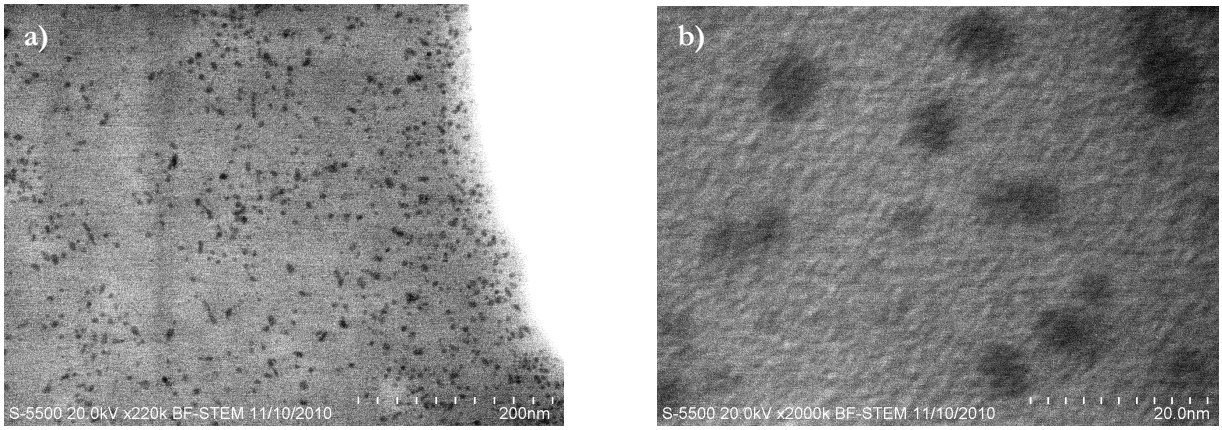

Figure 4.1: a) and **b)** STEM bright field images of product A−1 on a holey carbon grid [6].

The crystallinity of these quantum dots were confirmed by TEM investigation. In the high resolution TEM image in Figure 4.2, a striped pattern is visible for one of the quantum dots. This pattern is an image of the lattice planes, and is a clear sign that the quantum dots are crystalline. The lattice spacing was measured from 12 lattice fringes, and found to be 3.139 Å. This corresponds very closely to the lattice spacing between <111> planes in the diamond cubic lattice of silicon, which is 3.135 Å. Some of the most common lattice spacings for silicon are given in Appendix A. The lattice fringes are not very clearly visible, as the background tends to dominate the signal, making it difficult to obtain lattice imaging.

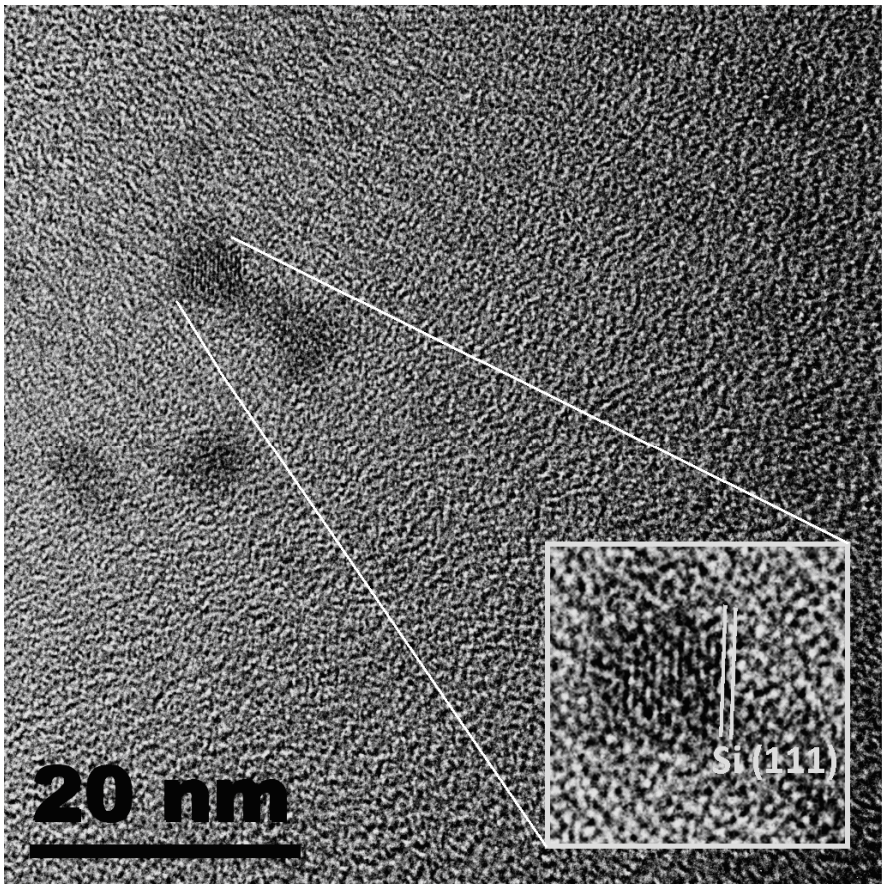

Figure 4.2: TEM bright field image of octoxy capped Si quantum dots (product A−1) on a holey carbon grid. Inset showing an individual 5 nm silicon quantum dot. The lattice fringes correspond to the lattice spacing between <111> planes in silicon.

Determination of surface chemical structure

The surface chemical structure of the silicon quantum dots was characterised by FTIR spectroscopy. The FTIR spectrum of the octoxy capped silicon quantum dots (product A−1) measured on a dried KBr pellet is shown in Figure 4.3. The strong and broad band between 1000 and 1100 cm^{-1} is characteristic for both the Si−O−Si bonding and the Si−O−C stretching vibration [41]. Because these bands are situated so close, and probably also overlap with each other, one can not say straight away whether the quantum dots are oxidised or not, based on the information from this band only. If the quantum dots have been successfully capped, this band should correspond to the Si−O−C bond on the surface of the quantum dots. The FTIR spectrum of amorphous silica is included in Appendix B−I to further confirm that the band between 1000 and 1100 cm^{-1} can not be used to say whether the quantum dots are oxidised or not. This is because no significant difference can be observed in this band when comparing the FTIR spectrum for the quantum dots and for silica.

Beyond that are the bands between 2800 and 3000 cm^{-1} noteworthy and indicate the presence of both CH_2 and CH_3 groups. This is consistent with the alkyl chain $-(CH_2)_7CH_3$ in the octoxy capping. C−H stretching in CH_3 has bands at 2871 and 2954 cm^{-1}, and C−H stretching in CH_2 at 2855 cm^{-1} and 2926 cm^{-1} [41]. The bands at 1378 cm^{-1} and 1462 cm^{-1} are due to CH_3 and CH_2 bending, respectively. The broad band which appears at 3300−3500 cm^{-1} relates to OH groups. The band for

Si−OH bonds will also show up in the range between 3200−3700 cm^{-1}. The band in this wavenumber range could come from water adsorbed on the KBr pellet, or it could indicate that the quantum dots have started to oxidise after they have been washed with water. This band will show up for oxidised Si QD because of hydrogen adsorption on the surface, and is for this reason also present in the FTIR spectrum for amorphous silica.

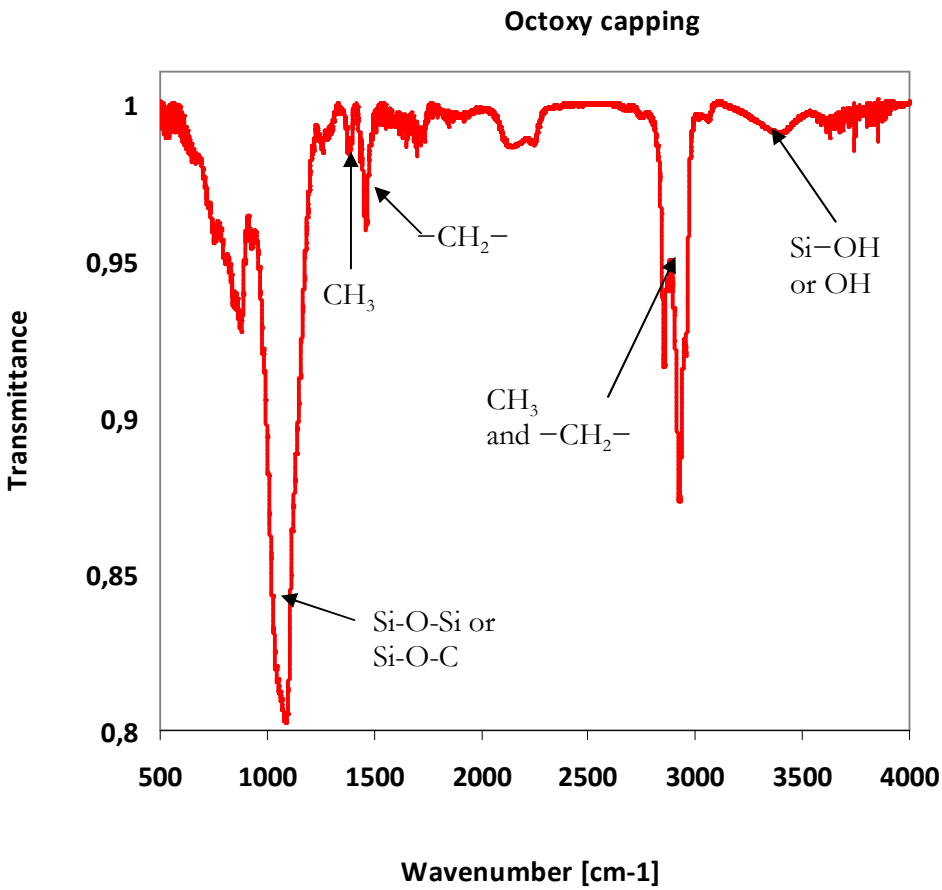

Figure 4.3: FTIR spectrum of product A−1, measured on a dried KBr pellet.

4.1.2. Pentenoxy and oxidised pentenoxy capping (A−2 and A−2 (ox))

Size distribution, degree of agglomeration and crystallinity

Product A−2 was investigated in the STEM on a holey carbon grid the day after the synthesis was finished. Pentenol had been added as the capping agent, and an STEM image of the resulting product is shown in Figure 4.4. It seems as if the quantum dots are quite well dispersed on the carbon grid and that the size distribution is quite narrow.

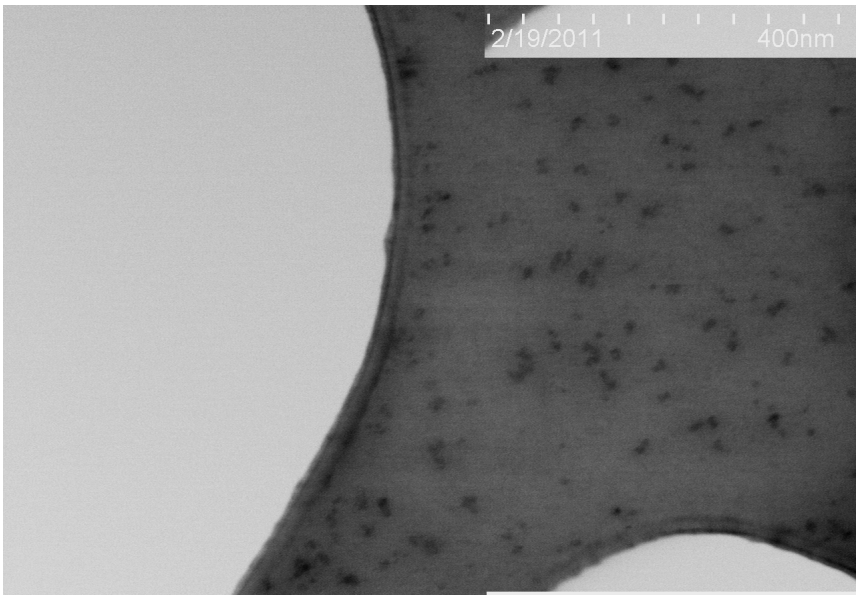

Figure 4.4: Bright field STEM image of product A−2, characterised on a holey carbon grid the day after the synthesis was performed.

TEM bright field images of these same quantum dots are shown in Figure 4.5. The TEM characterisation was done two weeks after the STEM characterisation of the same sample, deposited on a new carbon grid. A quitelarge amount of product could be observed on the grid, but the observed particles were agglomerated to a large extent, showing particles overlapping significantly with each other. No crystallinity could be detected for this product. Upon comparison with the STEM image in Figure 4.4, one can see that the particles agglomerate when they are stored. This agglomeration could also be observed upon visual inspection of the quantum dot dispersion, as the dispersion had become opaque after these two weeks of storage.

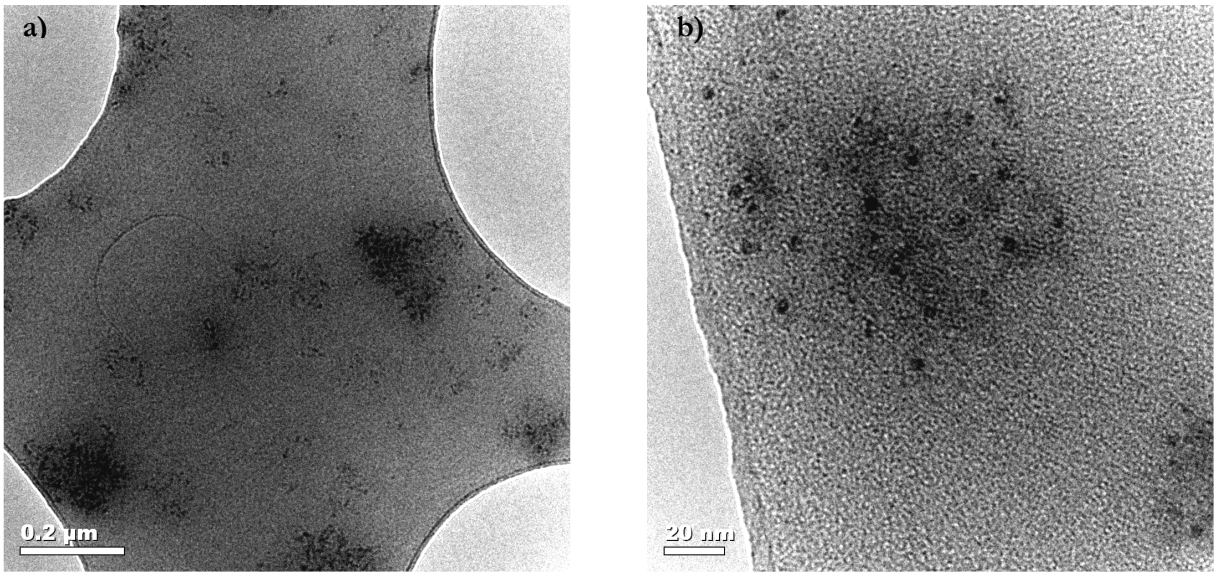

Figure 4.5: a) and **b)** TEM bright field images of product A−2 on a holey carbon grid, characterised two weeks after the synthesis was performed.

TEM images of the same quantum dots after the oxidation with water, i.e. product A−2 (ox) in Table 3.4, are shown in Figure 4.6 and in Figure 4.7. This characterisation was also done about two weeks after the synthesis was performed and the dispersion had become opaque during this storage. The material left on this grid had agglomerated to an even larger extent than product A−2 displayed in Figure 4.5, even though these particles were also well dispersed when investigating them on a holey carbon grid in the STEM just after the synthesis was finished. Only a couple of areas like that in Figure 4.6a were observed on the entire grid, whereas the circular dark spots as shown in Figure 4.6b were observed more frequently. The circular areas in Figure 4.6b contained some kind of smaller particles inside them, which disappeared very fast when the electron beam hit the sample, making it impossible to investigate these particles. Lattice fringes could only be observed for the kind of spots imaged in Figure 4.6a. A high resolution TEM image with lattice fringes can be observed in Figure 4.7.

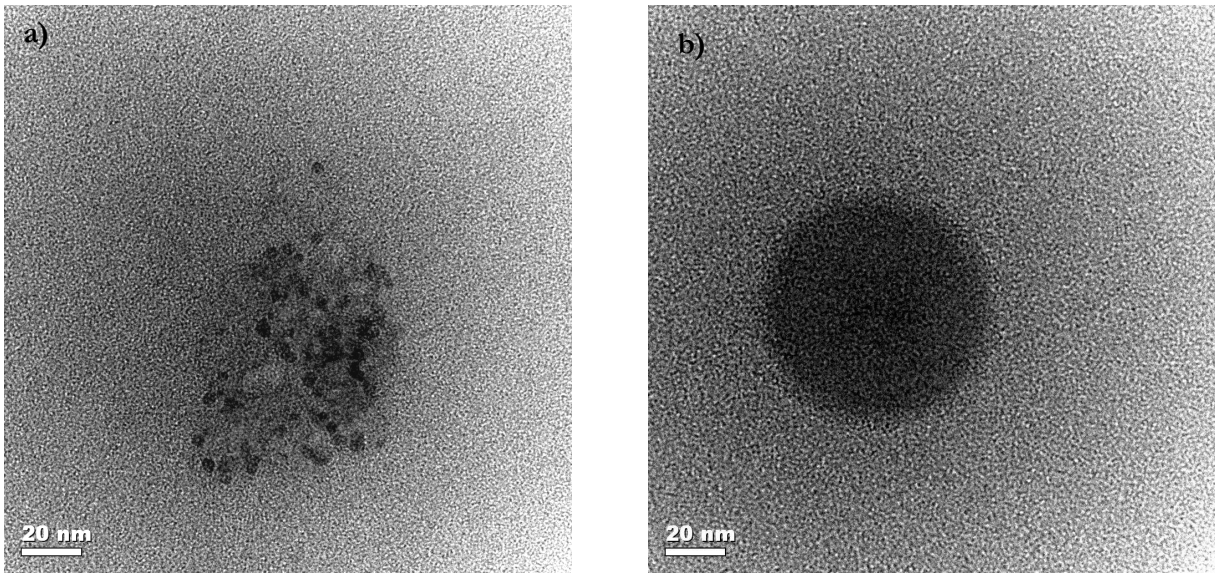

Figure 4.6: TEM bright field image of product A−2 (ox) on a holey carbon grid, characterised two weeks after the synthesis was performed. **a)** Agglomerated particles, only a few spots of this kind were observed on the entire grid, and **b)** more frequent circular dark areas containing unstable particles inside them.

In the TEM image in Figure 4.7, a striped pattern is visible for some of the particles on the grid. The lattice spacing was measured from 21 lattice fringes, and found to be 1.77 Å. The closest lattice spacing in silicon is between <311> planes, which is 1.64 Å, given in Appendix A. However, the lattice spacing between <222> planes in KCl is 1.82 Å, even closer to the observed value.

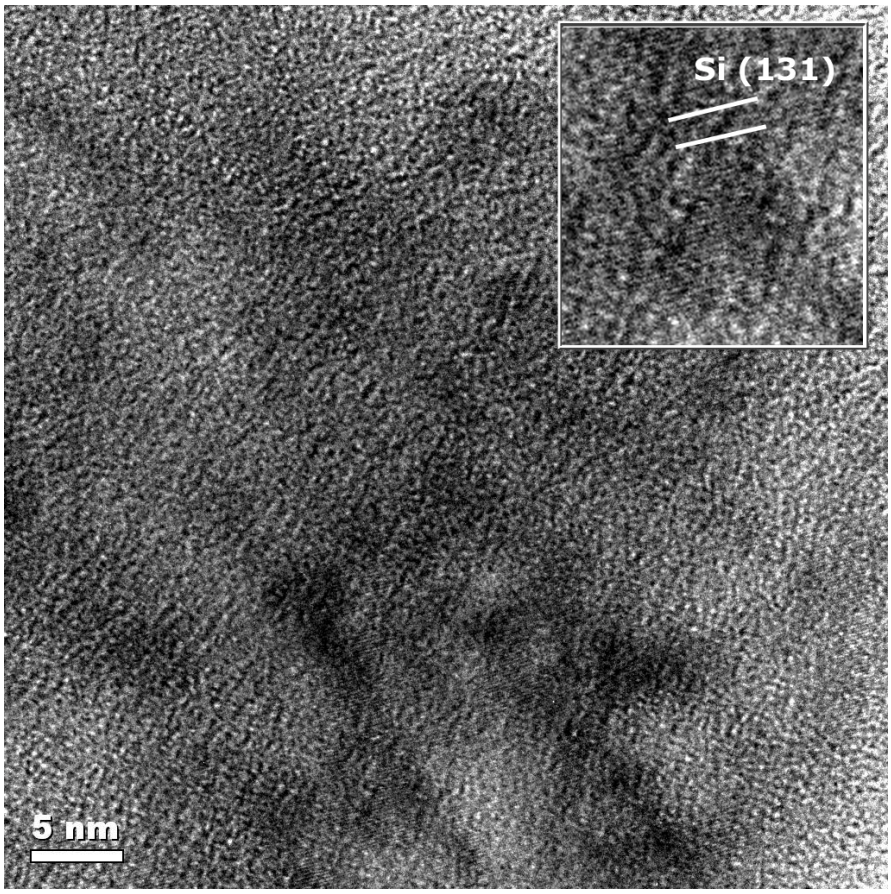

Figure 4.7: TEM bright field image of the material on the holey carbon grid when the product from synthesis A−2 (ox) was deposited. Higher magnification image of the material observed in Figure 4.6a. Inset showing lattice fringes possibly corresponding to the lattice spacing between <311> planes in silicon.

Determination of surface chemical structure

The FTIR spectra for the products of synthesis A−2 and A−2 (ox) are shown in Figure 4.8, the upper blue spectrum representing the pentenoxy capping (these quantum dots had not been washed), whereas the bottom red spectrum represents the measurement of the quantum dots with the oxidised pentenoxy capping. These spectra were both recorded from dried KBr pellets. There were some interference problems related to the measurements, as well as difficulties with obtaining low enough pressure in the sample chamber giving rise to high water levels, affecting the quality of the spectra. This plays a significant role especially for wavenumbers below 1000 cm^{-1}. The most striking difference between these two spectra is that the bottom curve has got an additional broad band at a wavenumber around 3400 cm^{-1} when compared to the upper curve. This band can be attributed to OH groups [41], and suggests that the intended oxidation of the terminating double bond was successful. Since these two spectra were recorded just after another, the humidity level should be about the same, so that the intensity of the OH bands in the two spectra can be compared.

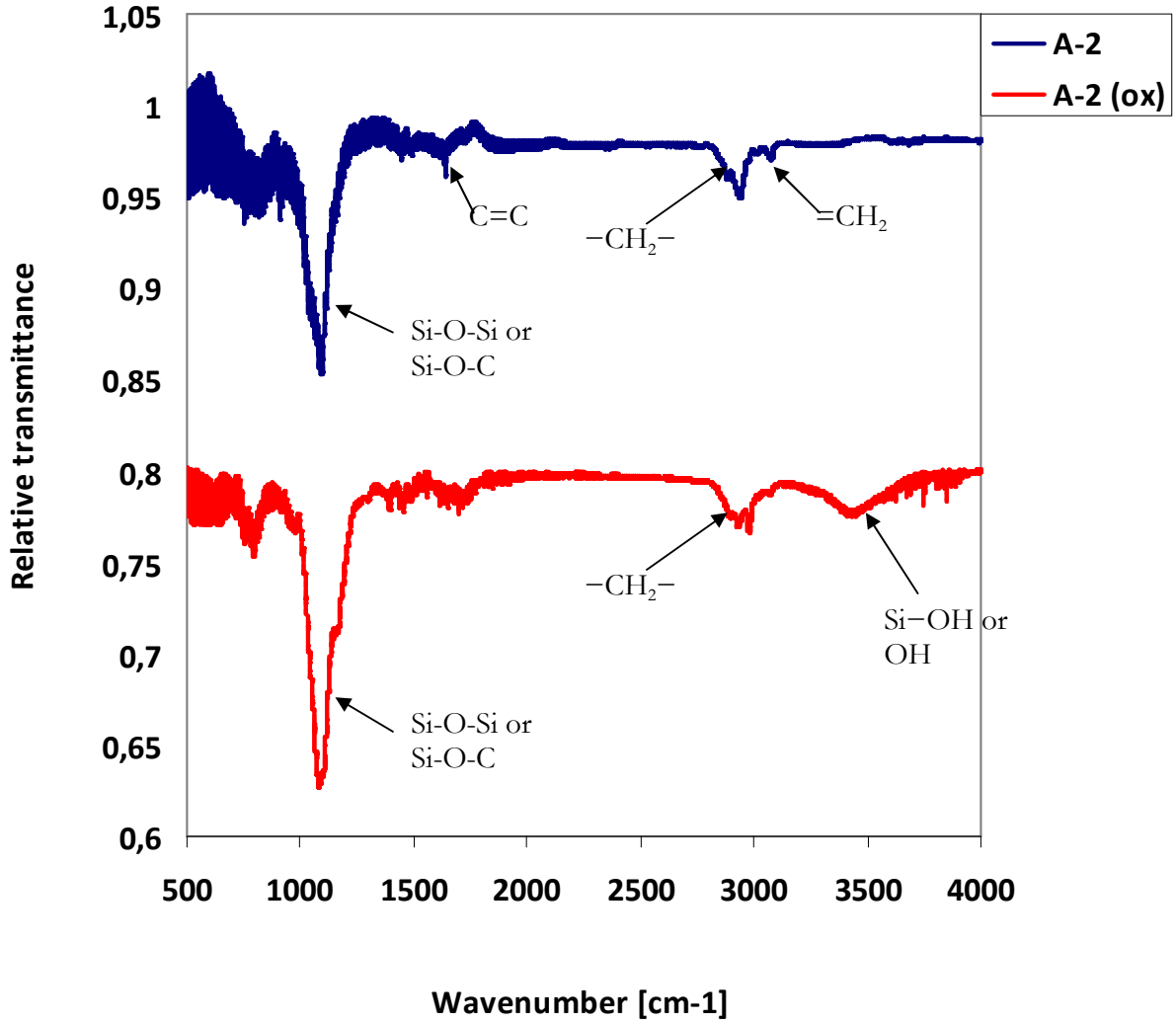

Figure 4.8: FTIR spectra of the products from synthesis A, after the addition of capping agent, measured on dried KBr pellets. Upper blue spectrum representing product A−2, whereas the bottom red spectrum represents the product A−2 (ox).

Two important bands indicate the presence of a carbon-carbon double bond [41]: First is a weak band close to 3100 cm^{-1}, second is a sharp band around 1650 cm^{-1}. The band close to 3100 cm^{-1} is due to terminal $=CH_2$ and is normally weak. It may be overlapped by the saturated C−H stretch near 2975 cm^{-1} and appear only as a shoulder, like for the bottom spectrum in Figure 4.8. These two signs of an alkene can be clearly seen for product A−2 in the upper blue spectrum in Figure 4.8. Since these two bands are hardly observable in the bottom red spectrum measured after the oxidation of the terminating double bond (product A−2 (ox)), this is a second indication that the surface modification is as intended and that the expected oxidation actually has taken place. The other bands present are the same as for the octoxy capped quantum dots and were presented when discussing Figure 4.3.

4.2. B−Sodium cyclopentadiene synthesis

The Na-cyclopentadiene route was the least investigated among the syntheses performed in this work. The most significant problem with this method was that it was difficult to remove the byproducts because of common solubility, and hence there were some challenges related to separation of the synthesised quantum dots and the byproducts formed.

4.2.1. Oxidised pentenoxy capping (B−2 (ox))

The oxidised pentenoxy capping was also tried for the Si quantum dots synthesised with the Na-cyclopentadiene route, listed as synthesis B−2 (ox) in Table 3.4. The dispersion became opaque just two days after the synthesis. Since it was observed from synthesis A−2 and A−2 (ox) that unclear dispersions contained agglomerated quantum dots according to the STEM and TEM characterisation, the same effect was assumed to cause the opaque appearance of the dispersion in this case. Because of this, the quantum dots were not investigated in the STEM on a holey carbon grid.

Determination of surface chemical structure

Even when the appearance of the B−2 (ox) dispersion was unclear and agglomeration had probably taken place, the surface chemical structure was characterised by FTIR measurements. The FTIR spectrum of the product from the Na-cyclopentadiene synthesis was measured after evaporation from a KBr pellet and also as a liquid in ethanol solution contained between KBr windows. The measurement was performed on the liquid sample because the reaction route was unknown, and it was not known which reactions could take place or whether the quantum dots oxidised or not when heating the KBr pellet to 120°C. The solid spectrum (upper red curve) and the liquid spectrum (bottom blue curve) of product B−2 (ox) are shown together in Figure 4.9 to give a comparison between the two measuring techniques.

The most important band visible is the strong and broad band between 1000 and 1100 cm^{-1}, which is characteristic for both the Si−O−Si bonding and the Si−O−C stretching vibration [41]. This Si band has a lower relative intensity for the liquid than for the solid sample. However, since this typical band is clearly present for the solid sample, the band in this wavenumber range for the liquid sample is probably also related to the Si bonds, possibly overlapping with the bands from the liquids. When measuring a liquid sample, all the bands related to the liquids in the mixture will be shown, in addition to or overlapping with the bands belonging to the sample to be investigated. The FTIR spectra of ethanol and 4-penten-1-ol are provided in Appendix B. When comparing the spectra, one can see which bands can be ascribed to the liquids, and these bands are marked in the liquid spectrum in Figure 4.9. Bands indicating OH-groups are present for both spectra around 3400 cm^{-1}, a shift to lower wavenumbers was observed for the liquid spectrum relative to the solid spectrum. This shift is consistent with the fact that increased strength of hydrogen bonding typically shifts the vibration to lower wavenumbers. This is reasonable since it can be assumed that hydrogen bonding is stronger in the liquid sample because of the contribution from ethanol and water molecules.

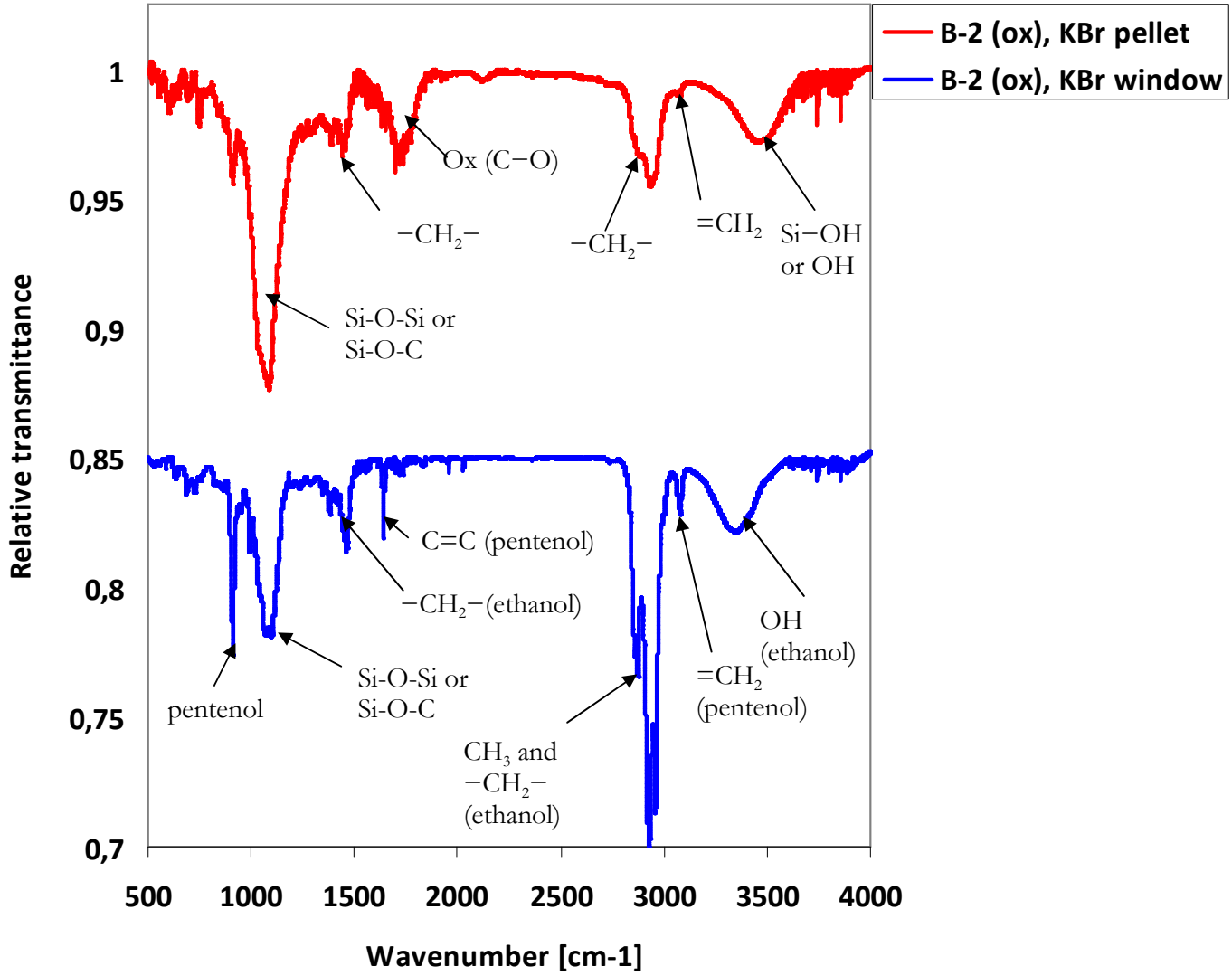

Figure 4.9: FTIR spectra of product B−2 (ox). Upper red curve is from the measurement on a KBr pellet and the bottom blue curve represents the measurement of the liquid sample with ethanol as the solvent between two KBr windows.

Beyond that are the bands between 2800 and 3000 cm^{-1} noteworthy and indicate the presence of CH_2 groups which is consistent with the alkyl chain $-(CH_2)_4-$ in the pentenoxy capping. The bands which can be attributed to alkyl chains have a much higher intensity for the liquid sample than for the solid sample, which is reasonable since ethanol is used as the solvent.

The bands indicating a C=C double bond are clearly present in the liquid spectrum, indicating that the intended oxidation of the double bonds was not complete. It was expected that the oxidation should take place on the free pentenol molecules to the same extent as for the pentenol molecules attached to the molecules, so the C=C bands should not be present in the case of complete oxidation. For the solid spectrum however, the band around 3100 cm^{-1} is much weaker and a broad band has arisen around 1730 cm^{-1}, possibly hiding the band for the carbon-carbon double bond at

1650 cm^{-1}. The band around 1730 cm^{-1} might indicate that oxidation of the double bond has happened upon heating of the sample to 120 °C, since C−O bonds tend to show up at this wavelength [41].

4.3. C−Alkalide synthesis

4.3.1. Octoxy capping (C−1)

Size distribution, degree of agglomeration and crystallinity

The product of synthesis C−1 was investigated on a holey carbon grid in the STEM, and the distribution of the particles on the grid is shown in the images in Figure 4.10. The particles are isolated from each other without significant overlap or agglomeration, which indicates that the functionalisation occurs on the surface of the quantum dots and prevent particle agglomeration. The size distribution seems to be narrow.

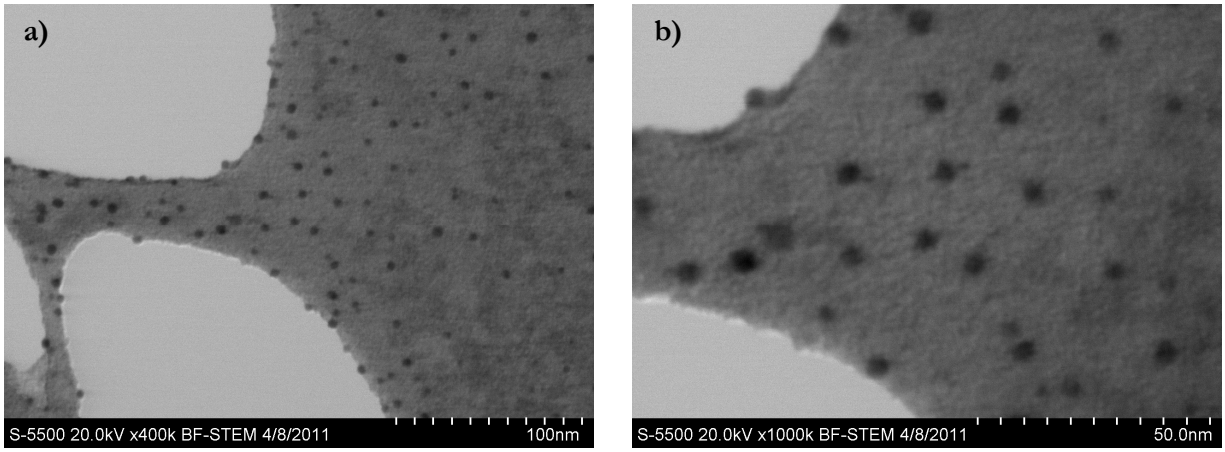

Figure 4.10: a) and **b)** STEM bright field images of the quantum dots from synthesis C−1 on a holey carbon grid.

The Selected Area Electron Diffraction (SAED) pattern in Figure 4.11 shows some of the diffraction rings obtained from this sample during TEM investigation. They correspond to the Miller indices <200>, <220>, <400> and <331> of the diamond cubic lattice of silicon. Some of the theoretical spacings of this crystal structure of Si are given in Appendix A. The relevant spacings and Miller indices together with the measured values obtained from the SAED pattern are given in Table 4.1 for comparison.

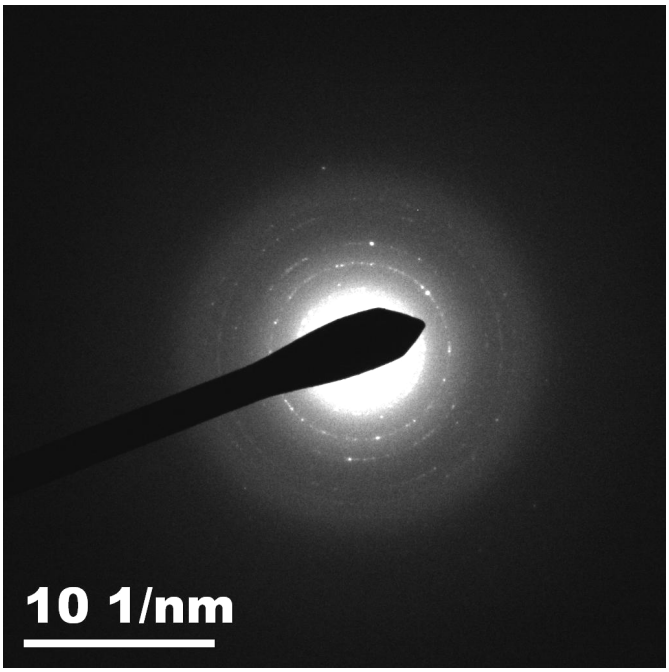

Figure 4.11: Selected area electron diffraction pattern obtained during the TEM investigation of the quantum dots from synthesis C−1.

Table 4.1: Comparison between measured lattice spacing from the diffraction pattern in Figure 4.11 for product C−1 and the closest value in the diamond cubic lattice for Si. The corresponding Miller indices are also given.

Measured lattice spacing (Å)	**Theoretical lattice spacing for Si (Å)**	**Miller indices**
2.77	2.72	<200>
2.12	1.92	<220>
1.94	1.92	<220>
1.35	1.36	<400>
1.24	1.25	<331>

Determination of surface chemical structure

The FTIR spectrum of product C−1 is shown in Figure 4.12. The same bands as those present for the octoxy capped quantum dots synthesised via synthesis A could be observed here, the reader is referred to Section 4.1.1 and the FTIR spectrum in Figure 4.3 for a presentation of them.

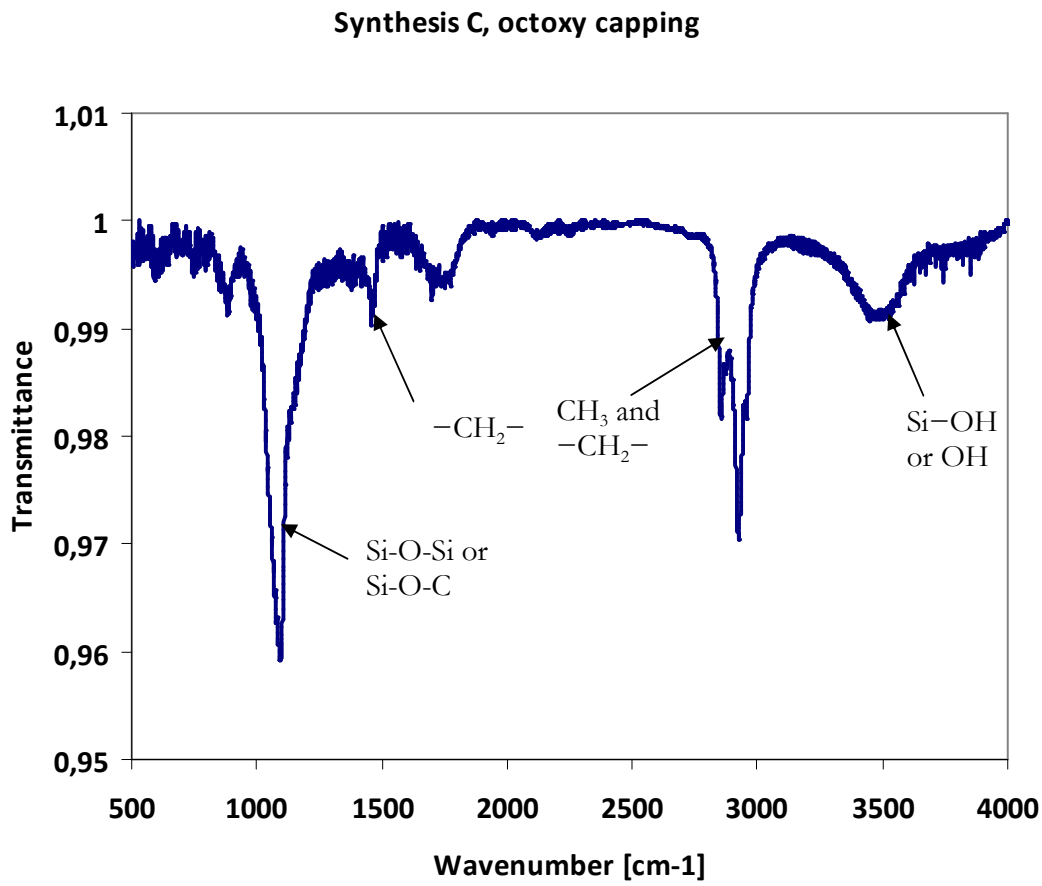

Figure 4.12: FTIR spectrum of product C−1, measured on a KBr pellet.

4.3.2. Oxidised acrylic acid capping (C−3 (ox))

The quantum dot dispersion to which acrylic acid was added formed a white precipitate which looked very similar to silica as the capping agent was introduced to the quantum dot dispersion, the liquid phase became opaque immediately. Because of this, product C−3 (ox) was not investigated on a holey carbon grid in the STEM since it was assumed that the quantum dots were oxidised and agglomerated.

Determination of surface chemical structure

The FTIR spectrum of product C−3 (ox) is shown in Figure 4.13, measured on a dried KBr pellet. Worth to note from this spectrum is that the bands around 2800−3000 cm^{-1} representing the alkane chain have very low intensities in this spectrum. This is an indication that the quantum dots have oxidised.

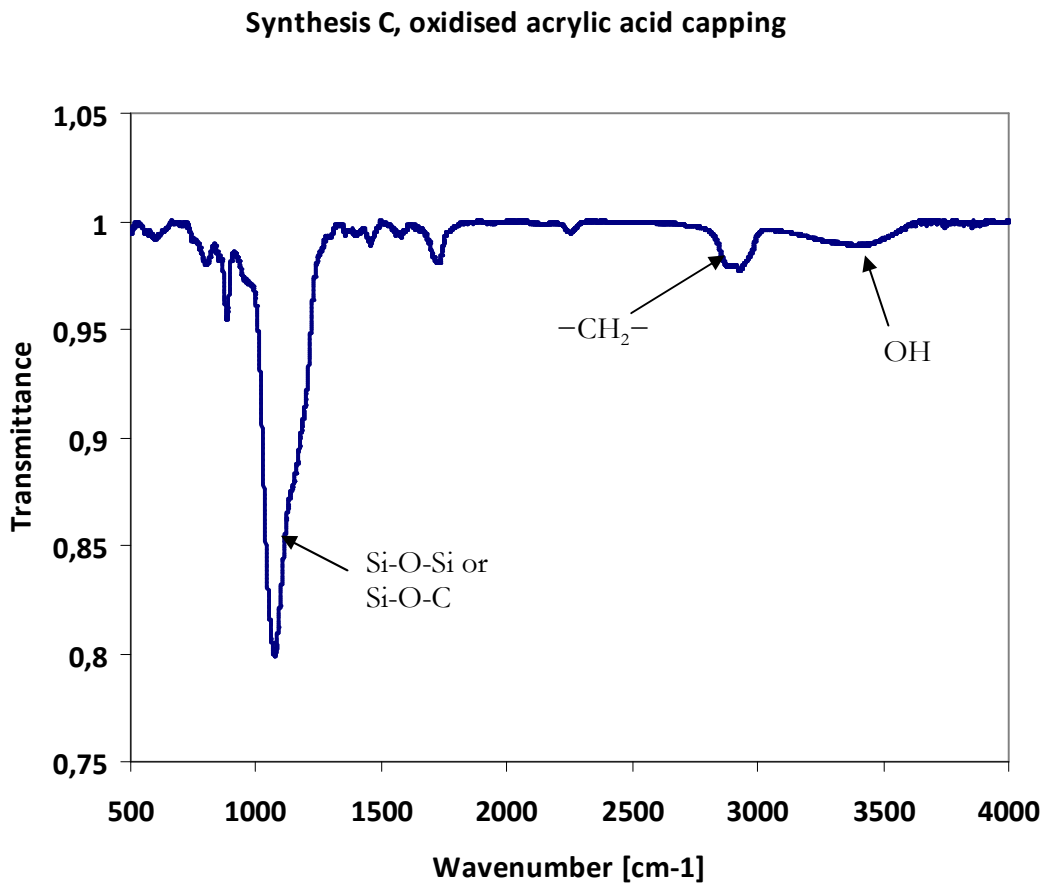

Figure 4.13: FTIR spectrum of product C−3 (ox), measured on a KBr pellet.

4.3.3. Ethanolamine capping (C−4)

Size distribution and degree of agglomeration

The product of synthesis C−4 (a) was dispersed on a holey carbon grid and investigated in the S(T)EM. Images from this characterisation are shown in Figure 4.14. Here, one can see that there were some quite large particles (on average about 50 nm in diameter) evenly spread on the grid. Instantly, some smaller particles could be observed inside the larger ones. These particles were not at all stable as the electron beam hit them, since they disappeared after being exposed to the electron beam for five seconds.

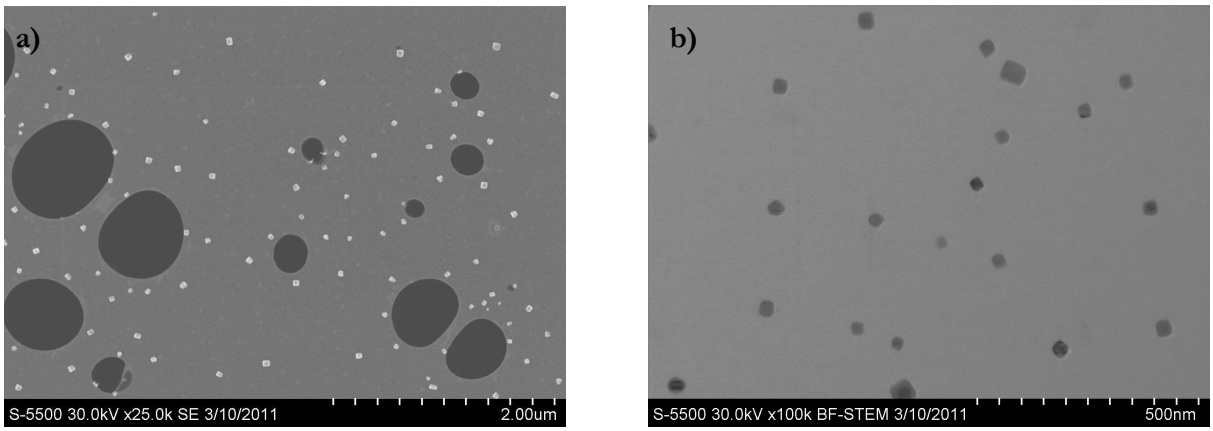

Figure 4.14: a) SEM image of product C−4 (a) on a holey carbon grid. **b)** STEM bright field image of the same sample.

EDS spectra were recorded at a point in the middle of one of the observed particles and also at a point where no particle was observed. The resulting EDS spectra are shown in Figure 4.15a and b, respectively. It is apparent from these spectra that the observed particles contain more potassium, chlorine, oxygen and silicon than other places on the grid. Both EDS spectra show certain amounts of aluminium and copper, which can be ascribed to the sample holder and to the supporting grid, respectively. These are the only peaks observed in Figure 4.15b. This observation indicates that the observed material on the grid consists of agglomerated particles containing some silicon compound together with byproducts from the synthesis containing K and Cl.

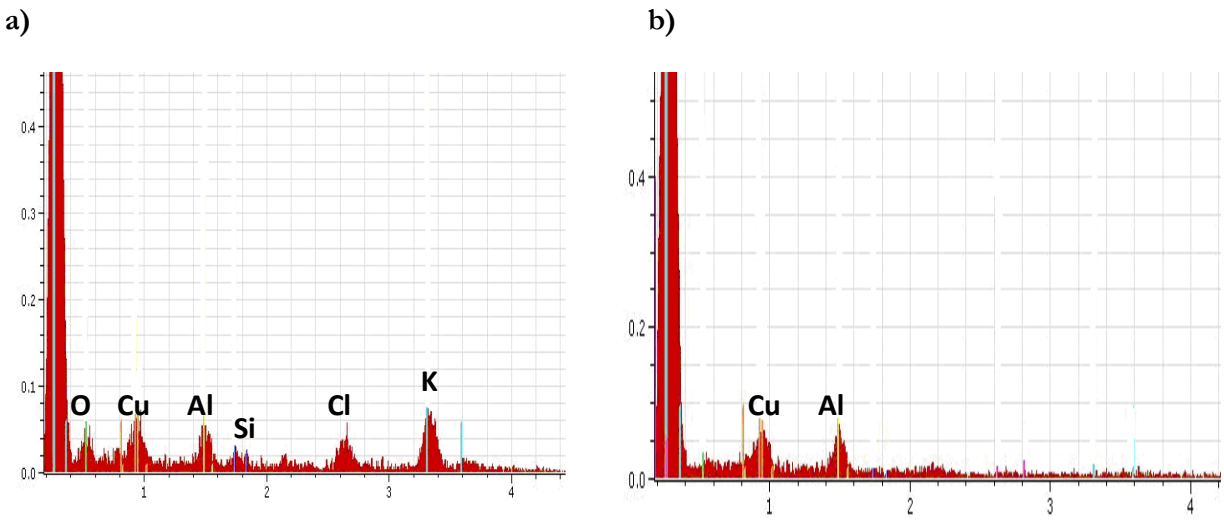

Figure 4.15: a) EDS spectrum recorded in the middle of one of the dark particles observed on the holey carbon grid during the investigation of a sample from synthesis C−4 (a), showing signals for O, Si, Cl and K. **b)** The EDS spectrum of the same sample, recorded outisde one of the dark particles, only showing peaks for Cu and Al, from the supporting grid and the sample holder, respectively.

Because of this apparent agglomeration of the product, the synthesis involving capping with ethanolamine was reproduced, resulting in product C−4 (b). This was done in case it was just a coincidence that the synthesis was not successful. The product of synthesis C−4 (b) was also

characterised in the STEM on a holey carbon grid. Exactly the same type of particles were observed during this characterisation.

Determination of surface chemical structure
The FTIR spectrum of product C−4 (a) was recorded. However, it turned out that the dispersion reacted with the KBr pellet, and the spectrum is because of this not included here.

4.4. Deposition of quantum dots on solid substrates

4.4.1. Deposition on Si substrate

CdSe quantum dots
Commercial CdSe quantum dots in a toluene dispersion were deposited on Si substrates. More on the results of this study are attached in Appendix C. Toluene does not wet a silicon surface very well. When toluene dispersions were forced to spread on a substrate which they did not wet, a thin liquid film formed on the substrate, which ruptured into a collection of droplets during the drying process. The film reached a final stage of disconnected droplets which formed a polygonal droplet pattern within hours. Between the droplets, strings of deposited material were observed, and these strings consisted of even smaller droplets.

Because of the bad wetting of Si substrates with toluene, it was tried to dilute the QD dispersion with ethanol which wets the Si surface much better than toluene does. However, diluting with ethanol resulted in agglomeration of the quantum dots and cloudy dispersions, even when adding some droplets of hydrochloric acid to the ethanol before the addition of the quantum dot dispersion. No difference could be observed in the degree of agglomeration for samples which had been deposited by solvent evaporation and spin coating. Because of this observation, the focus for the deposition process was put on the solvent evaporation technique since this was a simpler approach.

All the attempts for the deposition of quantum dots showed that avoiding agglomeration of the quantum dots was very challenging. An SEM image from the study of CdSe quantum dots is included in Figure 4.16 to show how these agglomerates appeared on the substrate. EDS spectra were used to confirm the presence of the quantum dots. From the EDS investigations it was concluded that the plasma cleaning provided too severe conditions for the quantum dots, because the signals for the quantum dot elements were lost when recording EDS spectra after the plasma cleaning.

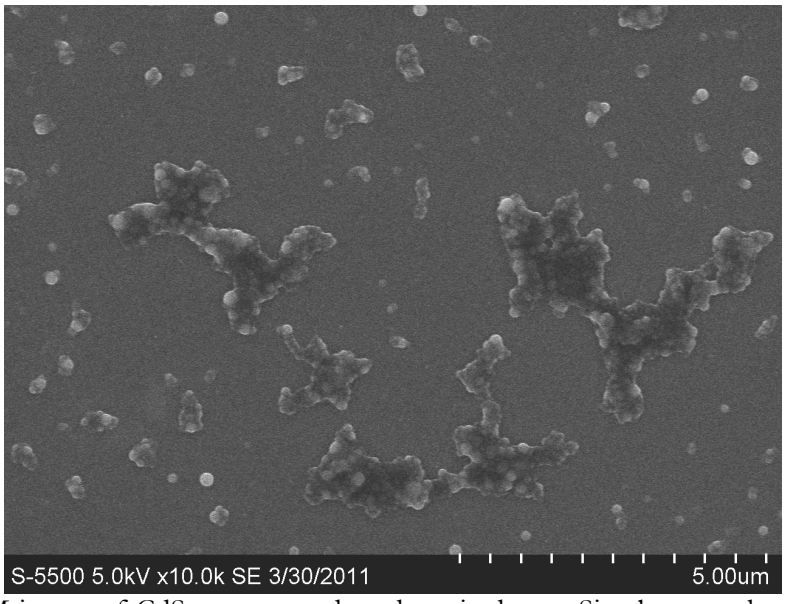

Figure 4.16: SEM image of CdSe quantum dots deposited on a Si substrate, showing the observed agglomerates.

Synthesis A−1

Octoxy capped quantum dots from synthesis A−1 were deposited onto plasma cleaned Si substrates, followed by evaporation of the solvent. When these quantum dots were dispersed on holey carbon grids and investigated in the STEM, well dispersed particles were observed on the grid, as can be observed in the STEM image in Figure 4.1. On the silicon wafer however, the liquid did not evaporate when heating the sample to 120 °C, so that the sample could not be investigated in an SEM afterwards. Because of this slow evaporation, plasma cleaning was performed also after the deposition despite the rigorous conditions provided during the treatment. This was done in order to be able to characterise the sample. An SEM image and the belonging EDS spectrum from this characterisation are given in Figure 4.17. The EDS spectrum was recorded on one of the observed particles, marked with the green cross in Figure 4.17a. Since the most intense peak in the EDS spectrum stems from oxygen and the particles are charging up, oxidation probably takes place during the plasma cleaning, but more important is it that only very large particles were observed on the substrate. However, these might be quantum dots which have agglomerated when they were deposited onto the Si substrate. Since EDS spectra were used to confirm the presence of quantum dots on the substrates, silicon is not the best substrate to use when investigating Si nanoparticles.

a) **b)**

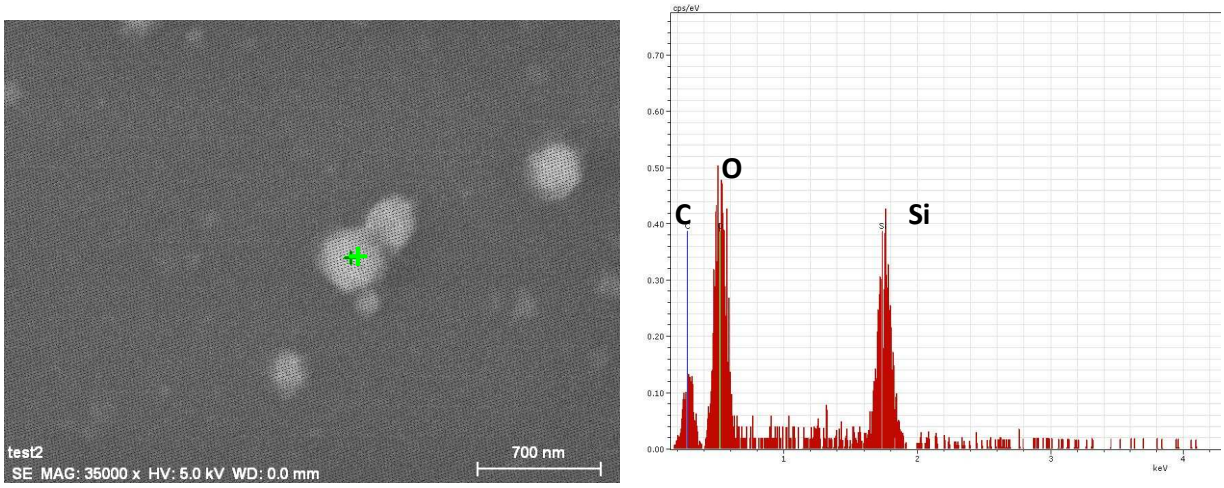

Figure 4.17: a) SEM image of product A−1 deposited on a Si substrate and **b)** the corresponding EDS spectrum. The spectrum is recorded at the position of the green cross, i.e. in the middle of one of the observed particles, showing signal from C, O and Si.

Synthesis C−1

Silicon quantum dots from synthesis C−1 were also characterised after deposition onto plasma cleaned silicon substrates, followed by solvent evaporation. When these quantum dots were investigated on holey carbon grids, well dispersed particles could be observed, as shown in the STEM images in Figure 4.10. The hexane/chloroform dispersion did not wet the silicon substrate well, having a tendency to form droplets on the surface which were moving over the substrate as the solvent evaporated. This resulted in a very inhomogeneous layer on the wafer, only smaller areas of the wafer were covered of material as a result of the droplet formation. An SEM image of one of those covered areas is shown in Figure 4.18a. This structure looks as if it consists of agglomerated particles. An EDS spectrum was recorded where this structure was observed, shown in Figure 4.18b. The EDS spectrum confirms the presence of Si, C and O. Because of the relatively large intensity for oxygen, the eventual quantum dot agglomerates are probably oxidised. Another explanation is that the observed material is a silicon alkoxide, which is a possible byproduct from the synthesis, formed by a direct reaction between silicon tetrachloride and octanol. It was also tried to deposit these quantum dots by spin coating, but then nothing was left on the substrate afterwards and it was assumed that the dispersion had been totally centrifuged away from the substrate during the spinning.

a) b)

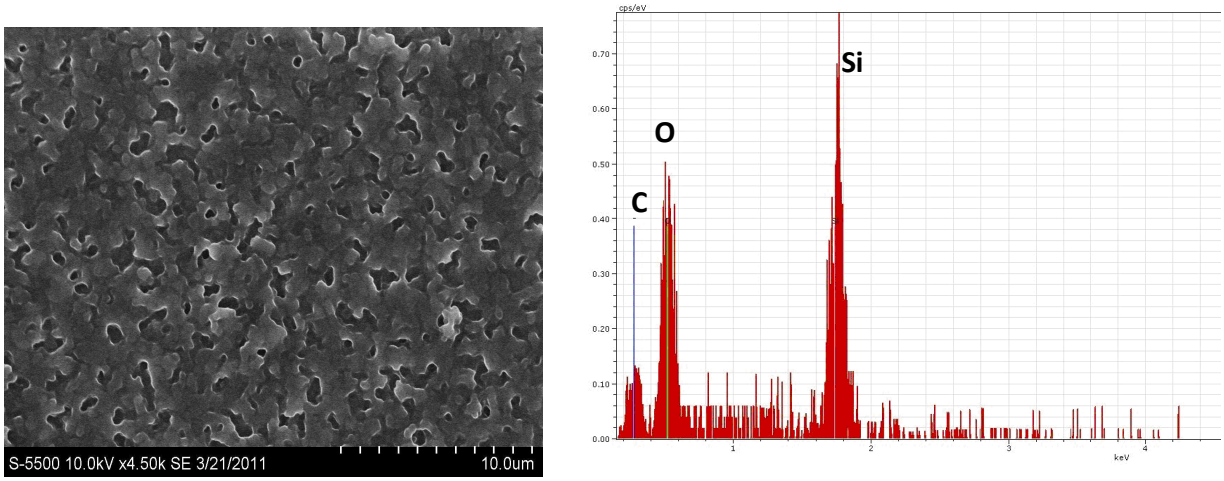

Figure 4.18: a) SEM image of covered area on the silicon wafer after deposition of product C−1 which was dispersed in a mixture of hexane and chloroform (3 : 1). **b)** The corresponding EDS spectrum, showing the presence of C, O and Si.

Synthesis A−2 (ox)

Silicon quantum dots from synthesis A−2 (ox) were deposited on silicon substrates, followed by solvent evaporation. These quantum dots were dispersed in ethanol which was wetting the Si substrate well. An image after the deposition is provided in Figure 4.19, and some regular crystals which were charging up could be observed on the substrate surface. This product has not been washed with water because of the expected water solubility of the quantum dots. These crystals are probably KCl crystals, which are believed to be the most important byproduct from the synthesis.

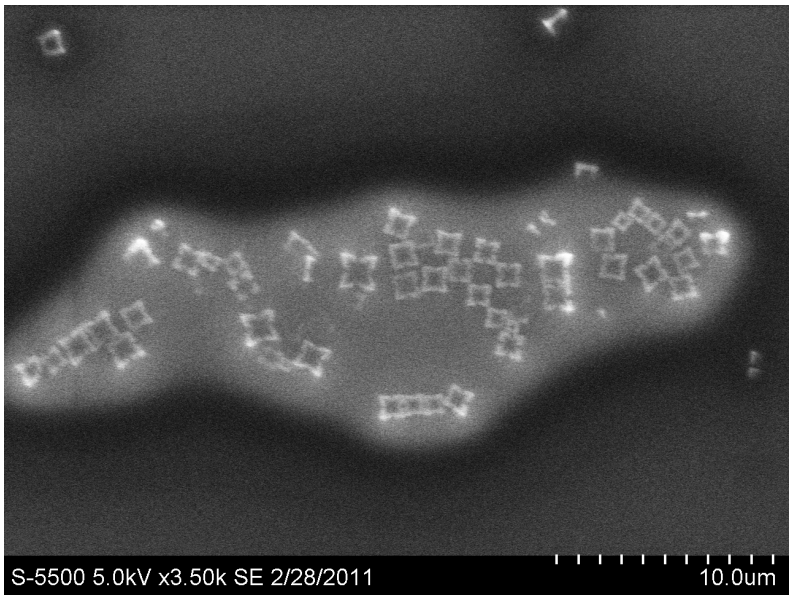

Figure 4.19: SEM image of product A−2 (ox) dispersed in ethanol, deposited on a silicon wafer.

4.4.2. Hydrophobic Si substrate

Because of the large extent of agglomeration and the bad wetting, it was tried to make the Si substrate hydrophobic before the deposition of octoxy capped silicon quantum dots. This improved the wetting of the substrate with the hexane/chloroform dispersion significantly.

Synthesis A−1

However, for the quantum dots from synthesis A−1, the liquid after the deposition did not evaporate when heated in a vacuum furnace at 120 °C. The temperature was further increased, and after heat treatment at 200 °C overnight, the liquid evaporated. A cracked layer was left on the substrate, which could not be investigated in the SEM because of beam damage. This layer was investigated by diffuse reflectance measurement in order to obtain some optical information from the material possibly explaining what it was, but no signal was obtained from the thin layer by this technique. The FTIR spectrum from the powder of this film is shown in Figure 4.20, showing bands for Si−O−C/Si−O−Si, the alkane chain and hydroxyl groups. All the bands present were also there in the FTIR spectra recorded from the quantum dot dispersion and indicate the presence of quantum dots in this film. The FTIR bands were discussed when presenting the spectra for the quantum dots in Section 4.1.1.

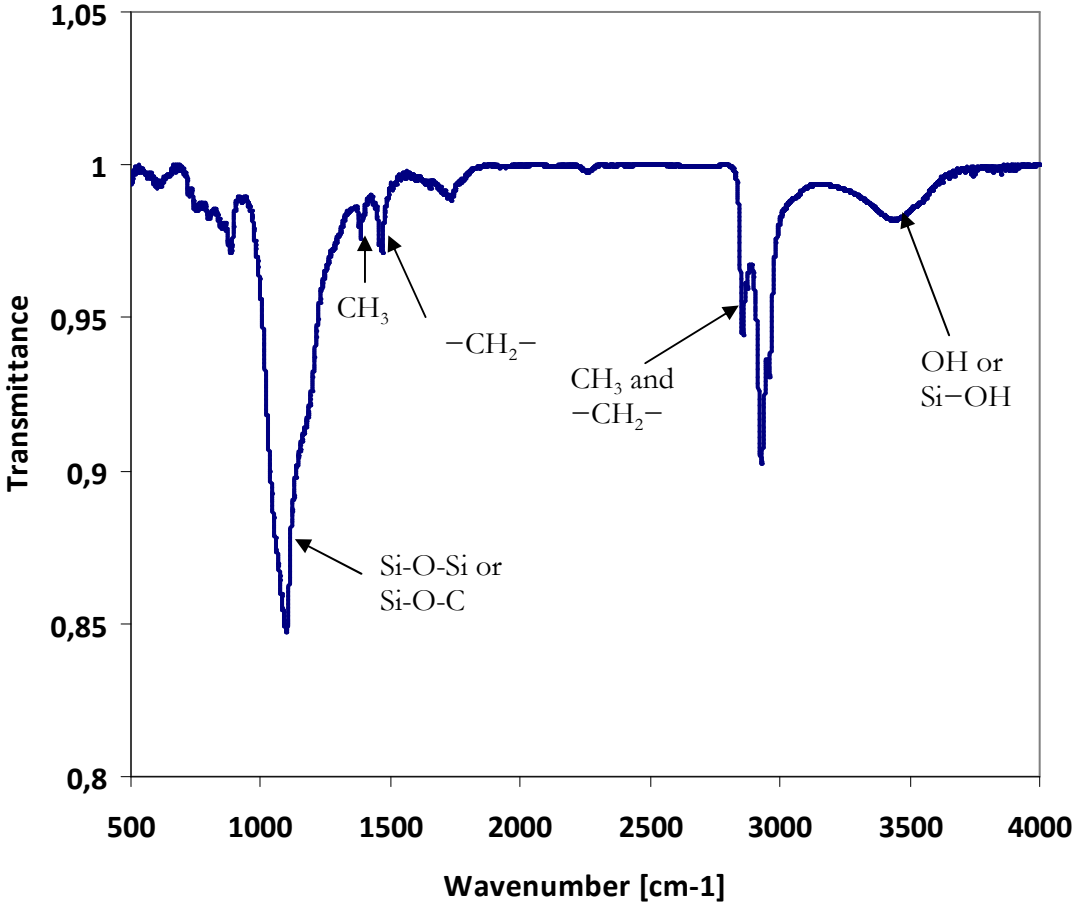

Figure 4.20: FTIR spectrum of the film after deposition of product A−1 on a hydrophobic Si substrate and heat treatment in a vacuum furnace at 200 °C overnight.

Synthesis C−1
When depositing quantum dots from synthesis C−1 on hydrophobic silicon substrates, the liquids evaporated upon heat treatment of the sample at 120 °C for four hours. Agglomerates still formed and were observed, as shown in Figure 4.21. Different concentrations and amounts deposited were investigated, but agglomerates like these were observed in every case. When this dispersion was spin coated onto a substrate, nothing was left on the surface afterwards.

a) **b)**

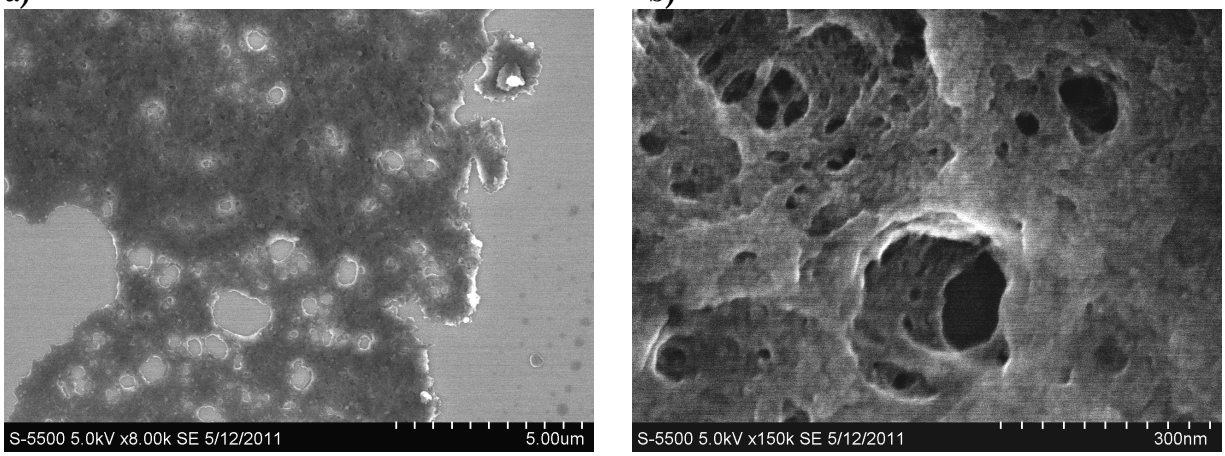

Figure 4.21: a) and **b)** SEM images of the quantum dot dispersion from synthesis C−1, showing agglomerated particles. Deposited on a hydrophobic Si substrate, followed by solvent evaporation.

4.4.3. Deposition on Al substrate

It was also tried to deposit quantum dot dispersions onto Al substrates, so that EDS could be used to confirm the presence of Si, and to see if it was easier to disperse the quantum dots on a different material because of the different nature and wetting of the substrate.

Synthesis A−1
Because the dispersion of product A−1 did not evaporate readily from the Si substrate, this was also expected to be the case when depositing the quantum dot dispersion onto an Al substrate. Due to this, the deposition was not done for sample A−1.

Synthesis C−1
The liquids after deposition evaporated when heat treated in a vacuum furnace at 120 °C for four hours. SEM images of different magnifications are shown in Figure 4.22. The belonging EDS spectrum to the image in Figure 4.22b is shown in Figure 4.23. The sample did not cover the substrate homogeneously; some regions were almost not covered at all, whereas quite thick layers with agglomerates were observed at other places. The images in Figure 4.22 are taken at positions which were well covered of sample. The EDS spectrum indicates that the observed particles consist of silicon, carbon and oxygen.

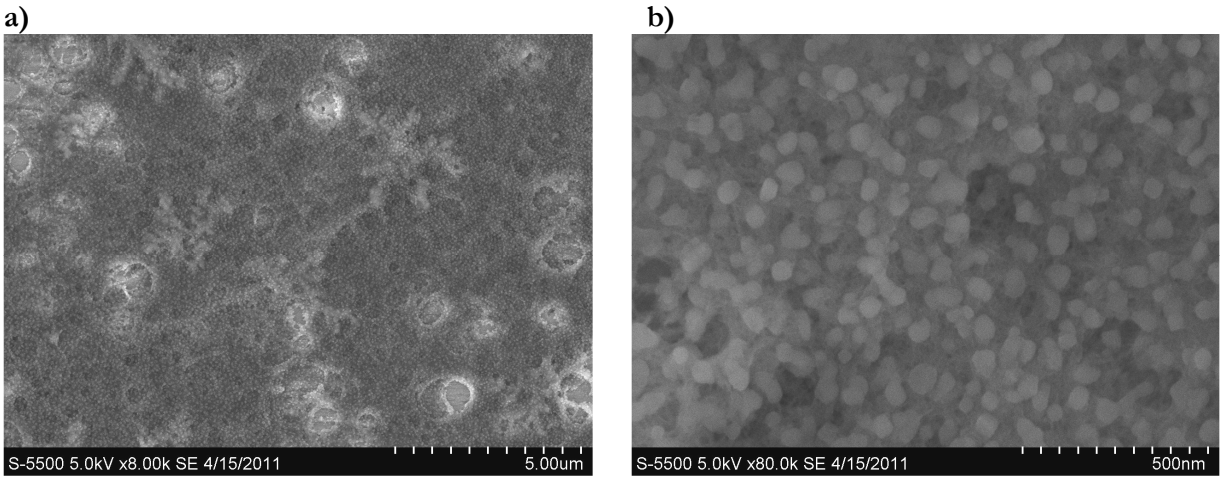

Figure 4.22: SEM images of product C−1. Solvent evaporation from Al substrate, followed by drying at 120 °C in a vacuum furnace. **a)** Overview image and **b)** an image with a higher magnification, showing agglomerated particles.

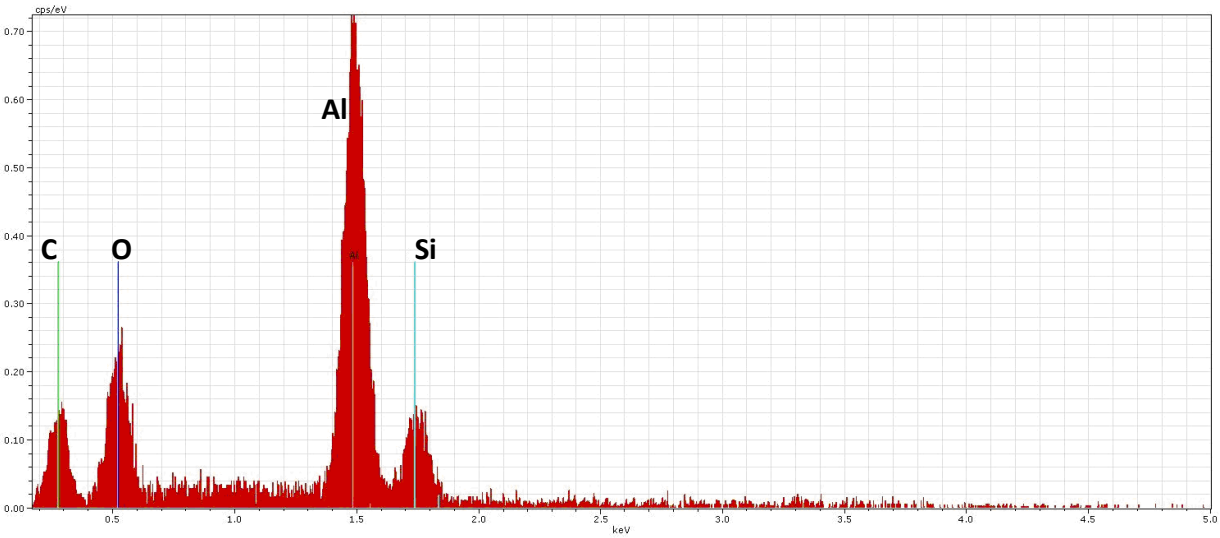

Figure 4.23: EDS spectrum corresponding to the SEM image in Figure 4.22b. Si Quantum dots from synthesis C−1 deposited onto an Al substrate.

At some places, some kind of structures was observed as a second phase above the agglomerates shown in Figure 4.22b. This phase is imaged in Figure 4.24. When an EDS spectrum was recorded at the position of this second phase, it showed peaks for potassium and chlorine, in addition to the peaks observed for the layer below. This EDS spectrum is given in Figure 4.25. Because of the signal from potassium and chlorine, it was assumed that this structure consisted of potassium chloride or the crown ether salt $K^+(15C5)_2Cl^-$, which was a byproduct from the alkalide synthesis. Further investigations are required to say which of these two salts were present.

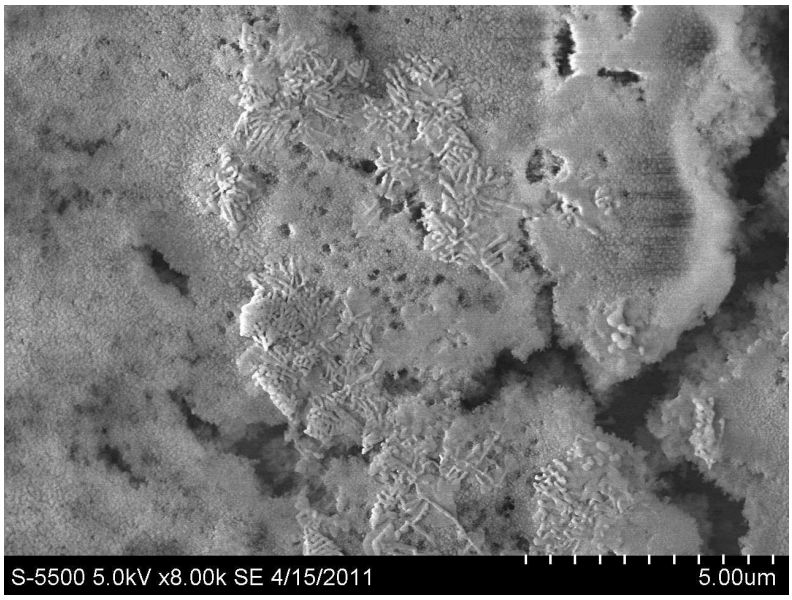

Figure 4.24: Material observed when the Si quantum dot dispersion of synthesis C−1 was deposited on an Al substrate.

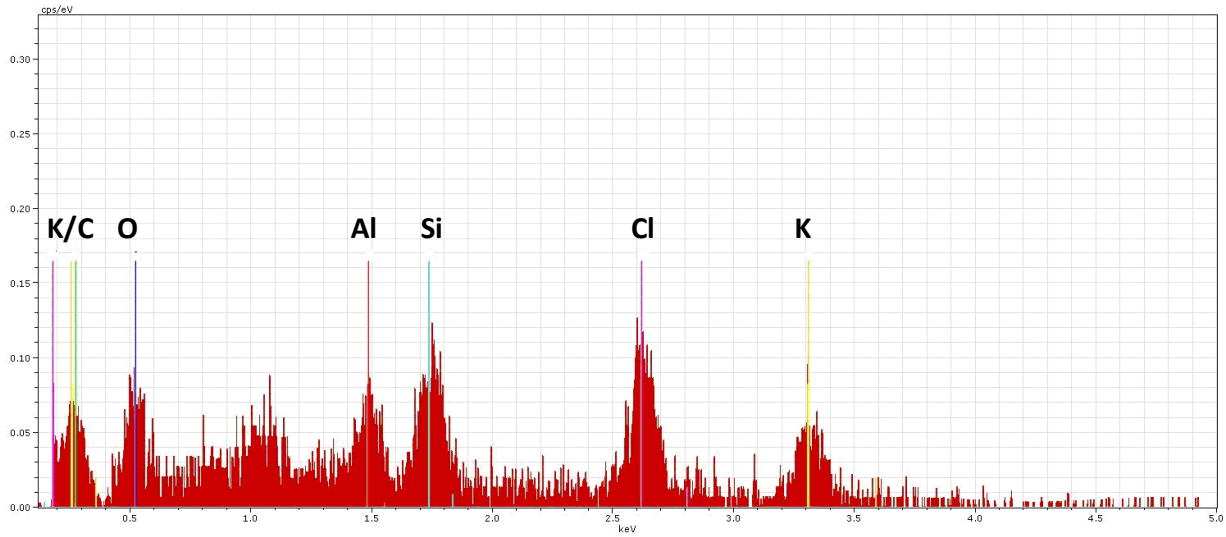

Figure 4.25: EDS spectrum of the dendritic structures imaged in Figure 4.24.

When smaller amounts (5 µl) of the quantum dot dispersion was deposited onto the Al substrate, the same type of agglomerates were observed on the surface as when larger amounts were deposited. However, the layer formed was somewhat thinner, and the agglomerates were slightly better separated from each other for lower amounts of dispersion deposited.

5. Discussion

5.1. Quality of quantum dots

5.1.1. Synthesis methods

Three different synthesis methods were utilised to synthesise silicon quantum dots. All of them were based on reduction of silicon tetrachloride with a reduction agent in homogeneous solution. The method involving reduction of silicon tetrachloride with potassium naphthalide was the most well known synthesis among the methods utilised here. Control over the size of the quantum dots prepared by this method has been obtained by adjusting the concentration of the reduction agent and duration of the reduction reaction [17]. For the alkalide synthesis, further work is required to be able to control the reaction completely, since the dissolution of potassium depends greatly on the concentration of the complexing agent and metal in the solvent. The correct balance between the reactants is demanding to predict and has to be derived from experience. This challenge is avoided in the sodium cyclopentadiene synthesis, since the metal is already dissolved and the concentration of metal is more certain. However, other challenges arise with this synthesis, related to the removal of unknown byproducts.

5.1.2. Functionalisation

For each of the synthesis methods, different functionalisations were investigated. The surface cappings were confirmed by FTIR spectroscopy, showing that quantum dots with different functionalisations had been successfully synthesised.

The band for OH or Si−OH for a wavenumber around 3400 cm^{-1} was present in the FTIR spectra for many of the samples. This band did also show up when an oxidation was not intended. It can not be distinguished between OH because of oxidation of the quantum dots, OH as a functional group and OH due to molecular adsorption of water on the KBr pellet due to humidity in the air. The trend was that for all the dispersions which had been washed with water, this band around 3400 cm^{-1} appeared. This may indicate that contact with water induced an oxidation process for the quantum dots, even when the time of contact with water was very short. The washing did not last any longer than ten minutes. It was also observed that for samples which had been washed with water, and the FTIR spectrum was recorded two weeks after the synthesis was performed, then the OH band got higher intensity in the spectra. One can therefore assume that oxidation of the quantum dots took place over time.

It was found that recording FTIR spectra from liquid samples contained between KBr windows could be useful when one is suspicious of oxidation upon heating. From the difference between the liquid and solid spectra in Figure 4.9, it was believed that oxidation took place when the sample was heated because of the arising band around 1720 cm^{-1}, indicating oxidation of the double bond. However, when interpreting liquid spectra, one should always be aware that the bands which show the functionalisation of the quantum dots tend to overlap with the bands for the liquids or residues of the liquids present in the liquid mixture. No significant difference in the Si−O−C/Si−O−Si around 1100 cm^{-1} was observed between the FTIR spectra recorded on the quantum dot samples and the FTIR spectrum of amorphous silica, so that this band alone could not be used to say whether the quantum dots were oxidised or not. Other bands, like the alkane bands slightly below

3000 cm^{-1}, should be taken into consideration when making a statement about oxidation, since these bands are not present for silica. However, both the alkane bands and the band between 1000 and 1100 cm^{-1} will be present for silicon alkoxides. These are compounds of silicon and an alcohol, and could maybe be formed as a byproduct when octanol is added for functionalisation of the quantum dots. This compound can not be distinguished from quantum dots just by considering their FTIR spectra, since the same bands will be present for both.

Even though the potential for using silanisation for the functionalisation of silicon quantum dots is promising, silanisation of quantum dots is somewhat limited by the commercial availability of adequate silanisation agents which provide water dispersibility. Silanisation also requires a relatively complicated synthesis procedure, which is difficult to control completely. Additionally, the quantum dot surface situation changes once silanising the surface and results in quantum efficiency decrease and altered optical properties for the quantum dots [33].

5.1.3. Purification

Silicon is especially oxophilic and reactive, making it difficult to separate the solvent and the byproducts without some oxidation. While the noble metals and some others such as Cu and Te can be separated from the water soluble byproducts (KCl/NaCl and the crown ether salt for the alkalide synthesis) by washing with methanol, more oxophilic metals like Si are oxidised by this procedure [28]. Other ways have to be found to obtain a pure product of non-noble metals. One possibilty is to wash with liquid ammonia without metal oxidation, but the low solubility of especially KCl in ammonia requires multiple washings. Other anions such as Br^- may improve the ability to wash away the byproducts. The reactive nature of nanoscale metals and the large surface area can lead to the inclusion of organic residues on the surface. This can be reduced by heating the samples to 100−150°C under vacuum. Vacuum heating could also remove some of the other impurities which are not water soluble. Such procedures, coupled with other washing solvents should improve the purity. With very oxophilic metals like silicon it might not be possible to prevent oxidation by reaction with the complexant or solvent.

Water dispersible quantum dots could not be purified by the normal procedure used for the hydrophobic quantum dots. The reason to this was that the most important byproducts KCl, NaCl and the crown ether salt were also water-soluble, so that the difference in solubility of the quantum dots and the byproducts could not be utilised for purification of the product. When the byproducts could not be removed from the quantum dot dispersion, this certainly affected the quality of the product significantly. However, when the method for making water dispersible quantum dots involved a two-step procedure, like for the pentenoxy capping and the following oxidation of the terminating double bond, there is an option for purification. This possibility involves washing with water in between the two steps, when the quantum dots are still hydrophobic with their double bonds, but before the oxidation with water which renders them water dispersible. Even though this method brings about oxidation of the quantum dots, it is better than no purification at all.

5.1.4. Water dispersible quantum dots

Synthesis of water dispersible quantum dots appeared to be much more demanding than the synthesis of hydrophobic quantum dots also for other reasons than the purification. It is a challenge to obtain water solubility of quantum dots prepared in organic solvents, since the water dispersible

capping does not necessarily mix with the organic solvent used in the synthesis. This problem could eventually be avoided by evaporation of the solvent before the addition of capping agent, but this would probably introduce other problems. This method tends to yield agglomerated particles which stick to the wall of the reaction flask. Additionally, the risk of introducing air or moisture to the quantum dots, which are very sensible when they are not yet capped and all the liquid is evaporated, will be quite large during the evaporation and addition of the capping agent.

Another problem with the water dispersible quantum dots is that these nanoparticles are not stable over time when stored in ethanol. This was observed from the STEM and TEM images in Figure 4.4 and Figure 4.5, since the degree of agglomeration was significantly larger after the dispersion had been stored for two weeks. For common nanoparticles, the elemental forces between the particles are van der Waals forces, however, for nanoparticles with polar groups, there is another strong interaction, hydrogen bonds, owing to the hydroxyl groups on the nanoparticle surface. The OH groups are interacting quite strong with other hydroxyl groups, and the existence of the hydrogen bonds will affect the dispersion and may also result in agglomerated particles [42].

If quantum dots which are dispersed in ethanol are not completely functionalised, i.e. there is some available space for molecules to attack the surface, ethanol can start to act as a capping agent rather than a dispersing medium. The quantum dots will then be partly functionalised with ethoxy groups. This is one of the reasons to why water dispersible quantum dots contained in ethanol are not stable over time. There will be water molecules present in this system, which may contribute to attractive interactions and agglomeration between quantum dots which are still functionalised with OH groups from the oxidised pentenoxy capping. A simplified illustration of the interaction between particles and the capping with ethanol is provided in Figure 5.1.

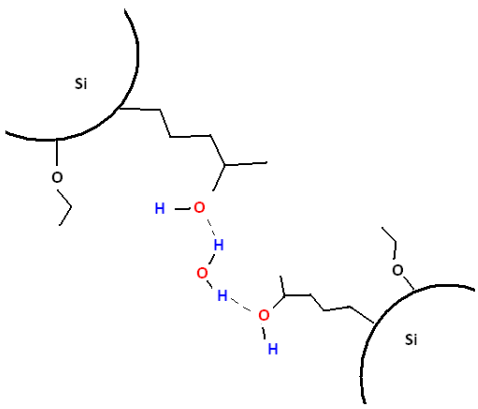

Figure 5.1: Illustration of how water molecules can act as a bridge between two water dispersible quantum dots and contribute to agglomeration. When dispersed in ethanol, the quantum dots can be functionalised with ethoxy groups if the original capping is not dense enough.

Another challenge for hydrophilic quantum dots is their optical stability. Prtljaga et al. [18] studied the optical properties of water dispersible silicon quantum dots, and found that silicon nanoparticles lack long-term photoluminescence stability in aqueous solutions due to a rapid and efficient surface oxidation.

5.2. Deposition of quantum dots on solid substrates

There are several important factors which influence the deposition process of a quantum dot dispersion on a solid substrate. Among them are the spontaneous tendency of the molecules to agglomerate, the evaporation of the solvent, the wetting properties between the solution and the substrate, the temperature, the concentration of nanoparticles in the dispersion and the byproducts present. The process is initiated once the solution is deposited on the substrate and the solvent starts to evaporate. Manipulation of the deposition process of quantum dots on a substrate requires control over the evaporation rate of the solvent and the temperature of the solvent.

It was observed that the structure of the deposited material on the substrates was always quite random. Large amount of agglomerated particles could be observed at some sites, whereas at other places no material could be observed at all. This might be due to the dynamics of the solvent evaporation process. This process is characterised by instabilities, in particular at its last stages when the solvent layer becomes sufficiently thin. The thin solvent layer is subject to convection, capillary waves and dewetting processes in which the layer ruptures into isolated solution droplets and "dry" regions free of solvent molecules [43]. These processes naturally lead to a random deposition, reducing the quality of the deposited material and limit the control over the deposition process.

5.2.1. Agglomeration

The octoxy capped quantum dots and the CdSe quantum dots [9] were well dispersed when deposited on holey carbon grids, which means that the quantum dots should also be well dispersed as contained in their respective dispersions. However, a homogeneous distribution was much more difficult to achieve when the same quantum dot dispersions were deposited on solid substrates, as agglomeration happened to a large extent for this kind of deposition. The probably most important reason to this altered behaviour on different surfaces is simply the changed nature of the substrate, leading to different interactions between particles and the substrate. Surface treatment of the substrate can control the binding of particles onto substrates to a large degree.

Agglomeration upon deposition onto solid substrates happens when the attractive van der Waals forces are stronger than the repulsion between the quantum dots in the dispersion, and the interactions between the particles are stronger than the interactions favouring attraction between the substrate and the nanoparticles. The functionality of the quantum dots control the interactions between nanoparticles to a large extent. For instance, long organic chains on the surface like octoxy capping provide steric hindrance towards agglomeration whereas short polar groups often have a tendency to stick more together. Another way to control the attractive forces between the particles is to introduce interparticle repulsion by charging up the quantum dots, which will keep the nanoparticles apart from each other by electrostatic repulsion and prevent them from gathering. The concentration of quantum dots in the dispersions will also have an effect on the degree of agglomeration, as there are more interactions between particles for higher concentrations. However, agglomeration was still observed when very dilute dispersions were deposited on the substrates.

5.2.2. Influence of solvent and wetting of the substrate

The type of solvent plays an important role in this kind of deposition, determining how fast the evaporation and growth takes place. As the solvent evaporates, the nanoparticles are moving on the substrate, determined by their interaction with the liquid, with each other and with the substrate. Adjacent nanoparticles tend to attract each other and aggregate in the absence of liquid. Because of this, solvent evaporation triggers the onset of agglomeration, after which the mechanism of growth is determined by nanoparticle diffusion. Nanoparticles have a very low mobility on a dry surface. Agglomeration is more pronounced when the solvent evaporates fast, and a very fast evaporation will destabilise the entire system. Generally, slow evaporation and growth is important to obtain ordered structures of quantum dots on substrates [36]. Because of this, it is an advantage to use a solvent which is not very volatile. The boiling points for the different solvents used are given in Table 5.1.

Table 5.1: Overview over the boiling point for the solvents used for the quantum dot dispersions which were deposited on solid susbtrates.

Solvent	Boiling point [°C]
Toluene	111
Ethanol	79
Hexane	69
Chloroform	61

Hexane and chloroform both have quite low boiling points, probably leading to a too fast evaporation to be able to obtain well dispersed quantum dots on the substrate. This was also observed during the experiments, as the evaporation happened more controlled when CdSe quantum dots dispersed in toluene were dispersed on the substrate, due to the higher boiling point. Despite this slower evaporation, agglomeration still happened. This could be explained by the strong attractive forces between the particles or by bad wetting of toluene on a silicon surface.

Wetting was another important consideration when the quantum dot dispersions were deposited on the substrates. Wetting is the ability of a liquid to maintain contact with a solid surface, resulting from intermolecular interactions when the two are brought together. Wetting is defined by a contact angle of less than 90 ° between the fluid and the substrate, illustrated in Figure 5.2. A non-wetting fluid will be repelled by the substrate. If quantum dots are dispersed in a solvent which is not wetting the substrate, this will make the dispersion of quantum dots on this surface impossible.

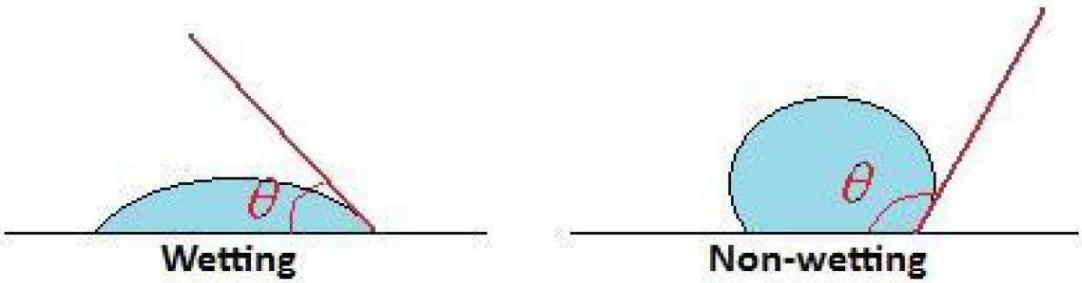

Figure 5.2: Wetting and non-wetting liquid on a solid surface. Wetting is defined by a contact angle of less than 90 ° [9].

What happens after deposition of a liquid onto a solid substrate which it wets badly, is that the thin liquid film on the substrate ruptures and forms droplets, through a process which is called dewetting. The droplet size and droplet spacing may vary over several orders of magnitude, since the dewetting starts from randomly formed holes in the film. There is no spatial correlation between the dry patches that develop. These dry patches grow and the material is accumulated in the rim surrounding the growing hole, forming a polygon network of connected strings of material. These strings then often break up into droplets, a process which is known as the Rayleigh-Taylor instability [44].

The solvent used determines the wetting degree on the substrate surface and consequently the final distribution on the substrate. The wetting was improved significantly when the substrate was made hydrophobic by silylation, and the hexane/chloroform mixture was deposited. However, agglomeration still took place when depositing octoxy capped quantum dots on these hydrophobic substrates, meaning that the fast evaporation characteristics and attractive forces between the particles were probably more important than improved wetting for the agglomerating behaviour of these quantum dots. The type of substrate used did also certainly affect the degree of wetting to a large degree, as seen when the Si substrate was exchanged with an Al substrate. This improved the wetting of the hexane/chloroform dispersion significantly. Surfactants can have a large effect on the wetting properties. When a surfactant is added, it will decrease the interfacial tension and allow wetting to occur.

5.2.3. Byproducts

Impurities were present in the quantum dot dispersions and could be investigated in an SEM after deposition onto solid substrates. Even when the quantum dots had been purified by the washing procedure with water, quite large amounts of byproducts could be observed on the substrate after deposition. This means that the purification procedure used is not sufficient for the complete removal of the byproduct salts, i.e. KCl and the crown ether salt $K^+(15C5)_2Cl^-$ for the alkalide synthesis. This may be due to limited solubility of the byproducts in the water so that the salts did not have the time to dissolve completely during the exposure to water. For the potassium naphthalide synthesis, one of the byproducts was naphthalene. This compound is not soluble in water and could not be removed during the washing procedure. The presence of naphthalene could be the reason to why dispersions prepared via the potassium naphthalide synthesis route did not evaporate when deposited onto substrates. It was expected that naphthalene should sublimate during heat treatment under vacuum at 120 °C, but an even higher temperature is probably needed for the complete removal. The presence of byproducts makes it challenging to characterise the substrates after the deposition of the quantum dot dispersions, and complicates the dispersion of the quantum dots on the substrates.

6. Further work

In further work with water dispersible silicon quantum dots, emphasis should be put on purification of the product and prevention against agglomeration in order to obtain high quality hydrophilic quantum dots and a stable dispersion of hydrophilic nanoparticles. Other dispersing agents than ethanol should be investigated to disperse these quantum dots. These solvents should preferably not be able to act as capping agents.

Improvements of the Si quantum dots are needed to be able to deposit them homogeneously on a solid substrate. These improvements should involve prevention against oxidation and agglomeration of the quantum dots. In further work, alternative washing procedures which do not induce oxidation should be investigated. A different purification procedure is also required for the complete removal of the byproducts from the final quantum dot dispersions. In this respect, the byproducts should be characterised more closely to find an optimal procedure to remove them. X-Ray Diffraction (XRD) and Nuclear Magnetic Resonance (NMR) are characterisation techniques which could probably be utilised for investigation of the quantum dots and the byproducts present in the dispersions.

6.1. Langmuir Blodgett deposition

The Langmuir Blodgett (LB) technique is one of the most promising techniques for preparing thin films of particles as it enables (i) the precise control of the monolayer thickness, (ii) homogeneous deposition of the monolayer over large areas and (iii) the possibility to make multilayer structures with varying layer composition. An additional advantage of the LB technique is that monolayers can be deposited on almost any kind of solid substrate. Amphiphiles or surfactants are the most used molecules for LB deposition, but the technique can also be utilised for functionalised nanoparticles. Such molecules will be aligned the same way on for instance a water surface, and by transferring this monomolecular layer onto a flat solid support by moving the substrate through the layer a Langmuir Blodgett film can form. The principle is illustrated in Figure 6.1.

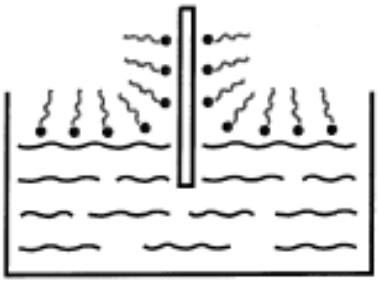

Figure 6.1: A monomolecular layer is formed by spreading amphiphilic molecules on a liquid surface. By moving a substrate through this layer, a Langmuir Blodgett (LB) film can form [45].

Factors that affect the LB film are, among others, the nature of the spread film, the surface pressure during the deposition, the deposition speed and the type and nature of the solid substrate. Careful control over the surface pressure of the monolayer is required during this process. Some preliminary investigations with stearic acid were done in this work with a Langmuir Blodgett trough from Joyce Loebl. This is an apparatus that is used to compress monolayers of molecules on the surface of a

given subphase (usually water) and measures surface phenomena due to this compression. The surface area of the trough is varied by sweeping movable barriers over the surface of the trough.

From the attempt to deposit Langmuir Blodgett films of stearic acid, it was found that even small contaminations can have substantial effects on the results. When an aqueous subphase is used, the water must be purified to remove organics and deionised to a resistivity not less than 18 MΩ/cm. Impurities as small as 1 ppm can radically change the behaviour of a monolayer. To eliminate contamination from the air, the LB trough can be enclosed in a clean room. The trough set-up may also be mounted on a vibration-free table, to further stabilise the monolayer. The exact calibration of the electrobalance which measures the surface pressure is very important for force measurements. This control has now been obtained, and the next step should be to try to deposit a monolayer of a quantum dot dispersion. This could for instance be done on a holey carbon grid followed by TEM or STEM characterisation to see whether the synthesised Si quantum dots can be dispersed by this procedure. This could be included in further work on deposition of Si quantum dots onto solid substrates.

7. Conclusion

Silicon quantum dots with different functionalisations were synthesised. Three different wet chemical methods were utilised for synthesising the quantum dots, they were all based on reduction of silicon tetrachloride with some reduction agent. The reduction agents used were potassium naphthalide, sodium cyclopentadiene and the alkalide of potassium. Both hydrophobic and hydrophilic cappings were investigated; these were functionalisation with octanol, oxidised pentenol, oxidised acrylic acid and ethanolamine. The surface modification of the quantum dots was confirmed by FTIR spectroscopy. TEM investigations showed that the octoxy capped quantum dots were crystalline since lattice imaging of the quantum dots corresponded well with the diamond cubic lattice of Si, further confirming the presence of high quality silicon quantum dots. It was also observed that the dispersion on a holey carbon grid was good and that the quantum dots had an average diameter of approximately 4 nm. It turned out to be more challenging to obtain high quality water dispersible quantum dots mainly because of challenges related to the removal of byproducts, as well as oxidation and agglomeration of the quantum dots in the dispersions.

Because of challenges related to the synthesis of water dispersible quantum dots, it was focused on deposition of the more known hydrophobic silicon quantum dots on solid substrates, mainly performed by solvent evaporation. This was done to find out whether it was possible to deposit quantum dots on solid substrates by this simple approach, to examine the tendency of the quantum dots to agglomerate and for the investigation of the byproducts present in the dispersions. The deposited films were characterised by SEM afterwards, showing that agglomeration played a prominent role for this kind of deposition and that large amounts of byproducts were present in the dispersions. The reason for the tendency to agglomeration was believed to be strong attractive forces between the particles, bad wetting of the solvents on the substrates and a too fast evaporation rate.

After all, improvements of the silicon quantum dots are needed for the application in down conversion layers for solar cells. The refinement should involve prevention against oxidation and agglomeration to increase the stability, as well as removal of the byproducts by finding alternative purification procedures for the quantum dot dispersions.

References

1. Conibeer, G., et al., *Silicon quantum dot nanostructures for tandem photovoltaic cells.* Thin Solid Films, 2008. **516**(20): p. 6748-6756.
2. Tsakalakos, L., *Nanostructures for photovoltaics.* Materials Science and Engineering: R: Reports, 2008. **62**(6): p. 175-189.
3. Richards, B.S., *Luminescent layers for enhanced silicon solar cell performance: Down-conversion.* Solar Energy Materials and Solar Cells, 2006. **90**(9): p. 1189-1207.
4. Zou, J., et al., *Size and Spectroscopy of Silicon Nanoparticles Prepared via Reduction of SiCl4.* J. Cluster Sci., 2006. **17**(4): p. 565-578.
5. Liu, S.-m., *Luminescent silicon nanoparticles formed in solution.* J. Nanosci. Nanotechnol., 2008. **8**(3): p. 1110-1125.
6. Århus, Å., *Wet-chemical deposition of silicon quantum dots for enhanced solar cell efficinecy*, in *Department of Materials Science and Engineering.* 2010, Norwegian University of Science and Technology: Trondheim. p. 56.
7. Markvart, T., *Solar Electricity.* Second ed. 1994, Chichester: Wiley. 280.
8. Evident_technologies, *How Quantum Dots Work.* 2008, Available from: http://www.evidenttech.com/quantum-dots-explained/how-quantum-dots-work.html. Cited: 03.10.2010.
9. Sletnes, M., *Master Thesis*, in *Department of Materials Science and Engineering.* 2009, Norwegian University of Science and Technology: Trondheim. p. 99.
10. Warner, J.H., H. Rubinsztein-Dunlop, and R.D. Tilley, *Surface Morphology Dependent Photoluminescence from Colloidal Silicon Nanocrystals.* J. Phys. Chem. B, 2005. **109**(41): p. 19064-19067.
11. Atkins, et al., *Inorganic Chemistry.* 4th ed. 1990, Oxford: Oxford University Press. 810.
12. Conibeer, G., et al., *Silicon nanostructures for third generation photovoltaic solar cells.* Thin Solid Films, 2006. **511-512**: p. 654-662.
13. Warner, J.H., et al., *Water-soluble photoluminescent silicon quantum dots.* Angew. Chem., Int. Ed., 2005. **44**(29): p. 4550-4554.
14. Sa'ar, A., *Photoluminescence from silicon nanostructures: the mutual role of quantum confinement and surface chemistry.* J. Nanophotonics, 2009. **3**.
15. Kravitz, K., et al., *Solid state synthesis of water-dispersible silicon nanoparticles from silica nanoparticles.* Journal of Solid State Chemistry, 2010. **183**(6): p. 1442-1447.
16. Baldwin, R.K., et al., *Room Temperature Solution Synthesis of Alkyl-Capped Tetrahedral Shaped Silicon Nanocrystals.* Journal of the American Chemical Society, 2002. **124**(7): p. 1150-1151.
17. Balci, M., et al., *Synthesis of Silicon Quantum Dots via Potassium Naphtalide Reduction Route.* 2010, Norwegian University of Science and Technology. p. 2.
18. Prtljaga, N., et al., *Photoluminescence of hydrophilic silicon nanocrystals in aqueous solutions.* Nanotechnology, 2011. **22**: p. 215704 (9pp).
19. Cho, W.-J. and S. Lee, *Synthesis of Silicon Nanocrystals.* Journal of the Korean Physical Society, 2003. **42**: p. pp. S629629~S632.
20. Shirahata, N., S. Furumi, and Y. Sakka, *Micro-emulsion synthesis of blue-luminescent silicon nanoparticles stabilized with alkoxy monolayers.* J. Cryst. Growth, 2009. **311**(3): p. 634-637.
21. Baldwin, R.K., et al., *Solution reduction synthesis of surface stabilized silicon nanoparticles.* Chem. Commun. (Cambridge, U. K.), 2002(17): p. 1822-1823.
22. LaMer, V.K. and R.H. Dinegar, *Theory, Production and Mechanism of Formation of Monodispersed Hydrosols.* Journal of the American Chemical Society, 1950. **72**(11): p. 4847-4854.

23. Dye, J.L., *Alkalides and Electrides*, in *Encyclopedia of Supramolecular Chemistry*, M. Dekker, Editor. 2004: East Lansing, Michigan. p. 8.
24. Dye, J.L. and K.-L. Tsai, *Small Alloy Particles formed by Co-reduction of Soluble Precursors with Alkalides or Electrides in Aprotic Solvents.* Faraday Discuss, 1991. **92**: p. 45-55.
25. Gokel, G.W., *Crown Ethers*, in *Encyclopedia of Supramolecular Chemistry*, M. Dekker, Editor. 2004: St. Louis, Missouri. p. 8.
26. Carey, F.A., *Organic Chemistry*. 7th ed. 2008, Virginia: McGraw Hill. 1229.
27. Jedlinski, Z. and M. Sokol, *Solubility of alkali metals in non-aqueous supramolecular systems.* Pure & Applied Chemistry, 1995. **87**(No. 4): p. pp. 587-592.
28. Tsai, K.-L. and J.L. Dye, *Synthesis, Properties, and Characterization of Nanometer-Size Metal Particles by Homogeneous Reduction with Alkalides and Electrides in Aprotic Solvents.* Chem. Mater., 1993. **5**: p. 540-546.
29. Shiohara, A., et al., *Chemical Reactions on Surface Molecules Attached to Silicon Quantum Dots.* J. Am. Chem. Soc., 2009. **132**(1): p. 248-253.
30. Zou, J. and S.M. Kauzlarich, *Functionalization of Silicon Nanoparticles via Silanization: Alkyl, Halide and Ester.* J. Cluster Sci., 2008. **19**(2): p. 341-355.
31. Zou, J., et al., *Solution Synthesis of Ultrastable Luminescent Siloxane-Coated Silicon Nanoparticles.* Nano Lett., 2004. **4**(7): p. 1181-1186.
32. Yu, W., et al., *Water-soluble quantum dots for biomedical applications.* Biochemical and Biophysical Research Communications, 2006. **348**: p. 781-786.
33. Gerion, D., et al., *Synthesis and Properties of Biocompatible Water-Soluble Silica-Coated CdSe/ZnS Semiconductor Quantum Dots.* The Journal of Physical Chemistry B, 2001. **105**(37): p. 8861-8871.
34. Bréchignac, C., P. Houdy, and M. Lahmani, *Nanomaterials and Nanochemistry.* 2007: Springer.
35. Liu, S., et al., *Evaporation-induced self-assembly of gold nanoparticles into a highly organized two-dimensional array.* Physical Chemistry Chemical Physics, 2002. **4**(24): p. 6059-6062.
36. Shevchenko, E.V. and D.V. Talapin, *Semiconductor Nanocrystal Quantum Dots: Synthesis, Assembly, Spectroscopy and Applications*, ed. A.L. Rogach. 2008, Munich: SpringerWienNewYork. 372.
37. Güleryüz, H., *Investigation of the mechanisms governing the deposition of sol particles on a substrate*, in *Department of Materials Science and Engineering.* 2011, Norwegian University of Science and Technology: Trondheim. p. 155.
38. Richerson, D.W., *Modern Ceramic Engineering.* Third ed. 2006, New York: Taylor & Francis Group. 707.
39. Rabani, E., et al., *Drying-mediated self-assembly of nanoparticles.* Nature, 2003. **426**(6964): p. 271-274.
40. Lee, C.J., G.S. Kim, and S.H. Hyun, *Synthesis of silica aerogels from waterglass via new modified ambient drying.* Journal of Materials Science, 2002. **37**: p. 2237-2241.
41. Mayo, D.W., F.A. Miller, and R.W. Hannah, *Course Notes On the Interpretation of Infrared and Raman Spectra*, ed. N.J. Hoboken. 2003: John Wiley & Sons.
42. Wang, Y., et al., *Aggregate of nanoparticles: rheological and mechanical properties.* Nanoscale Research Letters, 2011. **6**(1): p. 114.
43. Iftach, N., et al., *Laser-induced aligned self-assembly on water surfaces.* The Journal of Chemical Physics, 2009. **130**(14): p. 144704.
44. Rosen, M.J., *Surfactants and Interfacial Phenomena.* 3 rd ed. 2004: John Wiley & Sons, Inc. 444.
45. Schreiber, F., *Structure and growth of self-assembling monolayers.* Progress in Surface Science, 2000. **65**(5-8): p. 151-257.
46. Advanced_Industrial_Science_and_Technology, *Spectral Database for Organic Compounds SDBS.* 2010, Available from http://riodb01.ibase.aist.go.jp/sdbs/cgi-bin/direct_frame_top.cgi cited 15.11.2010: web page.

Appendices

A Lattice spacings in silicon

Some of the lattice spacings in crystalline silicon and their corresponding Miller indices are shown in Table A−1. It is assumed that Si has the diamond cubic structure, with a = 5.43 Å.

Table A−1: Some of the lattice spacings for silicon and the corresponding Miller indices.

Lattice spacing (Å)	**<hkl>**
3.14	<111>
2.72	<200>
1.92	<220>
1.64	<311>
1.36	<400>
1.25	<331>
1.21	<420>
1.11	<422>

1

B−I FTIR spectra

The FTIR spectrum of amorphous silica is given in Figure B−1.

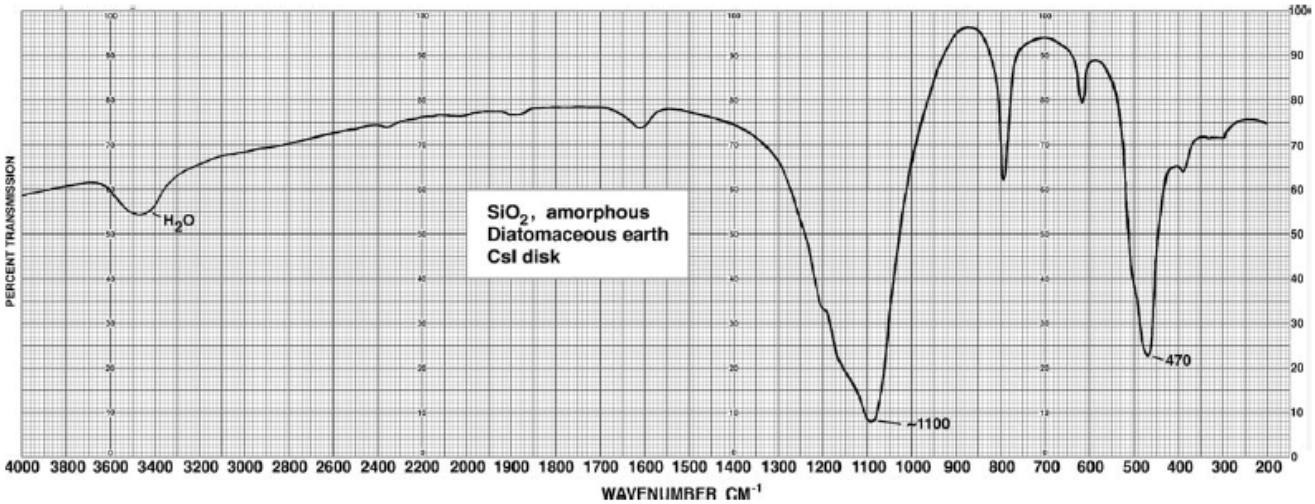

Figure B−1: FTIR spectrum of amorphous silica powder [41].

B−II

The FTIR spectrum of pure ethanol is given in Figure B−2.

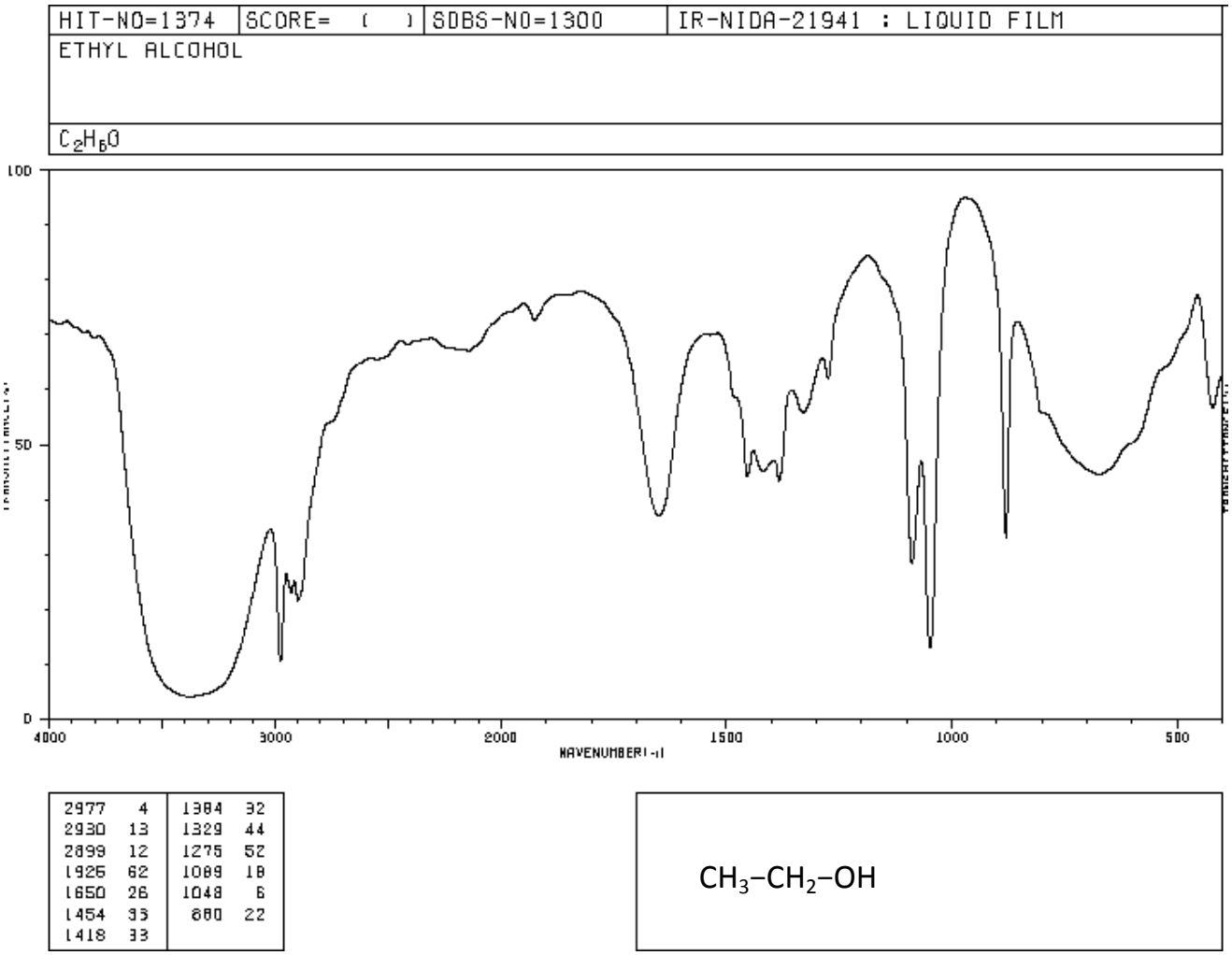

Figure B−2: FTIR spectrum of pure ethanol [46].

B−III

The FTIR spectrum of pure 4-penten-1-ol is given in Figure B−3.

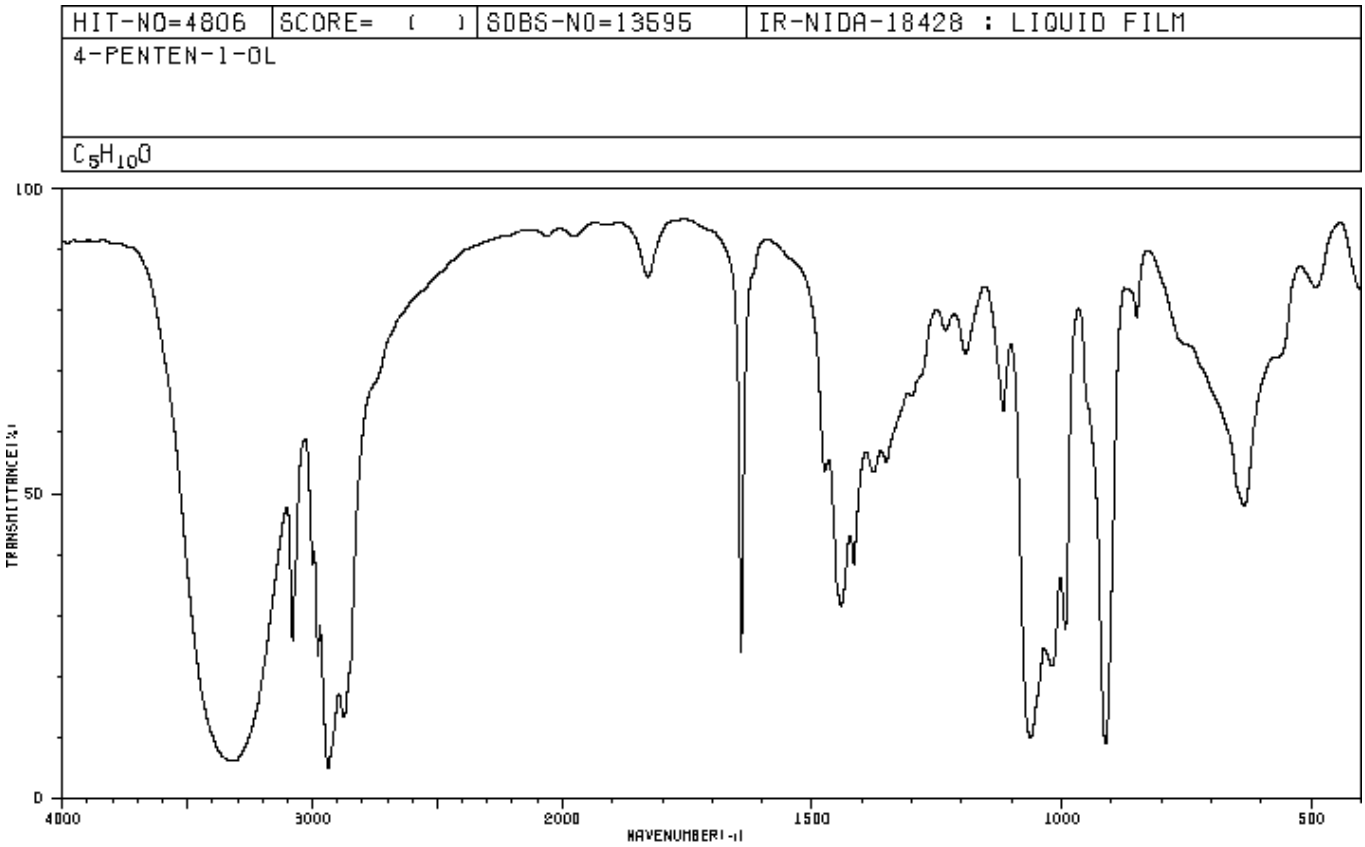

3332	6	1828	81	1233	74	860	77
3322	6	1642	23	1193	70	634	46
3079	25	1475	52	1117	80	491	61
2998	36	1442	30	1062	9		
2978	22	1416	37	1019	20		
2937	4	1378	52	993	26		
2873	12	1362	63	912	8		

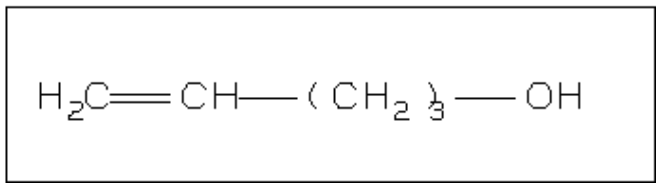

Figure B−3: FTIR spectrum of 4-penten-1-ol [46].

C Deposition of CdSe quantum dots on Si substrates

Solvent evaporation

Commercially available CdSe/ZnS core/shell quantum dots from Evident Technologies, with a diameter of 4 nm were dispersed on a silicon substrate, dried in air and finally plasma cleaned to see if it was possible to characterise quantum dots of a heavier element compared to the substrate. The CdSe quantum dots were supplied as a 49.9 nmol/ml dispersion in toluene, with an amine capping agent used as a stabiliser. The exact chemistry of the capping was unknown.

As a first try, the quantum dots were deposited as supplied, i.e. without further dilution. A quite thick layer formed, which was damaged as the electron beam hit the sample, even when the sample was plasma cleaned after the deposition. This means that it was not possible to investigate non-diluted samples by SEM. To try to avoid the thick layer and agglomeration, the CdSe quantum dots were diluted with toluene and with ethanol. Diluting with ethanol was done in order to improve the wetting properties of the dispersion on the silicon substrate, since toluene wetted the Si substrate badly. The quantum dots were first diluted ten times. However, the resulting layers were still too thick to be investigated and the quantum dots agglomerated to a large extent. A problem which arose upon dilution with ethanol was that agglomeration of the quantum dots took place, giving the dispersion an opaque appearance when ethanol was added.

The quantum dots were diluted even more, this time 200 times with toluene and ethanol. In Figure C−1, the SEM images from the characterisation for both solvents are shown. In Figure C−1a one can see that the wetting was an important issue, making it difficult for the liquid to stick to the surface, the quantum dot dispersion had in this case been diluted with toluene. The material left on the substrate after evaporation formed patches and strings consisting of small droplets on the surface, showing how the material accumulated. In b, one can see how the CdSe quantum dots which were diluted 200 times with ethanol appeared on the substrate after deposition. This image shows significant agglomeration of the material deposited, as was expected from the opaque appearance of the dispersion.

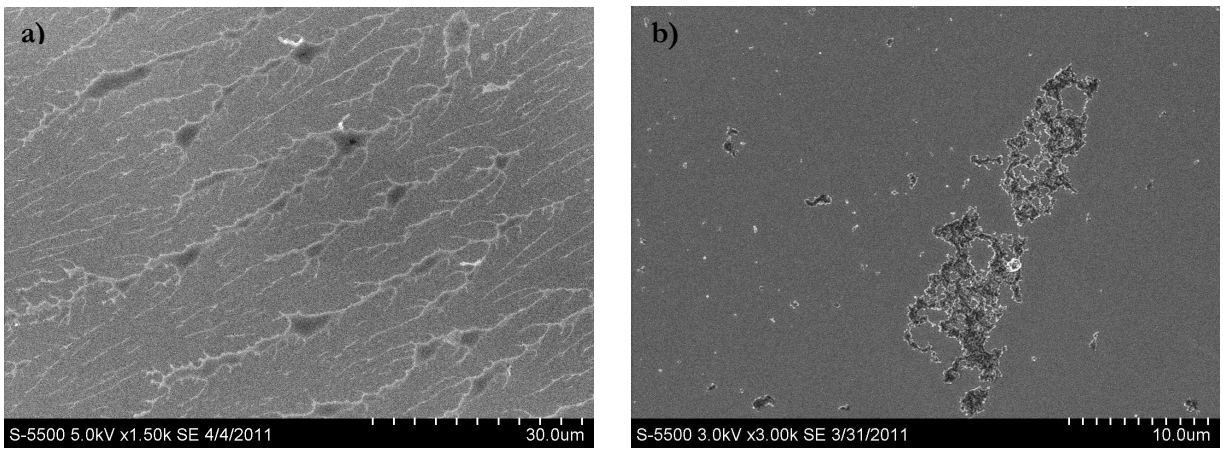

Figure C−1: SEM images of CdSe quantum dots deposited onto a plasma cleaned silicon substrate, diluted 200 times with **a)** toluene and **b)** ethanol. These samples have been plasma cleaned after the deposition.

In Figure C−2 it is shown a higher magnification SEM image of the agglomerates displayed in Figure C−1 b and the corresponding EDS spectrum. It looks as if the quantum dots are present on the

substrate from the signals from Zn and S, which are the elements forming the shell of the quantum dots. There are also weak peaks for Cd and Se. The largest peak stems from the silicon substrate. The following EDS spectra were recorded before plasma cleaning, as the signal from Cd, Se, Zn and S was lost when EDS spectra were recorded for the same samples after plasma cleaning. This indicates that treatment with plasma destroys the quantum dots. A clean silicon substrate was studied in the SEM before and after plasma cleaning, and it was found that the substrate oxidises during the treatment with plasma. It was concluded that the plasma cleaning is too vigorous as a treatment of quantum dots, and was not used for later samples.

a) **b)**

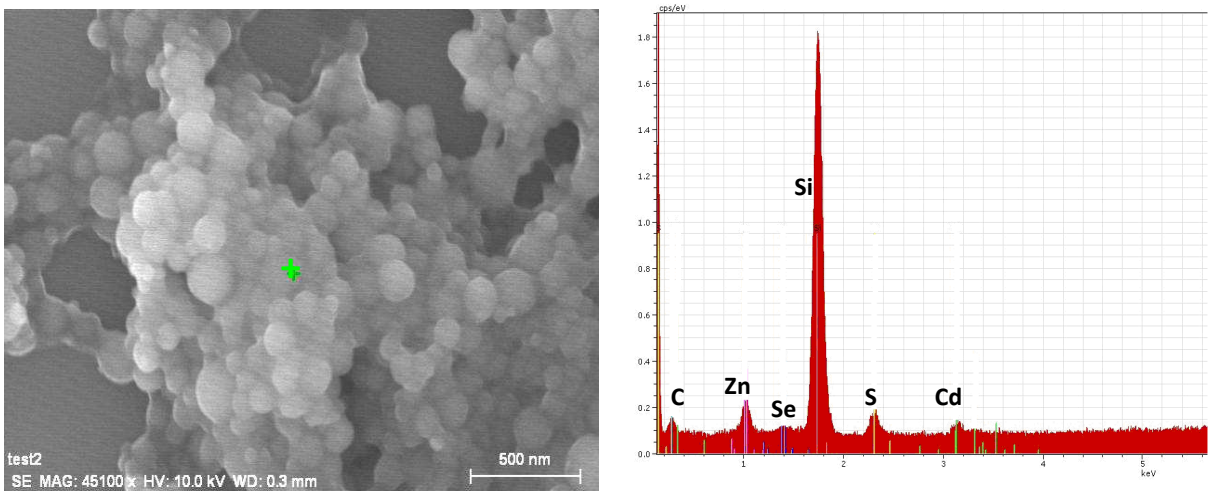

Figure C−2: a) SEM image of CdSe quantum dots diluted 200 times with ethanol and **b)** the corresponding EDS spectrum.

To avoid the agglomeration which took place upon dilution with ethanol, it was tried to add microlitre amounts of hydrochloric acid to the ethanol prior to addition of the quantum dot dispersion. Instantly, some large red particles formed, which dissolved as the liquids mixed with each other. This dispersion was deposited onto a Si substrate. An SEM image and the corresponding EDS spectrum of the agglomerates observed on the substrate are shown in Figure C−3. One can see that the agglomeration still took place to a large extent, and also that the added chlorine from the hydrochloric acid was present after evaporation. As a comparison, the EDS spectrum measured at a different position on the sample, where no particles were observed is shown in Figure C−4. At his point, none of the elements present in the quantum dots were observed, confirming the agglomerating behaviour of the quantum dots.

a) **b)**

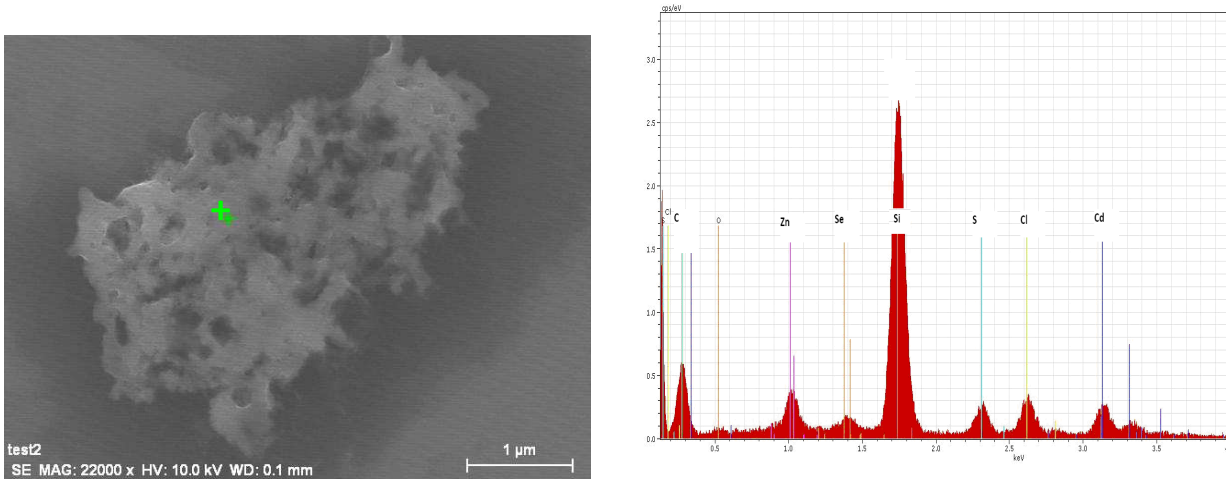

Figure C−3: a) SEM image of agglomerates formed when dispersing the CdSe quantum dots in ethanol and HCl, diluted 100 times, and **b)** the corresponding EDS spectrum. The green cross marks the position where the EDS spectrum was recorded, i.e. in the middle of the agglomerated particle.

a) **b)**

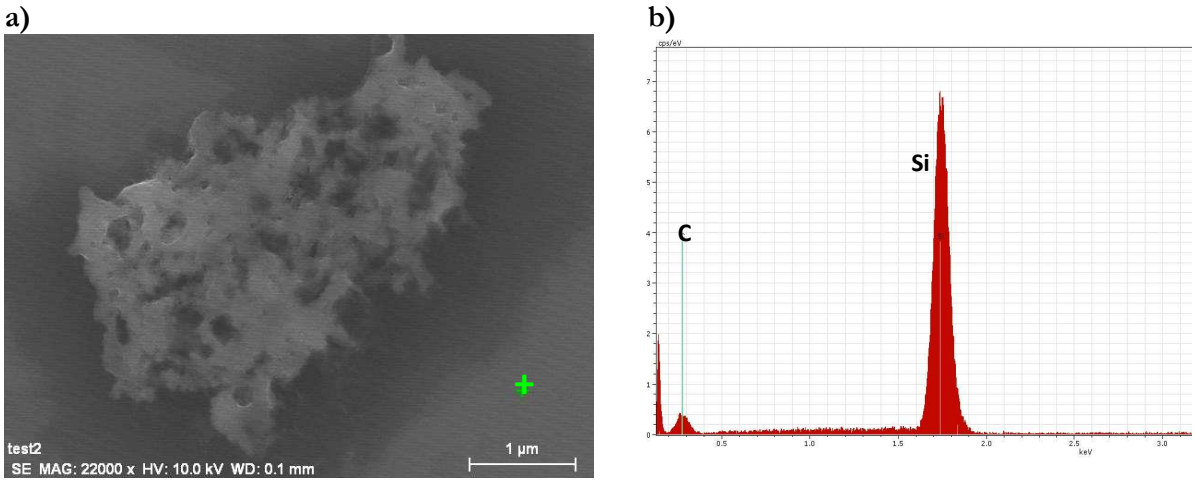

Figure C−4: a) SEM image of agglomerates formed when dispersing the CdSe quantum dots in ethanol and HCl, diluted 100 times and **b)** the corresponding EDS spectrum. The green cross marks the position where the EDS spectrum was recorded, i.e. outside an agglomerated particle.

Because of this apparent agglomeration upon dilution with ethanol, the solvent evaporation technique was further investigated when diluting the quantum dots with toluene, in spite of the bad wetting of toluene on the Si substrate. The bad wetting was shown in Figure C−1, an SEM image with a higher magnification is shown in Figure C−5a. The dark areas represent a track of the evaporated solvent. EDS spectra were recorded for these samples, see Figure C−5b, and it was observed that signals from the quantum dot elements were present everywhere in the dark areas. The brighter areas did not have a signal for these elements. This means that the quantum dots probably were quite homogeneously dispersed in these patches on the substrate.

a) **b)**

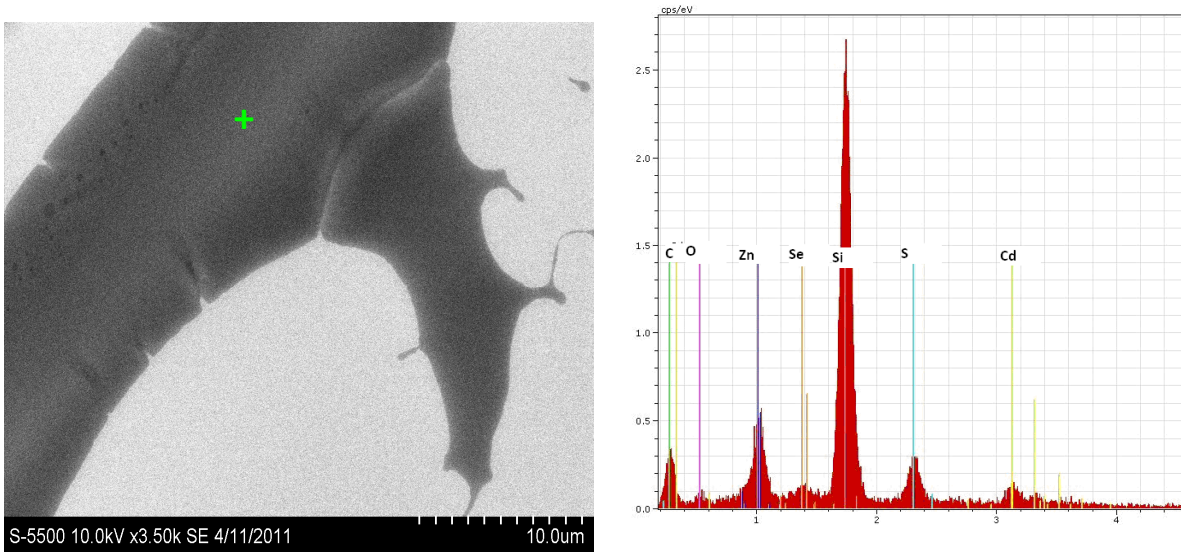

Figure C−5: a) SEM image of CdSe quantum dots diluted 200 times with toluene and **b)** the corresponding EDS spectrum, recorded in the dark area at the position of the green cross.

For higher concentrations of the quantum dots in the toluene dispersion, the quantum dots formed agglomerates, as shown in the SEM image and its corresponding EDS spectrum in Figure C−6. In this case, the quantum dots were diluted 20 times with toluene.

a) **b)**

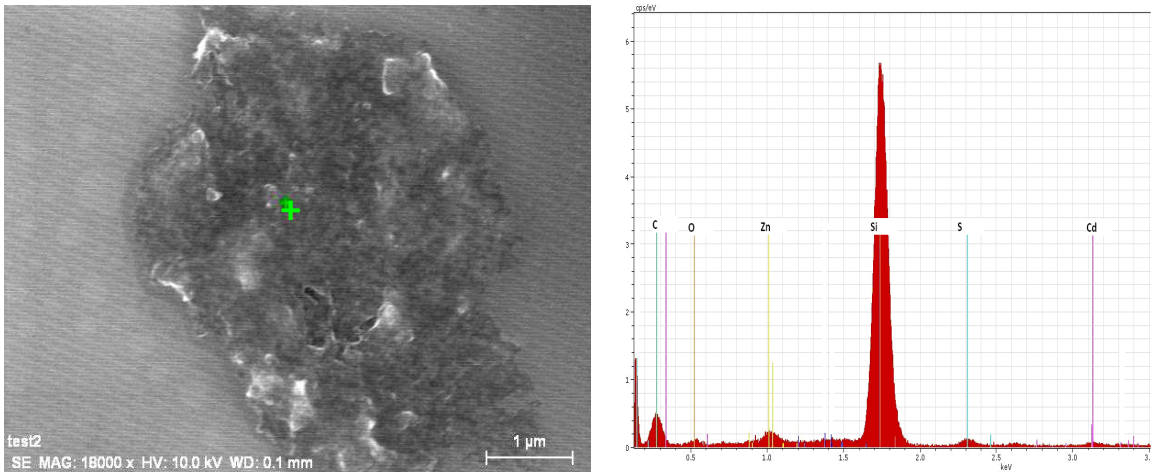

Figure C−6: a) SEM image of agglomerates formed when dispersing the CdSe quantum dots in toluene, and **b)** the corresponding EDS spectrum. The green cross marks the position where the EDS spectrum was recorded, i.e. right on top of the observed agglomerated material. The CdSe quantum dots had for this sample been diluted 20 times.

Spin coating

Because of the agglomeration when the technique of solvent evaporation was applied, spin coating was tried as an alternative deposition technique. However, for spin coating the ability to wet the substrate is even more important than for solvent evaporation. The dispersion of the CdSe quantum

dots was first diluted ten times with toluene and with ethanol for spin coating onto plasma cleaned silicon substrates. Spin coating of highly concentrated toluene dispersions was performed in spite of the bad wetting because of the agglomeration which took place when the quantum dots were diluted with ethanol. When investigated in the SEM, it was observed that the quantum dots agglomerated to a quite large extent when diluted with both solvents. The SEM images of the deposited quantum dot dispersions are shown in Figure C−7a and b for dilution with ethanol and toluene, respectively.

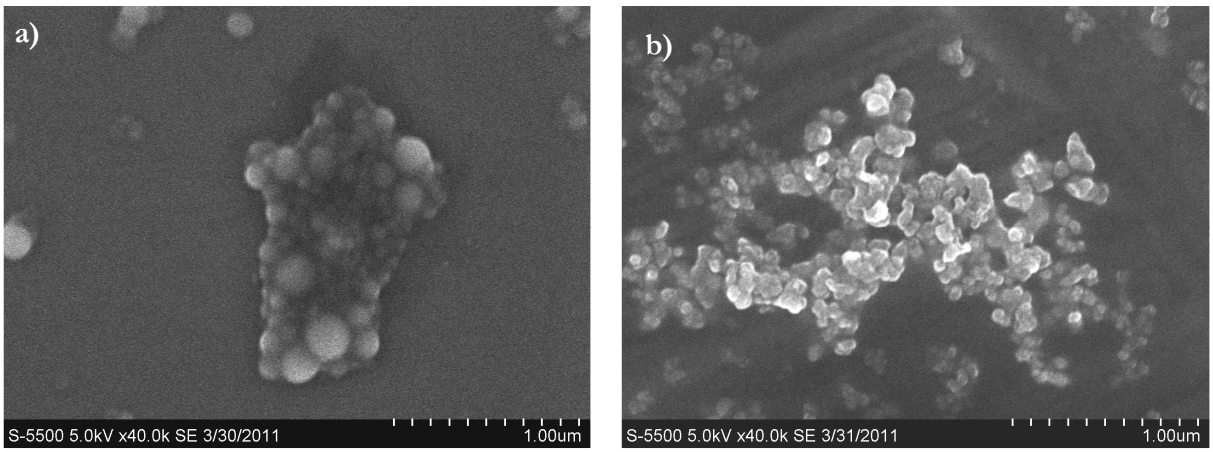

Figure C−7: Spin coated CdSe quantum dots, showing agglomerated particles, diluted ten times with **a)** ethanol and **b)** toluene.

Other concentrations were investigated for the spin coating. For lower concentrations of QD, only a very thin layer was left on the substrate after spin coating, hardly observable by eye. These layers were also too thin to be investigated by SEM. This was the case both when diluting with ethanol and with toluene.

It was also tried to increase the concentration of the quantum dots for the dispersion with ethanol and hydrochloric acid, since nothing was left after spin coating of dispersions with low concentrations. However, for higher concentrations, the colour changed to a more yellow one than for the dispersion of quantum dots with the same concentration in toluene. Since the capping of the quantum dots was unknown, and something apparently happened when hydrochloric acid was added, the dilution with ethanol and hydrochloric acid was not investigated any further.